# IRAM Annual Report 2012

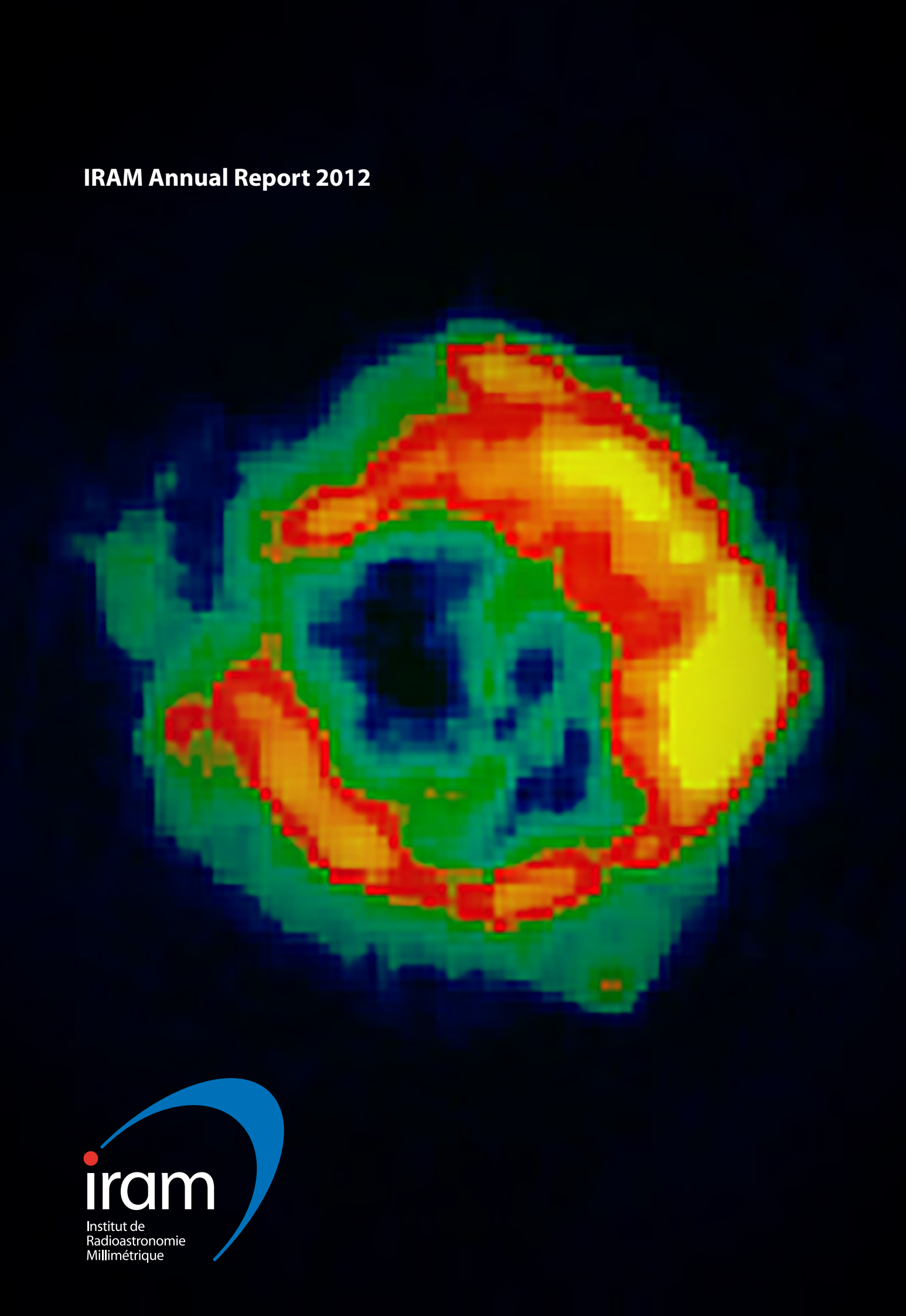

iram
Institut de
Radioastronomie
Millimétrique

# IRAM Annual Report 2012

Published by IRAM © 2013
Director of publication Karl-Friedrich Schuster

With contributions from:
Sébastien Blanchet, Michael Bremer, Walter Brunswig, Isabelle Delaunay, Frédéric Gueth, Carsten Kramer, Bastien Lefranc, Alessandro Navarrini, Santiago Navarro, Roberto Neri, Juan Penalver, Marc Torres

# Contents

# Introduction

2012 has been a pivotal year for IRAM with many important steps taken for the future. Most importantly NOEMA, the Northern Extended Millimeter Array Project started its transition from a mere concept to reality with important supplier contracts already signed, a well-advanced technology development and the organizational scheme well in place. Many details of the ongoing work for NOEMA can be found in this annual report. Current planning foresees first light for the first NOEMA antenna in spring 2014.

In parallel to NOEMA, the construction of the new cable car for an improved access to the Plateau de Bure has finally started this year and operation is also foreseen for early 2014. The two simultaneous projects, NOEMA and cable car construction, require a particular level of organization at the Plateau de Bure site, a real challenge to all participants in these projects. We are confident that with the detailed planning in place, this challenge can be met.

Meanwhile IRAM has continued to produce outstanding science with both observatories. At the IRAM 30m telescope, EMIR, the most powerful operating millimeter wave receiver, has allowed us to make a quantum leap in frequency surveys. GISMO and NIKA, the two prototype continuum arrays now produce unique science and pave the technological way to a future facility continuum instrument.

The PdBI Interferometer has produced a wide range of top-level science results ranging from very exiting investigations on galactic low mass star formation to observations in the distant universe with deep impact on the understanding of how galaxies form.

The year 2012 has also seen ALMA producing its first science results. The high success rate of proposals from members of the IRAM community clearly shows the advantage that our users have. A highly competent support through the IRAM ARC has been put into place and is receiving excellent user feedback. Towards the end of 2012, IRAM has successfully finished its production of ALMA B 7 cartridges. The first round of regular ALMA observations shows that this band with its excellent performance and reliability will play a central role in the operation of ALMA.

Undeniably the economic situation in Europe has degraded, and IRAM is forced to adapt with very tight budget constraints. It is remarkable that IRAM can pursue in such difficult times ambitious projects like NOEMA, a further proof of the outstanding support from the partner organizations CNRS, MPG and IGN. Although numerous investments on new instruments must be postponed due to the budget situation, basic technical developments can be continued (also with the help of European funding FP7 Radionet), a fact which will allow IRAM to maintain its know-how and leading position in mm-wave instrumentation.

At the time when this report is edited, another important change at IRAM has taken place. After more than 8 years of duty as the IRAM director, Pierre Cox has started his new position as the director of ALMA in Santiago, Chile. I thank Pierre Cox in the name of the IRAM staff and the IRAM partners for his collaboration, his continuous effort, and his involvement in numerous and sometimes difficult undertakings. Together with Frederic Gueth, the new deputy director, and the IRAM staff, we will continue with all our determination to keep IRAM up and ready for the many exciting things to come in the future of millimeter astronomy.

**Karl-Friedrich Schuster**
Director

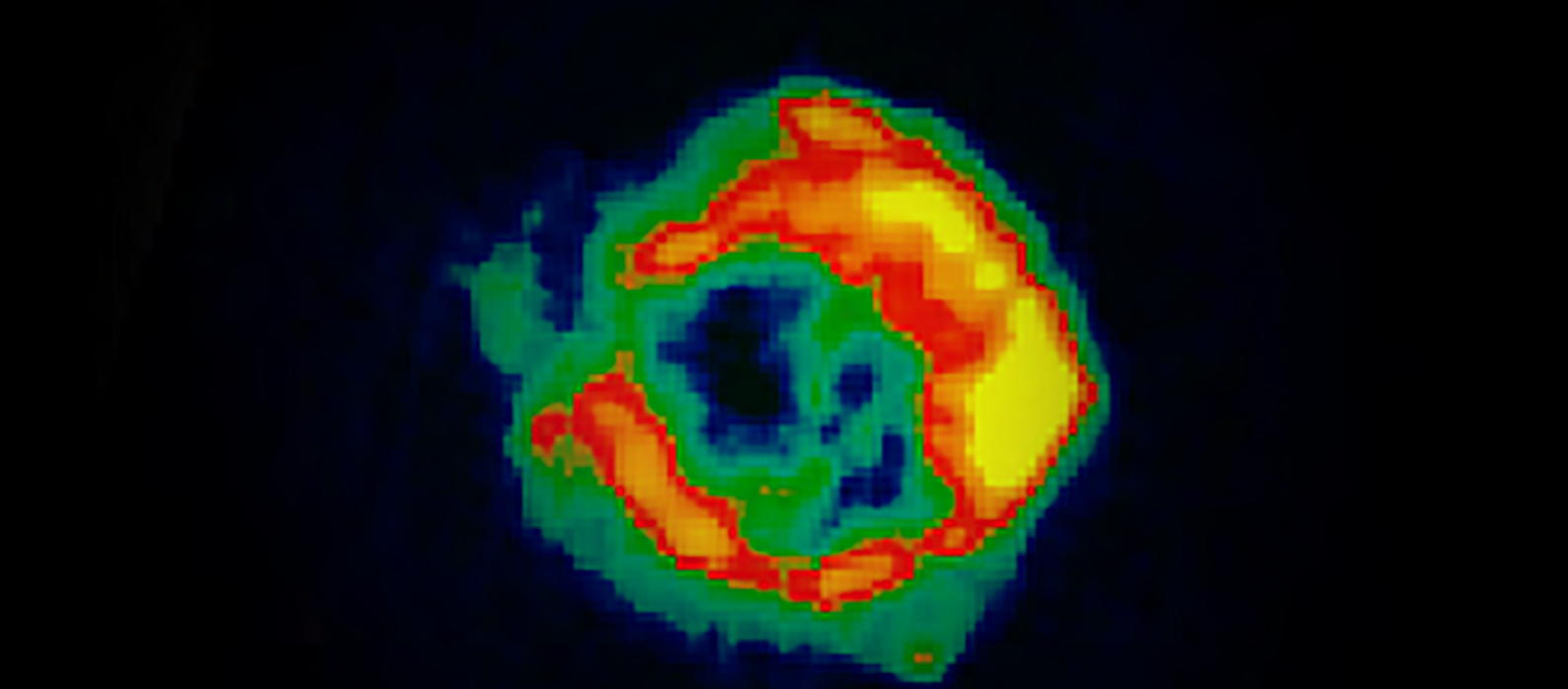

# Highlights of research with the IRAM telescopes in 2012

## LARGE FLUORINE RESERVOIRS IN THE HORSEHEAD NEBULA

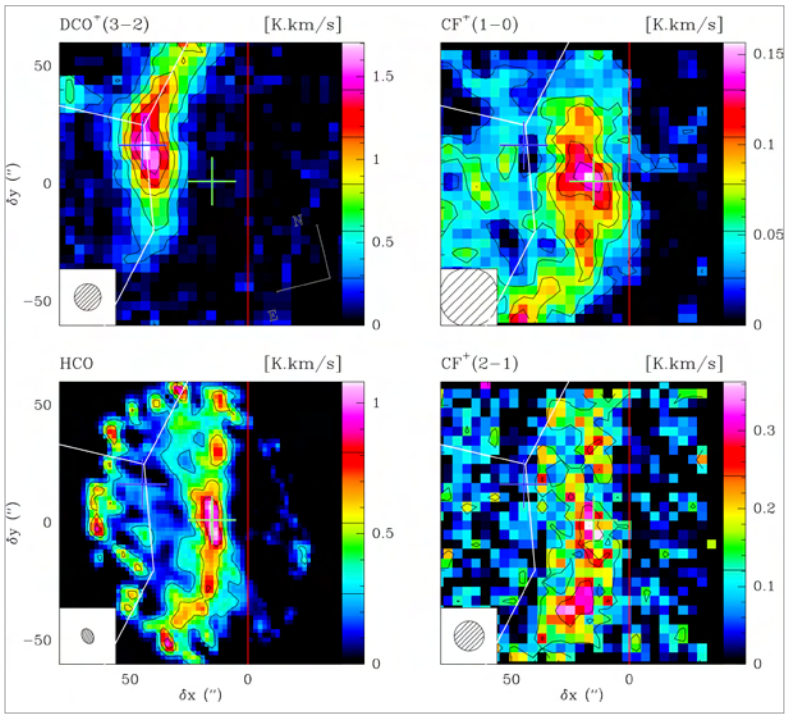


DCO⁺, HCO (left) and CF⁺ (right) integrated line intensity maps of the Horsehead Edge. The vertical line (red) identifies the edge of the photo-dissociation region (PDR); the crosses identify the center of the PDR (green) and of the dense adjacent molecular core (blue).
Work by Guzman et al. 2012, A&A, 543, L1

Understanding the chemistry of photo-dissociation-dominated regions (PDRs) is undoubtedly one of the key research areas in observational astrophysics. The goals are to measure reliable molecular abundances in PDRs, compare them to state of the art of astrochemical models to understand the formation and destruction mechanism at work, and dare to predict the existence of molecules, too rare to be observed but of critical importance for the chemical synthesis of new molecules.

Various efforts have been directed in the last years at astronomical line surveys, theoretical chemistry calculations of gas phase reaction rates and laboratory measurements. In an effort to provide observational constraints, Viviana Guzman (IRAM) and collaborators used the IRAM 30m telescope to conduct a line survey targeted at two positions in the Horsehead nebula: the warm UV-illuminated gas (PDR) and the cold UV-shielded gas (dense core).

Embedded within a forest of molecular lines from many species, Guzman et al clearly identified the weak chemical signature of $CF^+$, the fluoro-methylidynium ion. This molecule is not only of considerable interest to assess the chemical abundances and spatial distribution of HF and $C^+$ in the environment of PDRs but also to evaluate its reliability as a possible proxy for $C^+$ in the study of galactic chemical factories.

Guzman et al. combined the Meudon (Le Bourlot et al. 2012) photochemical model with the observed 30m telescope data to predict the abundances of $CF^+$, $C^+$ and HF in the PDR at the edge of the Horsehead Nebula, and concluded on a $CF^+$ abundance of ~$10^{-5}$ relative to $C^+$, and on a 4–8% amount of fluorine directly locked within $CF^+$. Chemical models predict that $CF^+$ and $C^+$ coexist; this strongly suggests that $CF^+$ is a good proxy for $C^+$ and is tracing the outer $C^+$ layer of the PDR.

## A PETROLEUM REFINERY IN THE MILKY WAY

The study of complex molecules in space is crucial for understanding the physical and chemical processes in the interstellar medium (ISM). As ISM regions are often characterized by a high diversity of molecular species, identifying the spectral signature and diagnosing their chemical properties is becoming a challenge in itself. The majority of interstellar molecules have been detected at millimeter wavelengths, as molecules with small moments of inertia are the most abundant and their rotational transitions are observable in the millimeter range. As of today, extensive spectral line surveying made it possible to identify the spectral signatures of about 200 molecules in the ISM.

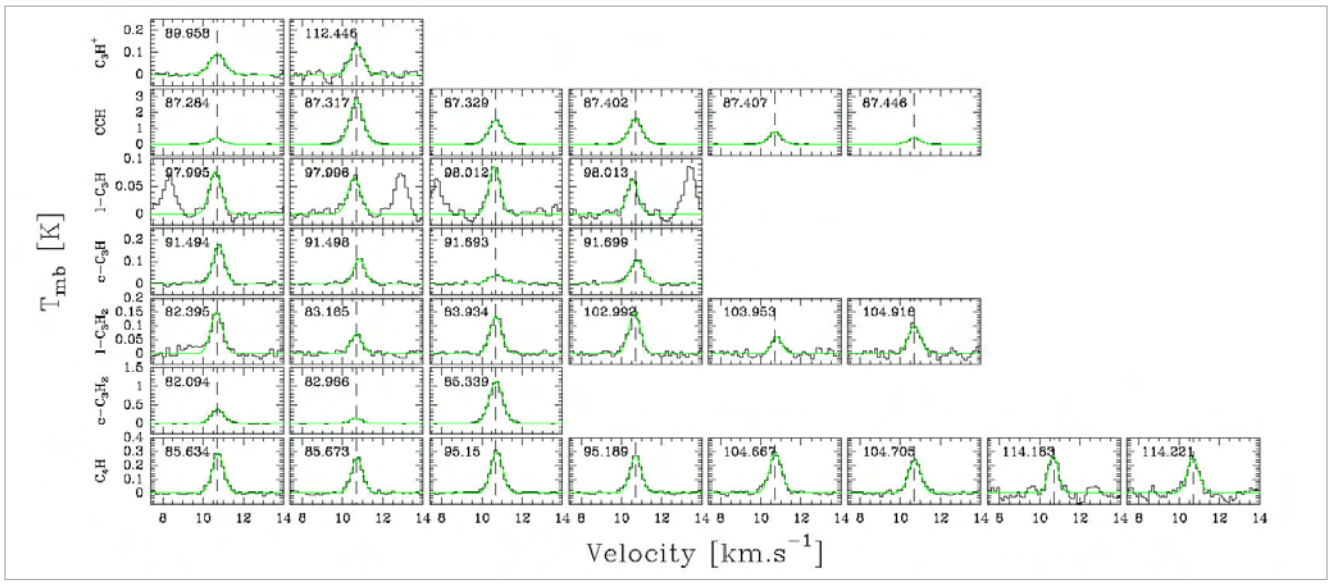


IRAM 30m EMIR/FTS spectra profiles and Gaussian fits (green) of l-$C_3H^+$, $C_2H$, l-$C_3H$, c-$C_3H$, l-$C_3H_2$, c-$C_3H_2$, and $C_4H$ towards the Horsehead PDR. Work by Pety et al. 2012, A&A, 548, A68

Inspired by the success of the EMIR receivers and of the Fourier Transform Spectrometer (FTS) at the IRAM 30m telescope, a team led by Jérôme Pety (IRAM/ LERMA) embarked on the Horsehead WHISPER survey. WHISPER is major effort aiming at characterizing the physical and chemical conditions in two areas of the Horsehead nebula: the photo-dissociation region (PDR) at the edge of the nebula and a nearby colder condensation. On analyzing the results generated by their complete spectral line surveys over three bands of the EMIR receivers, the researchers discovered a set of unidentified lines towards the PDR, and they tentatively assigned them to the spectral signature of l-$C_3H^+$. Laboratory measurements are needed now to refine the spectroscopic characterization of the newly detected molecule. This molecule, the so-called propynylidyne cation, is part of the hydrocarbon family, which composes one of the major energy sources on Earth, petroleum and natural gas. From the observations, the authors infer a column density of $5.10^{11}$ cm$^{-2}$ and a relative abundance of $10^{-10}$ for l-$C_3H^+$ at the edge of the Horsehead PDR, and in good agreement with the predictions of a photochemical model of the PDR. In contrast, the same model cannot account for the measured amounts of other small hydrocarbons like $C_2H$, $C_3H$, $C_3H_2$, and $C_4H$. Pety and collaborators suggest that these small hydrocarbons result from the fragmentation of PAHs by erosion through UV radiation. The mechanism is likely to be particularly efficient in regions like the Horsehead Nebula where the interstellar gas is directly exposed to the light of a nearby massive star.

The survey enabled the detection of about 30 molecular species. Among these small hydrocarbons like $C_2H$, l-$C_3H$, c-$C_3H$, l-$C_3H2$, c-$C_3H_2$, and $C_4H$ were found.

## FIRST IDENTIFICATION OF A PRE-BROWN DWARF

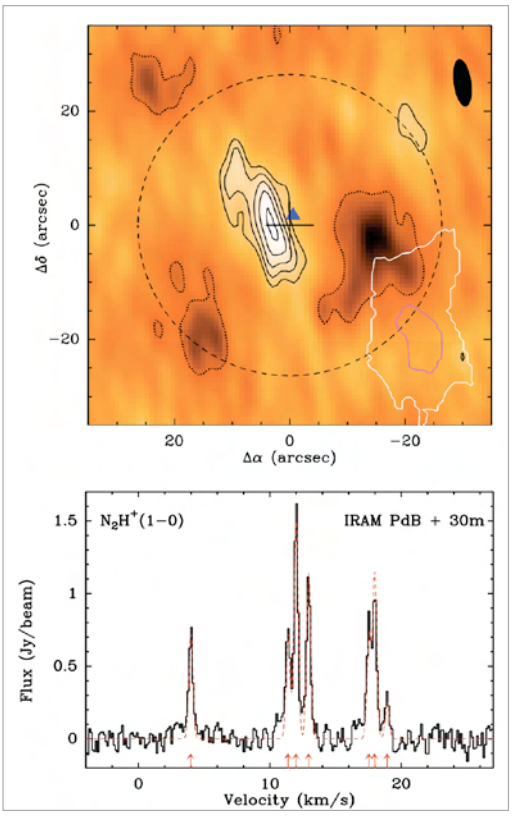


(top) $N_2H^+$(1-0) image of Oph B-11 obtained with the IRAM interferometer. The filled triangle shows the position of the 3.2 mm continuum peak. (bottom) $N_2H^+$(1-0) spectrum resulting from combined IRAM interferometer and 30m telescope observations. Work by André et al. 2012, Science, 337, 69

Brown dwarfs lie between planets and stars in terms of mass and composition. They are too light to undergo hydrogen fusion but too massive to be called a planet. Their predicted masses range from about 0.014 to 0.075 $M_\odot$, although the mass boundary with planets is subject to debate.

Today, two competing formation scenarios exist for brown dwarfs: 1) formation as a by-product of the process of disk fragmentation and/or ejection, 2) formation from the direct collapse of a self-gravitating condensation of gas and dust, a so-called pre-stellar core. In the second formation scenario, a large number of ultra-low mass cores are predicted to be dense enough to be gravitationally unstable to collapse. However, the existence of such pre-brown dwarf cores had never been confirmed observationally.

To demonstrate the existence of pre-brown dwarfs and provide support to models where brown-dwarfs form like solar-mass stars, Philippe André (CEA-IRFU) and collaborators pointed the IRAM interferometer on Oph B-11, a starless core in the cluster-forming region L1688.

They obtained a robust detection of the source in both the continuum at 3.2 mm and the $N_2H^+$(1-0) line. They fitted the visibilities with a Bonnor-Ebert core model and yielded a best-fit size of 1.0±1.8" for the outer angular radius, and a best-fit core radius of 140 AU. The continuum was detected at the 0.4mJy level and found consistent with emission originating from a region of cold gas and dust (≤10K) and of enhanced $H_2$ column density (≥·$710^{22}$ cm-2). From this, the gas and dust mass of Oph B-11 was estimated to 0.02-0.03 $M_\odot$. The linewidth of the $N_2H^+$(1–0) transition was found to be extremely narrow (0.2 km/s) indicating that the velocity dispersion of the gas within the core is nearly thermal and comparable to the isothermal speed of sound.

As no other stars or proto-stars were found to form close to Oph B-11, André and collaborators concluded from these observations that pre-brown dwarfs do exist and that brown dwarfs may form from the direct collapse of low-mass pre-stellar cores.

## PREBIOTIC CHEMISTRY IN PROTOPLANETARY SYSTEMS

Protoplanetary disks are rotating disks of gas and dust surrounding young stars. On their route to forming stars, they appear to dissipate remnant gas and dust and lead to the formation of planetary systems. As these objects are believed to be the birthplace of planets, detailed studies of their structure, composition and properties are expected to shed light on the origin of planets.

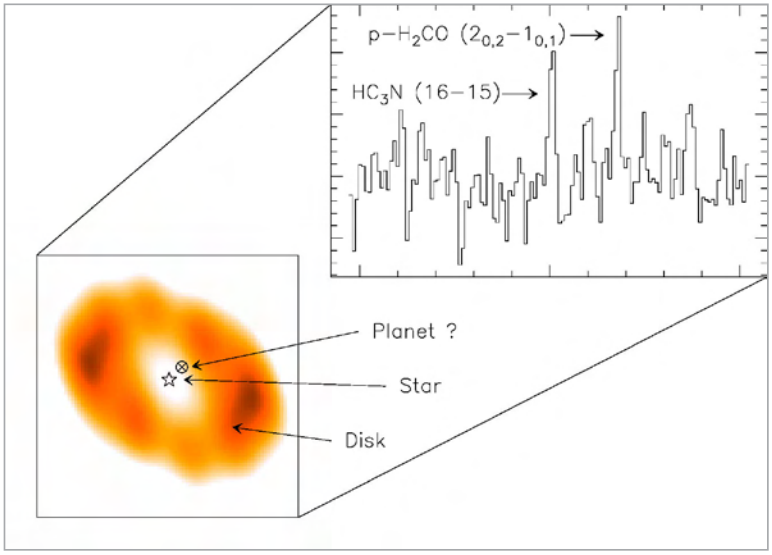


(top) low-resolution spectrum of $HC_3N$ and $H_2CO$ towards LkCa15 in the 3.5" beam of the IRAM interferometer, (bottom) high-resolution image (0.5") of the 1.3mm thermal dust emission from the circumstellar disk of LkCa15. Work by Chapillon et al. 2012, ApJ, 756, 58

Using the IRAM 30m and Plateau de Bure interferometer (PdBI), a team led by Edwige Chapillon (Academia Sinica) reported the detection of cyanoacetylene ($HC_3N$)

in the disks of two solar-like objects, the low-mass stars LkCa15 (PdBI, IRAM 30m) and GO-Tau (IRAM 30m), and of the more massive star MWC480 (IRAM 30m). LkCa15 is considered to be peculiar, as it shows a disk cavity, a telling sign of the formation of a planetary system. The authors presume a Jupiter-like planet, whose presence is inferred from infrared excess emission, carved it out.

$HC_3N$ is the heaviest and most complex molecule ever detected in a protoplanetary disk so far. It is the simplest cyanopolyyne, and presumably, also one of the key elementary bricks in the formation of complex organic molecules and in the emergence of life. According to current models of disk chemistry, $HC_3N$ is mainly formed through grain surface reactions in the colder regions (≤15 K) near the disk mid-plane. Contrary to $HC_3N$, simple molecules like CO and $H_2O$ are frozen onto the grains' ice mantle in the inner disk layers. These molecules can undergo a variety of reactions on an ice grain mantle to form more complex species. The newly formed molecules can then be released into the gas-phase by thermal evaporation or via induced desorption by ultraviolet radiation and cosmic rays. As the observed column densities of $HC_3N$ (~$10^{12}$ $cm^{-2}$) are found to be lower by two orders of magnitude than predicted, Chapillon and coauthors suggest that the mid-plane molecular chemistry is sensitive to the UV radiation field.

The discovery of $HC_3N$ in these three planetary formation regions is an important first step towards understanding the emergence of prebiotic molecules on Earth and exoplanetary systems.

## THE AFTERMATH OF TWO EXPLOSIVE MASS-LOSS EVENTS IN M2–9

Understanding the appearance and shaping of bipolar winds in the transition of stars from the late asymptotic giant branch (AGB) to the planetary nebula (PN) phase is one of the most challenging issues in stellar evolution. Bipolar winds are not only critical to unraveling the AGB to PN evolution timescales but also to characterize how PN properties are shaped by wind interactions. One mechanism invoked to account for the generation of bipolar winds is the presence of an orbiting binary star system at the nebula's center. While the direct detection of a binary companion is currently a challenge, its presence can be inferred indirectly through its dynamical influence on the surrounding circumstellar material. Currently, the best way to measure its dynamical imprint in regions, which normally are hidden to optical telescopes, is with sensitive interferometric observations in the millimeter waveband.

M2–9, which is one of the few established examples of a bipolar planetary nebula in the making, is one of the most promising candidates to gain initial insights into the orbital geometry of the presumptive binary star system. IRAM Plateau de Bure interferometer observations of M2–9 by Arancha Castro-Carrizo (IRAM) and collaborators have recently unveiled two ring-shaped structures in the waist of the nebula, both fitting remarkably well the basal point of departure of the optical lobes.

The rings were ejected during two short episodes (of ≤40 yr), about 1400 yr and 900 yr ago. The centers of the two rings were found offset by 220 AU and their systemic velocities by 0.6 km/s. According to the authors these findings provide sound evidence for the presence of a binary star system in M2–9.

The two rings were very probably ejected by one of the stars, in a very late AGB or very early post-AGB phase. Different positions in the stars orbital motion explain the measured position and velocity offsets between the rings. At the same time, two independent mass-loss events seem to have corseted the expanding nebula into the classic hourglass shape typical of many PN. By analyzing the kinematics of the equatorial rings and assuming a mass of 0.5 – 2 $M_\odot$ for the primary star, Castro-Carrizo and collaborators estimated the mass of the secondary to ~0.2 $M_\odot$ and its orbital speed to ~1 km/s. They also suggested the binary system is composed of a red giant and a dwarf, separated by ~20 AU, a distance considered too large for the stars to have undergone a common envelope phase, or for being interacting members of a symbiotic system.

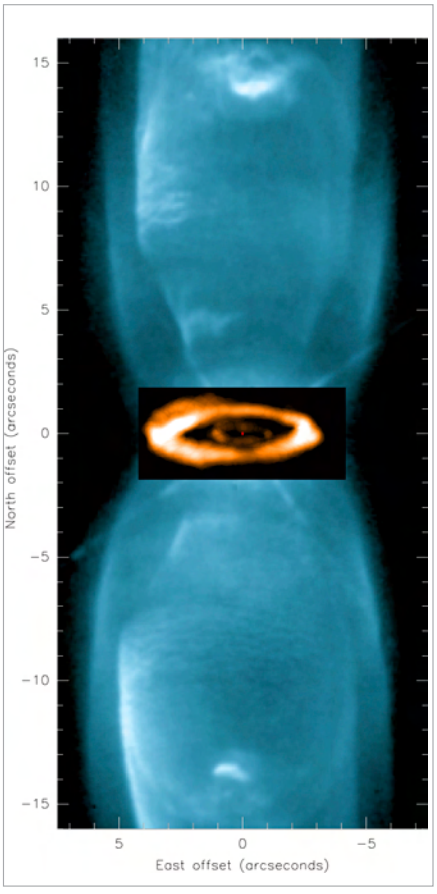


Velocity integrated 12CO J=2-1 line emission towards M2–9 (inset) superposed on the HST/WFPC 2 image (light blue).
Work by Castro-Carrizo et al. 2012, A&A, 545, A1

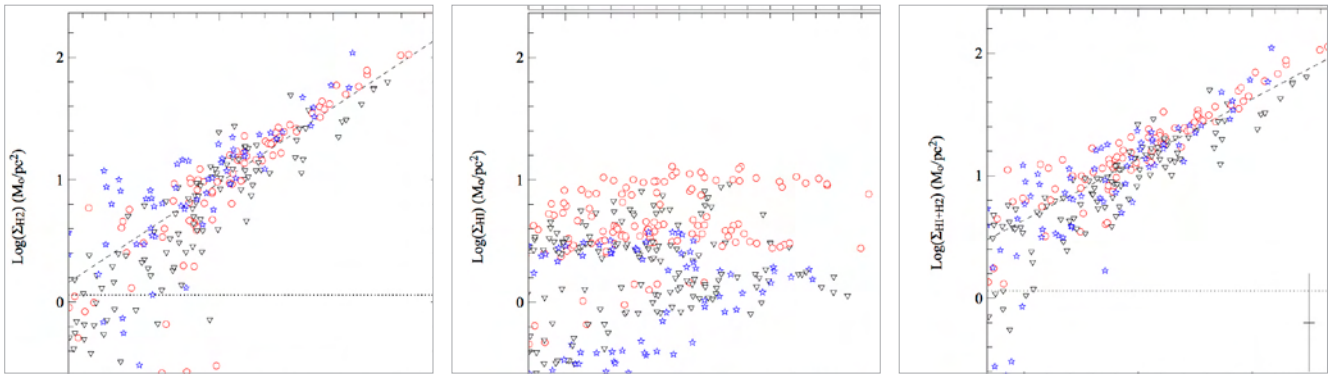


Surface mass densities of molecular (left panel) and atomic hydrogen (middle panel), and total gas (right panel) as a function of the FIR surface brightness at 250 µm. Different symbols distinguish non-deficient (red circles), slightly HI-deficient (black triangles), and HI-deficient galaxies (blue stars).
Work by Pappalardo et al. 2012, A&A, 545, A75

## ENVIRONMENTAL EFFECTS ON VIRGO CLUSTER GALAXIES

The stellar and gas distributions in a cluster galaxy can be drastically modified through environmental effects. While a spiral galaxy can lose a considerable fraction of its neutral gas (HI) through tidal interaction with neighbor galaxies and/or ram-pressure stripping, molecular gas is more bound to the galaxy potential and therefore less prone to removal via stripping. Indeed, in Virgo, a young, close (D~17 Mpc) and still dynamically active cluster, the environment effects are clearly seen for the atomic gas but are less evident for the molecular gas phase. Also while the global dust-to-stellar mass ratio is found to decrease as a function of HI deficiency, the dust-to-total-gas ratio is found to increases.

To develop a better understanding of the complex interplay between the different constituents of the ISM at various galactic distances and environmental effects, Ciro Pappalardo (INAF/Arcetri) started an international collaboration. The team observed a sample of 7 Virgo galaxies in the $^{12}$CO (1-0) and (2-1) transitions with the IRAM 30m telescope and combined the results with literature data. It estimated the integrated mass of molecular hydrogen for the galaxies observed in the CO lines and inferred molecular-to-total gas mass fractions between 0.04 and 0.65, and integrated dust-to-gas ratio ranges between 0.011 and 0.004.

According to Pappalardo and collaborators, both the molecular gas and the dust distributions show steeper radial profiles for HI-deficient galaxies and the average dust-to-gas ratio for these galaxies increases or stays radially constant. On scales of ~3 kpc, they find a strong correlation between the molecular gas and the 250 µm surface brightness. The correlation, is found tighter than average for non-deficient galaxies, and becomes linear if the total gas surface mass density is considered. The inclusion of atomic hydrogen does not improve the statistical significance of the correlation.

## THE METALLICITY DEPENDENCE OF THE CO/$H_2$ CONVERSION FACTOR IN Z>1 SFGS

$H_2$ is the primary but elusive component of the reservoirs of cold, dense gas that fuel star formation in galaxies. Estimates of gas masses and surface densities are therefore often derived from observations of CO using the galactic CO/$H_2$ conversion factor. While the canonical value of $\alpha_{CO}$=4.36 is adopted for a Milky Way like ISM, surface densities derived from CO are likely to be biased if the same conversion factor is used for galaxies with a metallicity (or dust-to-gas ratio) very different from that of the Milky Way.

To explore the metallicity dependence and evolution over cosmic time of the CO/$H_2$ conversion factor in z>1 "main-sequence" star-forming galaxies (SFG), Reinhard Genzel (MPE) and collaborators used a first systematic sample of CO measurements from the IRAM interferometer, and metallicities derived from [NII]/Hα estimates and stellar-mass-metallicity relations at the SFG redshifts. The survey encompasses a sample of 37 SFGs, including 21 galaxies from two IRAM Large Programs.

According to the study, the molecular gas depletion rate inferred from the ratio of star formation rate (SFR) to CO luminosity is ~1 Gyr$^{-1}$ for near-solar metallicity galaxies with stellar masses above $M_S$~$10^{11}$ $M_\odot$. In this regime, the depletion rate does not vary more than a factor of two to three as a function of molecular gas surface density or redshift between z~0 and 2. Below $M_S$ the depletion rate increases rapidly with decreasing metallicity.

The researchers argue that this trend is not caused by starburst events, by changes in the physical parameters of the molecular clouds, or by the impact of the fundamental-metallicity–SFR–stellar mass relation. A more probable explanation is that the conversion factor is metallicity dependent and that star formation can occur in "CO-dark" gas.

The trend is also expected theoretically from the effect of enhanced photodissociation of CO by ultraviolet radiation at low metallicity. From the available z~0 and z~1–3 samples they constrain the slope of the log ($\alpha_{CO}$)–log (metallicity) relation to range between –1 and –2, fairly insensitive to the assumed slope of the gas–SFR relation. Because of the lower metallicities near the peak of the galaxy formation activity at z~1–2 compared to z~0, they suggest that molecular gas masses estimated from CO luminosities have to be substantially corrected upwards (by factors of 2 to 10) for galaxies below $M_S$.

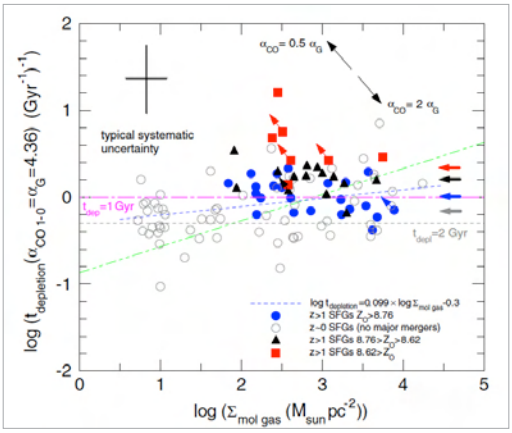


CO-based Molecular gas depletion rate as a function of molecular gas surface density. The open gray circles are non-mergers, near-main-sequence, and moderately high-mass SFGs at z~0. Blue circles, black triangles, and red squares denote z>1 SFGs from the IRAM LP program and other data in three metallicity ranges. In this form of the KS-relation, constant molecular depletion times or rates are horizontal lines. Work by Genzel et al. 2012, ApJ 746, 69

## NITROGEN EMITTERS AT HIGH REDSHIFT

Forbidden atomic fine-structure transitions are important cooling lines of the interstellar medium (ISM). They provide effective cooling in cold regions where allowed atomic transitions cannot be excited, and thus are critical diagnostic tools to study the star-forming ISM. One of the most important cooling line is the forbidden $^2P_{3/2}$–$^2P_{1/2}$ fine-structure line of ionized carbon at 158 µm, which alone accounts for 0.1%–1% of the total continuum far-infrared (FIR) luminosity in local, star forming galaxies. Other main cooling atomic transitions are provided by the FIR lines of [OI], O[III] and [NII]. Due to its ionization energy, the fine-structure line of [NII] 205 µm is generally an excellent tracer of the ionized medium around star-forming regions.

Last year's annual report showed the results of the highest redshift detection (z = 5.24) of [NII] at 205 µm. New observations have now been made by a team led by Roberto Decarli (MPIA) that yielded secure fine-structure line detections in two millimeter-bright and strongly lensed objects: APM08279+5255 (*z*=3.911) and MM18423+5938 (*z*=3.930). Both objects were observed with the IRAM Plateau de Bure Interferometer by using the capabilities of the band 4 receivers (275 – 373 GHz)..

The data revealed intrinsic [NII] line luminosity of ~1.8 $10^9$ L⊙/µ for APM 08279+5255 and ~2.8 $10^9$ L⊙/µ for MM 18423+ 5938.

The high-resolution map of the [NII] and 1.0 mm continuum emission in MM 18423+ 5938 clearly resolves an Einstein ring in this source and reveals a velocity gradient in the dynamics of the ionized gas.

The authors measure a [NII]/FIR luminosity ratio of ~9.0 10-6 on APM 08279+5255 and of ~5.8 $10^{-6}$ in MM 18423+5938, which they found in agreement with the decrease at high FIR luminosities observed in local galaxies.

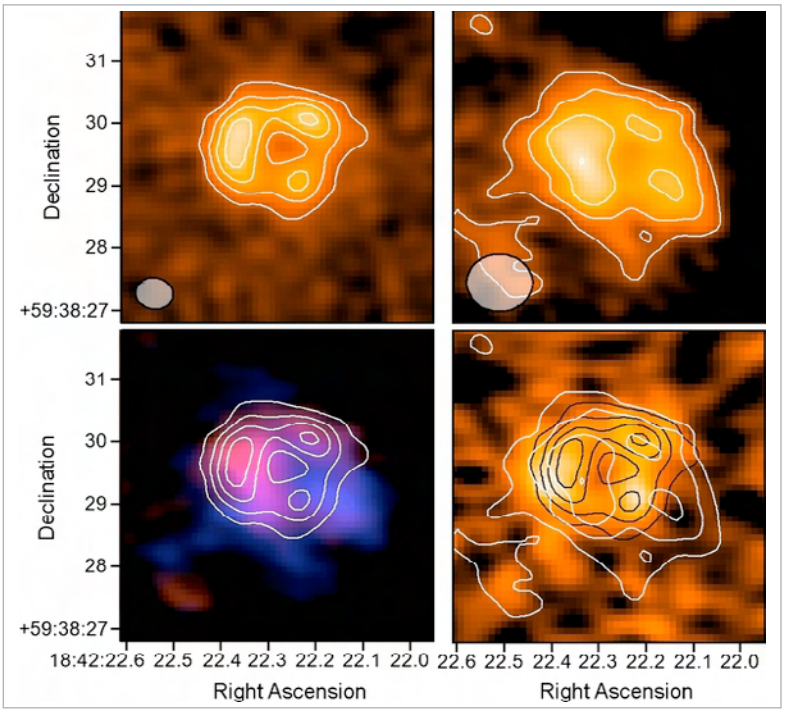


High-resolution (0.6"x0.5") map of the line-free continuum emission in MM 18423+5938 with contours in steps of 4σ (top left); continuum subtracted map of the [NII] emission with contours in steps of 2σ (top right); color-composite image of red and blue [NII] line emission wings with overlaid the contours of the continuum map (bottom left). Bottom right: comparison of the [NII] line map (white contours), the continuum emission (black contours), and the $^{12}$CO(2–1) map published by Lestrade et al. (2011) (color scale). Work by Decarli et al. 2012, ApJ, 752, 2

## LUMINOUS WATER VAPOR EMISSION AT HIGH-Z

Spectra of the $H_2O$ (left, ($2_{11}$–$2_{02}$) or ($2_{02}$–$1_{11}$)) and $^{12}CO$ (right, 3–2, 4–3, 5–4 or 7–6) emission lines observed at the IRAM interferometer towards six lensed *H-ATLAS* galaxies (top), lensing corrected $H_2O$ to infrared luminosity ratio for a sample of ultra-luminous infrared galaxies at low and high redshift (bottom). Work by Omont et al. 2013, A&A, 551, 115

Water is a molecule of key importance in astrophysical environments. In cold molecular clouds, water is in the form of icy mantles on dust grains but in warm and dense (≥100K, ≥$10^5$ cm$^{-3}$) clouds, such as in starbursting galaxies or galaxies with a luminous active galactic nucleus, water can evaporate from the dust grains when the grain temperature becomes sufficiently high or via photodesorption by exposure to high-energy radiation. Water is then one of the most abundant oxygen-bearing molecules after CO and an important coolant of the warm and dense gas, and as such it must play an important role in the process of star formation.

To evaluate the potential of water as a key diagnostic tool to probe both the extreme physical conditions and the infrared radiation in the warm dense environments of high-redshift starbursting galaxies, Alain Omont (IAP) and coauthors observed a sample of six, strongly lensed Herschel *H-ATLAS* galaxies with the IRAM interferometer.

The team was able to report the detection of water vapor line emission in the warm and dense core of all six galaxies with redshifts in the range from 1.57 to 4.24. The derived $H_2O$ luminosities corrected for lensing magnification show a strong ~$L_{IR}^{1.2}$ dependence on the galaxies' infrared luminosity. Though the measured slope of the $L_{H2O}/L_{IR}$ relation is affected by uncertainties in the lensing factors, the relation suggests that infrared pumping is playing a key role in the excitation of the $H_2O$ lines. Water emission is therefore expected to become very strong in the most luminous ($L_{IR}$>$10^{13}L_\odot$) galaxies.

Omont et al detections of the water vapor emission lines in these six luminous galaxies demonstrate that the millimeter/submillimeter transitions of water vapor provide a powerful tool to probe the warm, dense and dusty molecular environments in luminous infrared galaxies at high redshift. Observations in other water lines and molecular species are planned with ALMA and NOEMA and will possibly help to further constrain the excitation conditions and the water abundances in these regions.

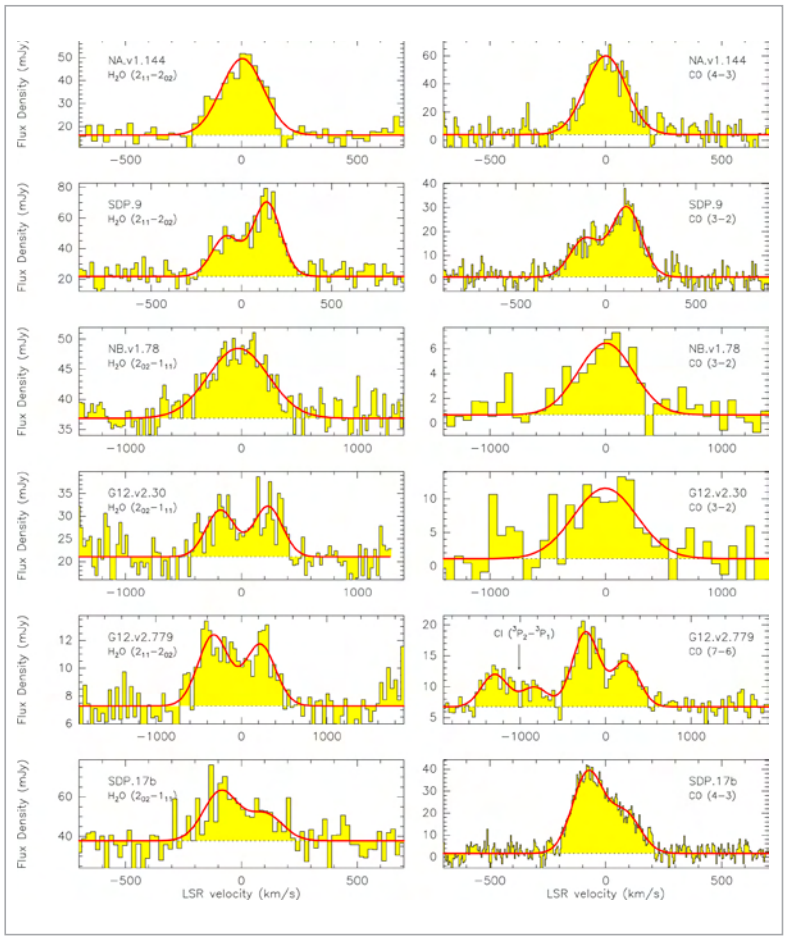


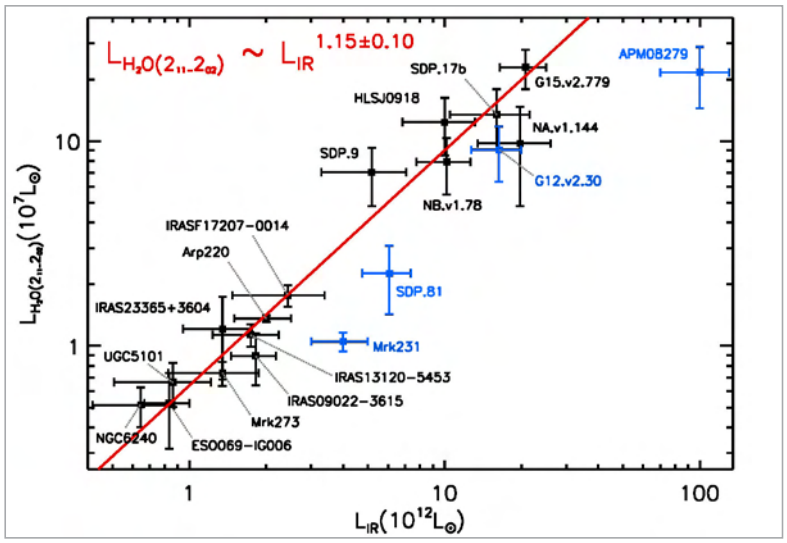

## MYSTERY OF GALAXY HDF850.1 FINALLY SOLVED

The region in the sky where HDF850.1 is located affords an almost unparalleled view into the deepest reaches of space. Known as the Hubble Deep Field (HDF), it was first studied extensively in visible light with the HST. Yet these observations only reveal part of the cosmic picture, and astronomers were quick to follow-up the Hubble observations with other telescopes operating at longer wavelengths. In the late 1990s, astronomers surveyed the region using the SCUBA/JCMT. The researchers were taken by surprise when they realized that HDF850.1 was the brightest submillimeter source in the field by far, a galaxy that was evidently forming as many stars as all the other galaxies in the HDF combined, presumably one of the most productive star-forming galaxies in the observable universe – and which was completely invisible in the observations of the HST.

An international team of astronomers led by Fabian Walter (MPIA) finally managed to determine the distance of HDF850.1 with the IRAM interferometer. Taking advantage of recent instrumental upgrades they were able to identify the (6-5) and (5-4) lines of $^{12}$CO and to detect the redshifted $^2P_{3/2}$–$^2P_{1/2}$ transition of [CII]. By combining these results with a $^{12}$CO (2-1) detection by the VLA, Walter and collaborators determined the redshift of HDF850.1 to 5.183 corresponding to a lookback time of ~12.5 Gyr. They also put first constraints on the physical properties of the host galaxy: the [CII] line luminosity was estimated to ~1.1 $10^{10}$ $L_\odot$, the FIR luminosity to ~6.5 $10^{12}$ $L_\odot$, the total dust mass in the host galaxy to ~2.8 $10^8$ $M_\odot$, and the global star-formation rate to ~850 $M_\odot$/yr. Based on the size of the [CII] emission region, the authors derived a star formation rate density of ~35 $M_\odot$/yr/kpc$^2$. The linewidth was estimated to 400 km/s (FWHM) and found narrower than in submillimeter-selected galaxies.

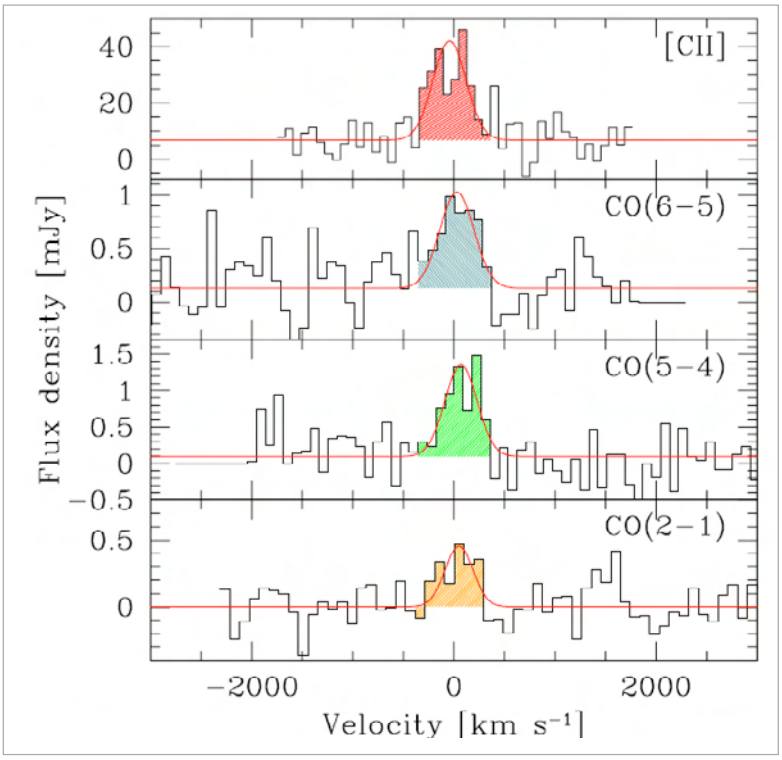


Spectra of the redshifted [CII] at 158 um and of the (6-5), (5-4) and (2-1) transitions of $^{12}$CO, with the underlying continuum. The (2-1) transition was marginally detected at the VLA. Work by Walter et al. 2012, Nature, 486, 233

Once the redshift was known, the astronomers were able to put the galaxy into context. Using additional data from published and unpublished surveys, they were able to show that the galaxy is part of a group of a dozen other galaxies, spread over six million light-years, all formed within the first billion years of cosmic history. At this redshift, only one other galaxy group like this is known so far (Riechers et al. 2010).

## EXTREME QUASAR FEEDBACK IN THE EARLY UNIVERSE

Most theoretical models invoke quasar driven outflows to quench star formation in massive galaxies, and this feedback mechanism is required to account for the population of old and passive galaxies observed in the local universe. The discovery of massive, old and passive galaxies at z~2, implies that such quasar feedback onto the host galaxy must have been at work very early on, close to the reionization epoch. Evidence for such feedback has been found only recently in quasar hosts through the discovery of massive outflows: Herschel Space Telescope spectra have revealed prominent [CII] emission associated with molecular outflows of nearby quasars but quasar-driven outflows have been uncovered also at high redshift.

In a concerted effort to advance understanding on quasar negative feedback, a team led by Roberto Maiolino (University of Cambridge) used the IRAM interferometer to observe SDSSJ1148+5251 at $z$=6.42 in the [CII] $^2P_{3/2}$–$^2P_{1/2}$ line, and discovered an exceptional outflow in the host galaxy of this remarkable quasar. The outflow velocity (~1300 km/s), luminosity (~7.3 $10^9$ $L_\odot$) and kinetic power (>1.9 $10^{45}$ erg/s) are clearly in favor of quasar radiation pressure as the main driving mechanism. Based on the interferometer data, the authors also estimated a lower limit to the total outflow rate (~3500 $M_\odot$/yr), which they found higher than the star formation rate in the quasar host (~3000 $M_\odot$/yr), and the extent of the outflow to smaller than 16 kpc.

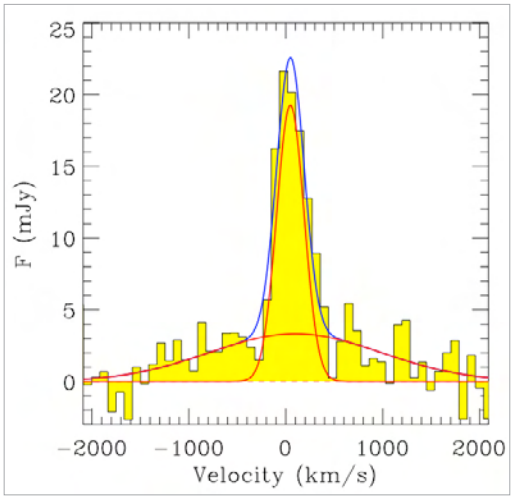


IRAM interferometer continuum subtracted spectrum of the redshifted [CII] $2P_3/2–^2P_1/2$ line towards J1148+5251.
Work by Maiolino et al. 2012, MNRAS, 425, L66

From all this, Maiolino and collaborators conclude that $SDSSJ_1148+5251$'s outflow is a cornucopia of superlatives: it is the most distant, most massive and possibly also the largest outflow ever detected.

The authors conclude that at the inferred mass-loss rate, the host galaxy's gas reservoir would be swept out in less than 6 $10^6$ yr and star formation in the galaxy host would rapidly be damped down. Their findings therefore support models ascribing the capability of cleaning entire galaxies, out to large radii, to quasar-driven outflows. According to Maiolino and collaborators, such a fast and efficient quenching mechanism, already at work at z>6, is what is required by models to explain the properties of massive, old and passive galaxies observed in the local Universe and at z~2.

# The 30-meter telescope

## OVERVIEW

Within the wide range of technical work one particular focus of 2012 was to further improve the integration of the newly installed Fast Fourier Transform Spectrometers (FTS) exploiting the large bandwidths provided by the eight-mixers receiver EMIR. The combination of FTS with EMIR is increasingly used for frequency surveys studying the complex chemistry of a variety of sources, from comets, pre-stellar cores, and Galactic star-forming regions, to the nuclei of nearby galaxies, and finally also for unbiased searches of CO and other lines to obtain accurate redshifts of distant galaxies. The study of the prototypical ultra-compact HII region Mon$R_2$ is just one example of such work, which also shows the power of combining frequency-surveys with spatial maps of the observed objects.

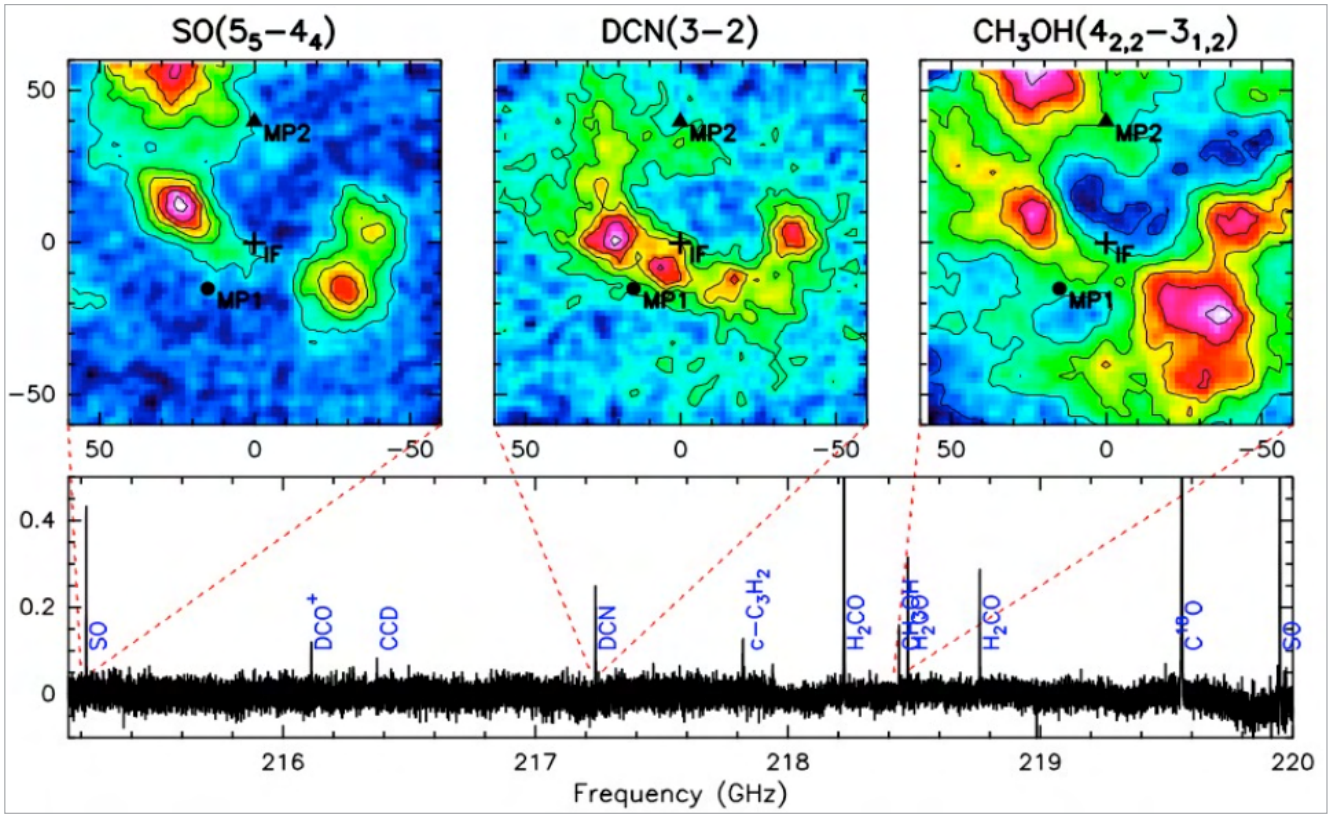


Frequency survey of the ultra-compact HII region Mon R 2 using EMIR and the FFT-Spectrometers (Trevino et al. in prep.)

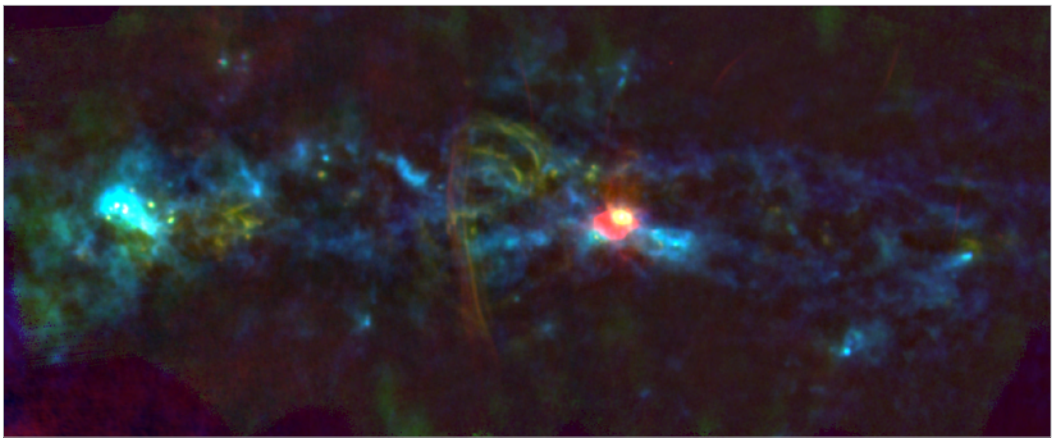

Galactic Center region observed with GISMO/30m at 2mm (green) in April 2012 with LABOCA/APEX at 850um (blue), and with the VLA at 20cm (red). (Morris, Staguhn et al. in prep.)

Another focus of work in 2012 has been to continue the integration and testing of the two new prototype continuum cameras GISMO and NIKA. In April 2012, GISMO was offered for the first time to the community during two weeks of pooled observations. One science high-light of this run has been the map of the Galactic Center region obtained during only 6 hours of observing time showing the importance of the 2mm emission tracing not only the extended molecular clouds, but also the thermal and non-thermal radio continuum filaments. Also, the NIKA camera with its two arrays of Kinetic Inductance Detectors (KID) working simultaneously at 2 and 1mm, made strong progress as discussed further below. One example of the test run in November 2012, is the successful mapping of the Sunyaev Zel'dovich (SZ) effect towards an X-ray cluster of galaxies improving on observations done about 10 years ago with the Diabolo-camera at the 30m telescope, and paving the way for SZ-studies of the hundreds of clusters found by Planck, ACT, and STP with the future, new, large field-of-view dual-band camera NIKA-2.

## ASTRONOMICAL PROJECTS

During the year 2012, a total of 208 projects were scheduled at the 30m telescope, including 4 large programs. A fraction of 26% of these projects was scheduled in the heterodyne and continuum observing pools. A total of 149 astronomers visited the telescope in 2012, 42 of which came to support the observing pools. About 20% of the scheduling units, mainly the shorter ones of typically less than 10 hours, were observed remotely. From the proposals eligible for RadioNet support, 32 were scheduled at the telescope, and 7 European astronomers were granted travel support.

The vast majority of the scheduled projects used EMIR (87%). The remainder is made up by HERA (5%) and the 2mm bolometer camera GISMO (8%). The total observing time was split by about half between Galactic and extragalactic projects.

## TIME DISTRIBUTION

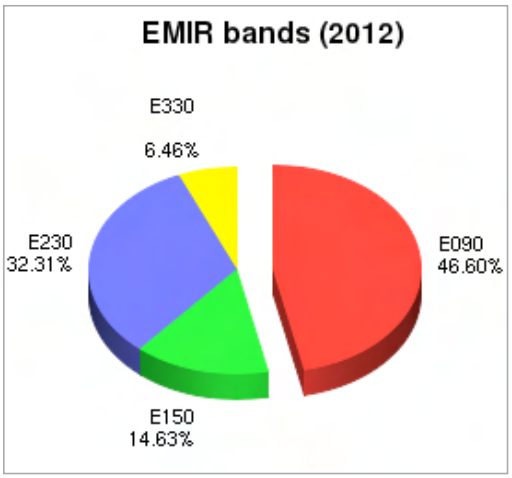


Usage statistics of all 4 EMIR bands in 2012

The IRAM 30m telescope operates 365 days per year, at 24 hours per day. The figure "Time distribution in 2012" shows that more than 70% of the total time was spent for astronomical observations, a number which has been very constant over the past few years. About 8% of the total time was used for maintenance and tests. Slightly more than one fifth of the total time were lost for astronomical observations due to adverse meteorological conditions, and less than 0.5% of the total time were lost due to technical problems, about half due to problems in the computer / network area (see the section on Computers).

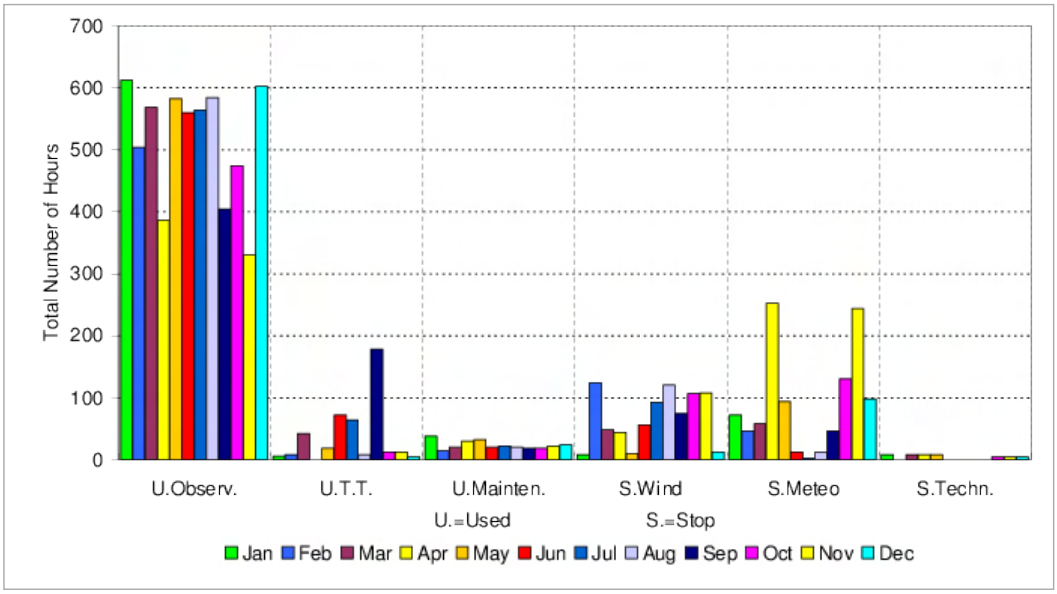


Monthly time distribution of observing time (U.Observ.), technical projects (U.T.T.), maintenance (U.Mainten.), time lost due to high wind speeds (S.Wind), or other adverse meteorological conditions (S.Meteo), or technical problems (S.Techn.).

## TELESCOPE OPERATION

In September 2012, the last two new gearboxes were installed at the 30m telescope. With this intervention the replacement of all six gearboxes, which started in 2010, has been successfully finished. The new gearboxes were built by the Germany company Desch which will also provide the gearboxes for the new antennas of NOEMA. In a series of detailed tests, we confirmed that their characteristic properties (stiffness, resonance frequencies, hysteresis, rolling friction, brake behaviour, vibrations) have reached or exceeded the specifications.

After more than 30 years of operation, several of the antenna surface panels have started to loose their top layer of paint. Images taken with an infrared camera show somewhat increased temperatures of the blackened panels when pointing near the sun. An investigation has started on how to possibly repaint the primary mirror. For this, Vertex and MT Mechatronics have provided samples of paint of different properties, put on small aluminium panels. Their mm-wavelength properties are now being characterized by the frontend group in Grenoble. In parallel, we have started to prepare again for holographic measurements of the primary surface using the 39GHz beacon of AlphaSat, a new satellite which is scheduled to be launched in June 2013 (see the section on Frontends).

In the course of 2012, several measures were taken to further improve safety at the 30m. On 20-June, we have simulated a human emergency inside the motors room of the 30m telescope. In this simulation, which was the first of its kind at the 30m, the local 061 service for medical emergencies, the service 112 for general emergencies, and the Guardia Civil worked tightly together with the IRAM staff at the telescope to "rescue" one of the staff members via helicopter to Granada. A video live-link to the 061 emergency support service has been prepared to receive medical advice if needed. On 14-June, the Granada fire brigade gave a general fire prevention training course, which we are conducting every 2 years at the observatory. On 15-October, 10 staff members participated at a specific training course of the Granada fire brigade on using the oxygen breathing equipment. We plan to repeat this course at regular intervals.

## FRONTENDS AT THE 30M TELESCOPE

After more than three years of continuous operation the EMIR receiver has proven to be the core of the frontend section at the 30m telescope. The receiver is being upgraded continuously, both by increasing its RF and IF bandwidths and by expanding the capabilities of the associated equipment. Examples of this are the modification of the IF switch box in order to allow new combinations of the 2mm band and the installation of a remotely controllable heating element for removal of quantum flux trapping on the E 230 band.

Shortly after the installation of the new 1.3 and 0.8 mm mixers, in fall 2011, a problem was detected on the E 230 band. Spurious lines were contaminating many of the frequencies on both sidebands and

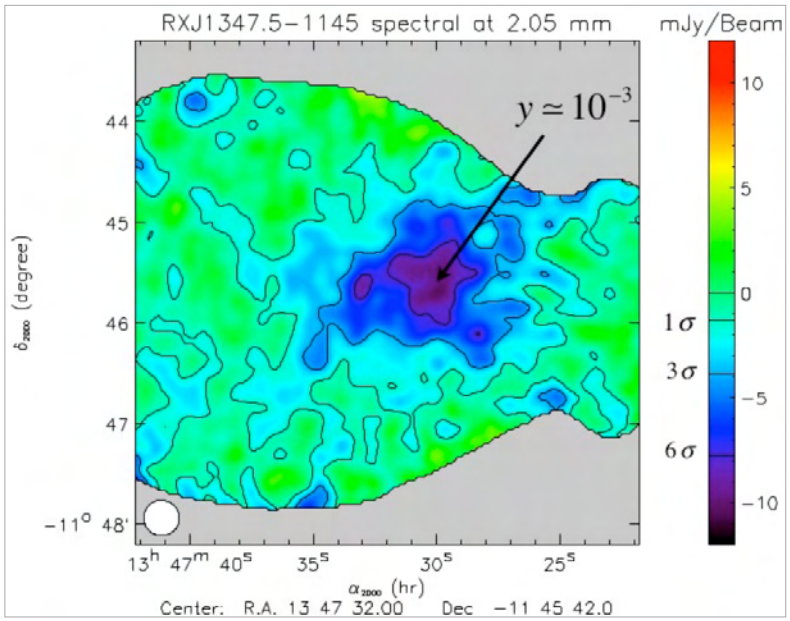


NIKA 2mm map of the Sunyev Zel'dovich decrement toward the X-ray cluster RXJ1347.5-1145 taken in November 2012. (Desert et al. in prep.)

polarizations. An intensive search for the cause, lead to the identification of internal oscillations in the mixer-cold IF amplifier assembly. The oscillations were eliminated in spring 2012 by modifying the bias and LO power level settings with none or little degradation in receiver temperatures.

The Goddard-IRAM 2mm 30m observatory (GISMO) camera has been offered to the astronomical community for the first time during two runs in April and November 2012, over a total of 4 weeks. This prototype camera uses super-conducting transition edge sensors (TES) and SQUIDs for readout. In preparation for the first open run of pooled observations, a new optics, which had been designed at IRAM/Grenoble, was installed using less mirrors together with a new extra cold baffle to improve the sensitivity by stray-light mitigation. GISMO was moved to a new place in the receiver cabin allowing observations at low elevations, and allowing a dual installation of GISMO together with NIKA. During the GISMO runs, IRAM receiver engineers learned handling of the cryostat. A long-standing leak problem on the GISMO cryostat was found and corrected by replacing the cryostat window. The improved vacuum reduced the cryogenic liquids consumption to half the previous rate. At present, GISMO needs to be recycled once per day. Median GISMO sensitivities have reached ~13mJy $\cdot s^{1/2}$, dominated by sky noise, with about 100 healthy pixels of the 8x16 array (1.8 arcmin x 3.7 arcmin). Data are now routinely processed by an automatic data pipeline using CRUSH (A. Kovàcs). The pipeline is producing preliminary results and puts them online. The relative flux stability has been better than 10% during the April run, and somewhat worse for the November run which suffered from poor weather conditions and from problems with the new taumeter. During the November run, we used the old taumeter for atmospheric calibration.

Tests with the prototype New IRAM KIDs Array (NIKA) continued during two runs in June and November 2012. NIKA is a dual-band prototype camera (P.I.: A.Benoit, Neel Institute/Grenoble) with two kinetic inductance detector (KID) arrays working at 2 and 1mm, using a 45deg dichroic mirror to split the wavebands. NIKA uses a 4K cryocooler and a closed-cycle dilution to achieve its 150mK working temperature. The data acquisition rate is 22Hz synchronously over each array. Fits files are provided that contain raw data and the central resonance frequency of each KID which is assumed to be proportional to the incoming millimeter power. The run in November 2012, showed that the best pixels reach sensitivities with 18mJy.sqrt(sec) at 2mm and 24mJy.sqrt(sec) at 1mm. The test runs allowed to progress in the development of the arrays, electronics, data readout, and data processing, while at the same time identifying a number of issues on which we will improve, in preparation of a commissioning run of NIKA in 2013, and in preparation also for the large, new continuum camera at the 30m telescope, NIKA-2.

The HEMT 3mm receiver was modified in Grenoble to include new metamorphic HEMT amplifiers designed within the AMSTAR+ project. The receiver was installed and successfully tested at the 30m telescope during the summer season. An optics with extended frequency range optics (75-116GHz) has been designed and is planned to replace the existing one in the future.

Work started on the modification to the holography receiver and the data acquisition system in preparation for measurements of the antenna surface. The acquisition part of the modification consisted in the migration from an obsolete Windows based PC operating system to a Linux based system together with subsequent software modifications. In addition, the frequency of the receivers had to be adapted to 39.4GHz.

## VLBI

In autumn 2012, the hydrogen maser for VLBI, EFOS-10, has been sent to $T_4$Science in Neuchatel/ Switzerland for repair with the aim to solve sporadic out-of-locks. Another maser, EFOS-21, has been rented by the MPIfR/Bonn and installed at the telescope to carry out observations during the 2012/13 winter period.

The European model of the Digital Base Band Converter (DBBC) VLBI backsend was installed with help from MPIfR engineers. It replaces the analog rack with Mark4 recorder. The new DBBC works with a new series of disk recorders Mark5B and Mark5C. With this backend a peak data rate of up to 8Gbits/s might be expected.

## BACKENDS AT THE 30M TELESCOPE

The 24 units of Fast Fourier Transform Spectrometers (FTS), which were installed in 2011, are working very well with no failures. Some observations using large bandwidth do however suffer from baseline "platforming" between individual FTS units. An investigation in the labs of the MPIfR in Bonn confirmed that small temperature drifts of the 8bit-ADCs cause small total-power drifts of the individual units against each other. This situation cannot be easily improved. The FTS are therefore of limited use as continuum detectors of faint sources.

To prepare for a future upgrade to 64GHz bandwidth using FTS/EMIR, and for the 3mm 5x5 dual-channel multi-beam 3mm receiver, we have studied jointly with the Grenoble backend group the option to use an optical microwave link to transport the intermediate frequencies (IF) to the backends. At present, they are transported via thick 4GHz coaxial cables through the cable spiral of the telescope into the backend room. The optical fiber was carefully evaluated through a combination of on-sky and laboratory measurements. These tests showed degraded baselines and insufficient dynamic range taking into account the large power level changes during calibration and the bandpass ripple of the receivers. We are therefore considering alternative solutions to the IF transport, as e.g. thin 3/8" coaxial cables.

The design of a barycentric reference progressed significantly in a joint effort by the backend groups in Granada and Grenoble. The goal is to eliminate the need for resampling of spectra taken with large bandwidths and high spectral resolutions. This software solution currently degrades the instrumental resolution when simultaneously observing with the same receiver widely separated lines (up to 24GHz with EMIR) or when observations taken at widely different dates are combined. It is planned to also use the barycentric reference in the future for NOEMA.

## COMPUTERS & SOFTWARE

The prototype continuum arrays GISMO and NIKA have been better integrated into the telescope control system NCS, which now offers functions which are specific for these instruments. The limits for several observing modes were reviewed and unified, in particular for the on-the-fly drift speed in LISSAJOUS, OTFMAP and POINTING. For NIKA, we introduced a special "tune" subscan type as an experimental feature. This allows, for example, antenna TIPs ("skydips") with an internal adjustment of NIKA at each elevation step.

In close collaboration with the GILDAS group in Grenoble, we have started work on a new calibration software package, MRTCAL, which will eventually replace the current software MIRA. And to support data processing of NIKA data, we have developed a new version of the raw data format IMBfits.

The TAPAS header database has been up and running since October 2009. Observation header data are continuously being transferred to this database without delay. After a proprietary period of 1 year a subset of these header data is regularly being transferred to the Centre des Données astronomiques de Strasbourg (CDS). In 2012, new functionality has been added to TAPAS. Observers can now use it as a logbook and enter comments to individual scans. Monitoring of the system performance has become a lot easier via new web forms and plots of e.g. the telescope pointing corrections, the receiver temperatures, and other calibration parameters like the derived sky opacities.

In addition to TAPAS, we are maintaining an internal project archive of all observational data. It contains the results of the online data processing, i.e. the 30m CLASS files of EMIR and HERA, and the FITS data files of GISMO and NIKA. The archive currently contains

all data since 2009, while older data are being added. During a limited time of one year, observers can access their project data online. This allows, for example, to quickly recalibrate data and retrieve project files for rescheduled projects.

Several measures have been taken to improve the computer network at IRAM/Granada. All network switches at the observatory have been replaced. The receivers and backends are now connected with optical cables to the central switch. In case of problems with an optical link, the switches automatically use twisted pair cables instead. A separate network switch has been installed in the receiver room for guest instruments like e.g. GISMO. This separates the instrument-specific network traffic from time-critical network traffic related to the control of the antenna. A 100Mbit/s radio-link is used to connect the observatory and the offices in Granada. We now offer WLAN in these offices and in all visitor rooms.

# Plateau de Bure interferometer

A.Rambaud / IRAM.

As in previous years, the 2012 operation of the Plateau de Bure Interferometer has been smooth on the whole. The instruments provided images of stunning quality and resolution suitable for the investigation of a wide range of cutting edge science.

The interferometer performed according to expectations with almost no downtime due to hardware upgrades, maintenance operations and work in preparation of NOEMA. The receivers and the antennas all worked well throughout the year. Scientific observations were performed in periods of excellent phase stability and atmospheric transparency in winter and autumn, but faced somewhat less favorable conditions in spring and summer, as in 2011. The recent move to the A configuration was deferred to January 09, 2013, and was so accomplished about two weeks earlier than in the winter 2011 / 2012 and about one week later than in the winter 2010 /2011. As in previous years, the scheduling of the A configuration was readjusted shortly after the beginning of the winter scheduling period to optimize the observing of A-rated projects with respect to Sun avoidance limitations and weather constraints.

As in previous years, the percentage of contiguous array-correlation-time scheduled for observing programs was on average 50% of the total time. Additional 20% have to be accounted for receiver tuning, related checks and other unavoidable observational overheads, array configuration changes, interferometer upgrades, surface adjustments and antenna maintenance; the remaining 30% were lost because of precipitation, wind and inadequate atmospheric phase stability.

The Program Committee met twice in 2012, around four weeks after the proposal submission deadlines, reviewed 203 proposals and recommended the approval of 128 proposals corresponding to 327 individual projects. In total, more than 230 different projects were scheduled at the Observatory in 2012, including 4 Large Programs, 7 proposals for Director's Discretionary time and the backlog of projects from

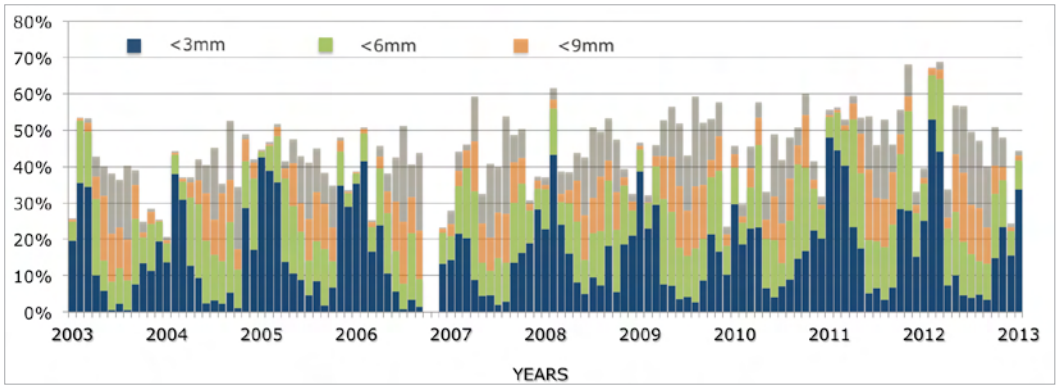


Plateau de Bure observing time and atmospheric water vapor statistics over the last ten years. The overall correlation time accounts for 49% of the total time in the year 2012. Band 3 (200 – 268 GHz) and band 4 (275 – 373 GHz) programs and observations in the most extended (AB) configurations are for the most part carried out in the winter months. The smooth increase in the observing efficiency over the years 2003-2012 results from a combination of weather statistics, technical improvements and reduced calibration overheads. Science operations were suspended in the autumn of 2006 for the installation of new receivers.

2011. The weight on extragalactic high-redshift research was considerable; the requested observing time was about 3-4 times higher than the time requested for each, nearby galaxies and young stellar objects. Also, a fairly large amount of observing time was invested in D-configuration between spring and fall in the detection of line-emission from molecular (e.g. carbon-monoxide, water) and atomic transitions (e.g. carbon, ionized nitrogen) in galaxies at high redshift. Annex I details all the proposals to which time was granted in the course of the year, and the list of projects testifies to the high scientific return of the Plateau de Bure Interferometer.

## VLBI NEWS

Both Plateau de Bure and Pico Veleta participated in the Global VLBI session of May 2012, which observed four projects. Due to meteorological limitations, Pico Veleta observed 53.2% and Plateau de Bure 48.1% of all scheduled observations (Bure did 52.3% of the observations without sun avoidance constraints). During a bad weather period, the Pico Veleta hydrogen maser EFOS-10 suffered a temporary out-of-lock. No observing time was lost due to this, but in summer the maser was sent to T4Science, Neuchâtel for a revision and subsequent monitoring. The autumn GMVA session was cancelled in 2012, so the absence of the maser was tolerable. However, a submitted and accepted VLBI 1mm proposal for Spring 2013 would have suffered from the absence of a high stability frequency standard on Pico Veleta. MPIfR Bonn kindly agreed to finance a rental maser until the return of EFOS-10.

## ONGOING WORK AND ACTIVITIES

A number of investigations and developments took place in 2012 that deserve to be mentioned:

In the frame of the NOEMA project, we investigated the possibility to have a common LO reference signal for band 2 (129 GHz to 174 GHz) and band 3 (200 GHz to 268 GHz) receivers. For this purpose, a waveguide switching system was installed on antenna 1, in between the Gunn oscillator module and the band2/band3 frequency multipliers, and its performance evaluated over a period of several months. The results validated the use of the waveguide switch and led to the decision to equip all NOEMA antennas with it.

Inspection of the subreflector of a Plateau de Bure antenna during regular maintenance operations.

To reduce the ripple levels in the IF outputs of the band1, band2 and band3 receivers of all six antennas, an experimental study was carried out in September on antenna 1 that consisted in the replacement of the six entrance windows of the receiver cryostat i.e. all four bands and the two 15K stages, and the associated infrared filters. It was found that changes made to the receiver optics had not lived up to expectations, and that further work is necessary to fully meet this objective.

To prepare for the arrival of the NOEMA antennas, it was decided to renovate the control servo drive system of one antenna, monitor its performance over a period of several months, and validate the usability of the prototype system. The renovation work was carried out at the end of the summer maintenance period on antenna 5 and consisted in the replacement of the azimuth and elevation motors, in the refurbishment of the closed-loop feedback systems, and in the modernization of the control software. Due to technical difficulties and scheduling issues it has not been possible to compare and validate the performance of the new system before the end of 2012. The final evaluation is expected to take place in the spring of 2013.

As in previous years, the surface quality of all of the antennas was verified by means of holographic measurements at the end of the maintenance period. Surface panels were readjusted when deemed necessary. The final overall surface precision achieved by holography was 35µm (weighted by

illumination) for antenna 1 and better than 45µm for all other antennas.

In the frame of the observatory's antenna surface improvement program, a significant effort was made in the maintenance period 2011 on replacing the central struts of the ring 2 to ring 6 panels of antenna 6. These panels are known to stress and deform in conditions of a significant thermal gradient between the central supporting strut (5th point) and the set of corners struts. To eliminate this misbehavior and contain surface efficiency losses within allowable tolerances, all central struts were replaced with a set of thermal gradient compensating struts. After more than one year of operation with the new struts and regular monitoring of the panels surface precision by holographic techniques, we feel confident that we have succeeded in correcting the problem.

To address the maintenance issue associated with the arrival of new antennas and related to displacing individual antennas on the east-west and north-south tracks from a remote position to inside the hangar, it was decided to add two sidetracks, one on the east (E 12) and one on the west (W 05) track. The construction of these two sidetracks, which will reduce the number antenna displacements and the associated expenditure of time and effort, has started in the summer of 2012 and is scheduled to achieve completion in the summer of 2013. During summer the STM Pugnat company completed contracted work, which started in 2010 and continued in 2011, to repair and resurface the pavement with concrete in between the rails along the east-west and north south tracks.

In the spring of 2014 Plateau de Bure's Science Operations Group (SOG) will be in the forefront of an institute-wide effort to validate the characteristics of the seventh antenna. To prepare for this major effort, support future antenna maintenance operations and provide an additional powerful platform to test software, a new mode of operation was developed that allows the control of two independent antenna sub-arrays. While one sub-array would operate in science mode to address and meet the needs of the astronomical community, the second sub-array would be set up to test and validate novel and upgraded equipment and software. First observations with the current six-element array in the so-called double-array mode were successful but to fully assess and implement the new operating modes a continuation of this development effort is being planned for the spring of 2013.

Plateau de Bure's phase switching (180°) and sideband separating (90°) scheme is based on a 32-element set of Walsh functions. The same set of functions will be available for the NOEMA array. To prepare for the arrival of the new antennas while building on the experience with the six-element array, a study was conducted that investigates the optimum choice of Walsh code sequences for NOEMA's 12-antenna array. An optimization was performed that yields the highest phase-switching frequency and simultaneously produces the smallest summed squares of crosstalk. We plan to implement the new sets of Walsh functions for the arrival of the seventh antenna.

Sidetrack construction and pavement refurbishment work on the western track, as of June 05, 2012.

The radiometers on the Plateau de Bure have operated without major problems. Minor disturbances like two 15V power supply failures and a defective load arm were quickly resolved. In the context of the NOEMA project, plans for an upgraded multi-channel radiometer are under development.

With the continuous and rapid developments in wireless services and satellite communication, more and more sources of radio frequency interference (RFI) are found to operate in the millimeter range. To spot and locate new sources of RFI in the frequency range covered by the 22 GHz radiometers and to be able to react accordingly, we have set up a prototype interference monitoring system. The system uses a wide-band spectrum analyzer connected to the IF output of the radiometer to record spurious changes in the power levels of adjacent spectral channels. The prototype, which operates across the 19 to 26 GHz RF-band of the radiometers, was installed on antenna 5. The system is presently undergoing testing.

The pointing accuracy of the Plateau de Bure antenna is limited by thermal gradients in the antenna structure and by changes in the antenna

inclination. The latter appear to be linked to positional instabilities of the station on which the antenna is clamped. To correct for these changes, the inclination of every antenna is continuously measured with a high-precision (1") dual-axis tiltmeter placed in the antenna yoke at the high end of the azimuth axis. With the disappearance of Leica's NIVEL-20 tilt-meters from the market and the arrival of new antennas, we have started a monitoring program to evaluate the performance of a competitive tiltmeter manufactured by Jewell Instruments. According to the results of the investigations, the new tiltmeter are fully adapted to needs and will equip the NOEMA antennas.

During the regular operations of the cold-heads maintenance 2011, the vertical polarization of the band 4 mixer (275 to 373 GHz) on the receiving system of antenna 4 had gone open-circuit. This fault was cleared during the antenna maintenance period of 2012. In parallel, it was necessary to replace the band 2 (129 GHz to 174 GHz) LO frequency doubler-modules in two antennas, as they began to show signs of fatigue.

## USER SUPPORT

The Plateau de Bure Science Operations Group (SOG) is staffed with astronomers that regularly act as astronomers on duty to optimise the scientific return of the instrument, directly on the site or remotely from Grenoble, provide technical support and expertise on the Plateau de Bure interferometer to investigators and visiting astronomers for questions related to the calibration, pipeline-processing and archiving of Plateau de Bure data, interact with the scientific software development group for developments related to the long-term future of the interferometer, perform the technical reviewing of the proposals, and collaborate with technical groups to ensure that operational requirements are being met. Six astronomers were appointed to the group at the beginning of 2012.

As in previous years, work was continued in the context of extending and improving the Plateau de Bure data calibration pipeline. In 2012, efforts were directed to improve the pipeline's robustness, refine the antenna-based RF passband calibration, ensure consistent phase calibrations in both the horizontal and vertical polarization, and release an automatic assessment routine for projects aiming at detecting a weak emission line and continuum. In parallel, work was made to improve the accuracy of the absolute flux calibration scheme. An effort was directed to narrowing down antenna gain factors: visibilities of the radio source MWC 349 are now fitted to a frequency- and size-dependent, modelled visibility function. Another effort was started on modelling the mm-SED of the optically thick core surrounding LkHa101. The aim is to calibrate it better than a few percent and thereby establish an alternative high-precision flux calibration reference to MWC 349.

In 2012 assistance was given to 34 investigators from Europe and overseas visiting IRAM Grenoble for a total of 139 days to reduce data from the Plateau de Bure Interferometer. Advice and support was also provided to a number of experienced astronomers from Caltech/Pasadena, CSPF/Copenhagen, ESO/Garching, MPIA/Heidelberg, LERMA/Paris and EPFL Geneva for a total of 51 days to reduce and analyze Plateau de Bure Interferometer data remotely from their home institutes. Assistance was provided to 58 projects in total. IRAM astronomers collaborated on 69 projects in which they were directly involved.

As in previous years, in a continuing and successful effort with the Centre de Données astronomiques de Strasbourg (CDS), data headers of observations carried out with the Plateau de Bure Interferometer are conjointly archived at the CDS, and are available for viewing via the CDS search tools. In 2012, the archive contained coordinates, on-source integration time, frequencies, observing modes, array configurations, project identification codes, etc. for observations carried out in the period from January 1990 to September 2011. The archive is updated at the CDS every 6 months (May and October) and with a delay of 12 months from the end of a scheduling semester in which a project is observed in order to keep some pieces of information confidential until that time.

SOG members holding their weekly meeting with a video call to the Observatory

## RADIONET USERS

As in 2011, travel funds have been made available to RadioNet eligible astronomers from non-IRAM partner countries for expenses incurred during their stay at IRAM for reducing data from the Plateau de Bure Interferometer. These funds, which were initially made available by the European Commission for the institutes participating in the FP 6 TransNational Access (TNA) initiative, are today granted by the FP 7 program. Because of budget restrictions in the RadioNet program, only expenses related to accommodation or travel were covered in 2012. For the same year, the Program Committee received 42 eligible proposals (25% more than in 2011) and recommended 22 proposals (5 A-rated, 17 B-rated) for observations with the Plateau de Bure Interferometer. Taking into account proposals accepted in 2011 but continued in 2012, time was allocated to 17 eligible proposals corresponding to a total of 25 projects and 325 hours of observing time. Since the beginning of RadioNet, access time was allocated to 112 eligible proposals (12 in 2004, 11 in 2005, 11 in 2006, 13 in 2007, 14 in 2008, 6 in 2009, 14 in 2010 and 14 in 2011) for observations with the Plateau de Bure Interferometer, corresponding to a total of ~2500 hours (272 in 2004, 239 in 2005, 272 in 2006, 326 hours in 2007, 334 in 2008, 140 in 2009, 266 in 2010 and 327 in 2011) of observing time. User responses to questionnaires of the European Commission and to the RadioNet management in Bonn show that IRAM continues to maintain an excellent reputation concerning the assistance and service given by scientists and support staff to visiting astronomers.

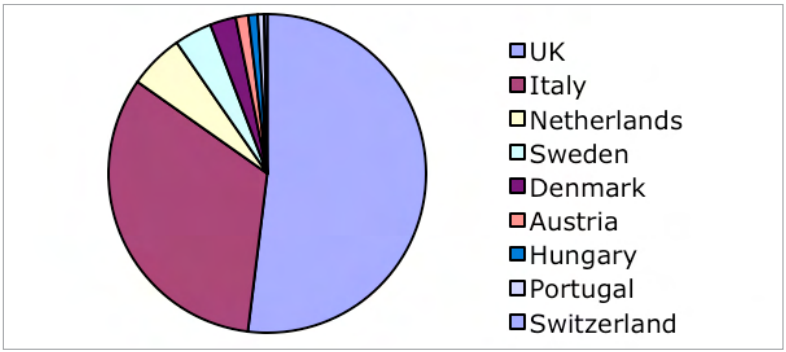


RadioNet observing time was allocated to eligible principal investigators from United Kingdom (percentage of total time is 52%), Italy (32.8%), the Netherlands (5.6%), Sweden (3.8%), Denmark (2.6%), Austria (1.3%), Hungary (1.0%), Portugal (0.6%), and Switzerland (0.3%) with a balanced distribution between PhD students and post-doctoral researchers (51%) and senior scientists (49%).

# Grenoble Headquarters

## FRONTEND GROUP

The IRAM Front End Group had a busy year in 2012 with maintenance, upgrade and development activities for both NOEMA and the 30 m telescope, as well as for the upgrade of the laboratory instrumentation and the development and tests of prototype receiver and components for the European AMSTAR+/AETHER collaboration and the ALMA Band 2&3 projects. The year 2012 also marked the end of the ALMA Band 7 cartridge production, totalling 73 cold cartridge assemblies delivered from IRAM to the ALMA project.

## DEVELOPMENT OF NOEMA FRONTEND

The NOEMA Front-Ends specification requires a re-design of the current PdBI Front-Ends, which have been in continuous operation since their installation in 2006. The design of the NOEMA Front-Ends has started in collaboration with the IRAM Mechanical Group. Such Front-Ends will be state-of-the-art dual-polarization quadri-band heterodyne receivers based on SIS superconducting mixers that cover the 3 mm (Band 1), 2 mm (Band 2), 1.3 mm (Band 3) and 0.8 mm (Band 4) bands using a sideband separating (2SB) mixer technology with two 7.744 GHz wide (3.872-11.616 GHz) IF bands per polarization. Therefore, the Single Side Band (SSB) backshort-tuned SIS mixers delivering 4 GHz IF bandwidth per polarization channel, which is currently adopted for PdBI Bands 1-2-3, will be upgraded to the 2SB technology delivering two 7.744 GHz wide IF band per polarization channel. Also, the four RF bands of the NOEMA receivers will be slightly larger than the ones of the current receiver generation. The main NOEMA Front End specifications are given in the following table.

The two main goals of the Front-End Group during the coming years are to build four new receivers for the four new NOEMA antennas (Phase A of the project) and to upgrade the six PdBI receivers to the NOEMA specification.

A view of the inner part of the NOEMA Front-End, with two out of the four bands, is shown in the following Figure.

Current PdBI receiver specification and NOEMA 2SB receiver specification.

| | Current PdBI receivers | | | | 2SB NOEMA receivers | | |
|---|---|---|---|---|---|---|---|
| Band | RF [GHz] | Mixer scheme | IF [GHz] | Notes | RF [GHz] | IF [GHz] | Notes |
| 1 | 83-116 | SSB | 4-8 | Backshort tuning | 78-116 | 3.872-11.616 | RF band extension down to 72 GHz under study |
| 2 | 129-174 | SSB | 4-8 | Backshort tuning | 127-179 | 3.872-11.616 | New mixer with integrated IF superconducting hybrid |
| 3 | 200-268 | SSB | 4-8 | Backshort tuning | 200-276 | 3.872-11.616 | EMIR E2 type 2SB mixer with permanent magnets |
| 4 | 277-371 | 2SB | 4-8 | One IF used | 275-373 | 3.872-11.616 | ALMA Band 7 mixer chip and integrated IF hybrid |

## CRYOGENIC OPTICS MODULES

The first prototype of NOEMA cryogenic optics module was designed and fabricated for Band 3 (200-276 GHz). It comprises two ellipsoidal mirrors thermalized at 15 K, as well as a polarization splitting wire grid and two single-polarization broad-band feed-horns which will be maintained at 4 K. The various parts are supported by a 6060 Aluminium frame and use G 11 fiberglass tabs to thermally split the 15 K optics and the 4 K parts. Unlike the current generation PdBI cryogenic optics modules, the new design allows to keep the module assembled after its room temperature tests on the antenna range, before its final integration into the receiver cryostat. The design of the different parts of the module was also simplified to ensure a better alignment on the sky between the two receiver polarizations. We will adopt this same design philosophy for the cryogenic optics modules of NOEMA Band 1 and 2.

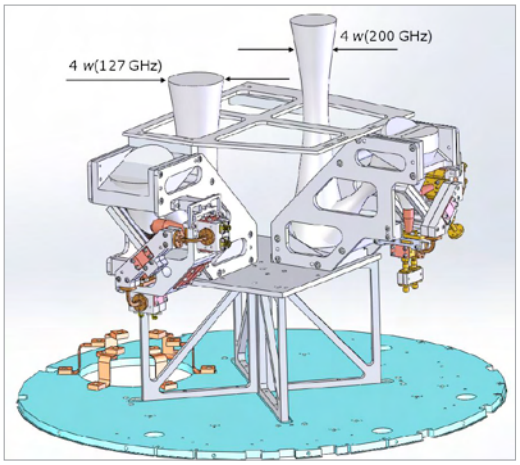


Inner view of the NOEMA cryostat showing the 15 K plate on which the four RF cryogenic modules will be mounted (only the modules for Band 2 and Band 3 are shown). Two of the RF beams (4 w at the lowest frequency edge of the band) are also shown.

## 2SB SIS MIXERS

After the successful experimental results obtained with the EMIR E2 2SB mixer in 2011, and after that mixer proved to work reliably in the 30 m antenna, we decided to adopt the same type of mixer for NOEMA Band 3; the mixer required only slight modifications to the mechanical blocks.

After a decision was made to specify the NOEMA IF band across 3.872-11.616 GHz, some key components of the IF chain required some slight modification with respect to those operating over the more standard 4-12 GHz band (used for example for the ALMA Band 9&10 IFs). In particular, new prototypes of cryogenic isolators and IF cryogenic

# PLATEAU DE BURE INTERFEROMETER MAINTENANCE AND NEW TEST EQUIPMENT

## MAINTENANCE

The maintenance work concerned the Sumitomo cryogenerators, which took place during the summer period. Starting from 2012, the maintenance of the cryogenerators is regularly made, approximately every 15000 hours of operation. The on-site intervention uses the "hot-swap" method, which consists in changing the active parts of the cold heads without removing the cryostat from the receiver cabin. The three cold-heads installed on Ants. #1, #3, and #6 were hot-swapped, then sent to Sumitomo-Germany for servicing. On Ant. #4, the Band 4 (275-373 GHz) receiver module that had a SIS mixer chip in short circuit (in Pol H) since September 2011 was swapped with a spare one. This spare module had been previously characterized in the laboratory. A maintenance work was made on the 22 GHz Water Vapour Radiometers on Ant. #2 (room temperature load measurement was repaired) and on Ant. #6 (the radiometer was serviced after a water leakage into the cabin due to weathering). A number of Local Oscillator (LO) systems were repaired following failure of Gunn oscillators, attenuators and frequency doublers. The HDPE vacuum windows and IR Teflon filters of the four PdBI receiver bands on Ant. #1 were swapped with new broader band ones having corrugations similar to those mounted in the Pico Veleta EMIR receiver. The goal is to understand and try to improve the problem of ripple in the measured noise temperature across the 4-8 GHz IF frequency.

## NEW TEST EQUIPMENT AT THE SITE

A waveguide switch that drives a LO signal to either the Band 2 or the Band 3 SIS receiver modules was tested in the laboratory and then installed on Ant. #1 in October 2012. The role of this WR12 waveguide switch is to deliver a monochromatic LO signal across the 69.3-88.1 GHz frequency band generated by a common Gunn oscillator to either the frequency doubler of the Band 2 receiver or to the frequency tripler of the Band 3 receiver. Site tests with the PdBI interferometer were started to verify if such switch, situated outside the PLL loop which locks the fundamental oscillator frequency from the Gunn module, worked well and could be adopted for NOEMA. This would allow replacement of the two 69.3-88.1 GHz Gunn LO systems that independently drive the Band 2 and Band 3 receiver modules by a single Gunn LO system cascaded with the switched waveguide. A radio frequency interference (RFI) monitoring system for the 18-26.5 GHz band was installed on Ant. #5. The system is based on a spectrum analyser (Textronix 492BP) connected to the 2-10 GHz IF monitor output of the water vapour radiometer and was set to detect spurious signals across 18-26.5 GHz over –110 dBm at the radiometer input using a 3 MHz bandwidth. A lower frequency low-cost rack mounted spectrum analyzers (from Aaronia) was also tested in the laboratory. It was found to be suitable for the direct detection of RFI disturbances of up to 9.4 GHz and across most of the IF frequency band from the 18-26.5 WVR through its IF monitor output. This low-cost analyser should replace the most expensive one.

low noise amplifiers covering 3.8-11.7 GHz were developed by external institutes and validated to work well for the NOEMA Front-End. Laboratory test results demonstrated that the NOEMA Band 3 mixers, which delivers two 3.872-11.616 GHz IF bands, perform as well as the EMIR E2 mixer, which delivers two similar IF bands across 4-12 GHz.

We also focused our developments on the mixer for NOEMA Band 2. An IF coupler chip covering the 4-12 GHz frequency range (also suitable for 3.8-11.7 GHz) was developed. The design is based on three coupling sections using superconducting striplines. The simulated performances of the chip are shown below.

The great advantage of this IF chip compared to commercially available couplers is its planar design, which makes it suitable for integration with the mixer chip into the mixer block, so resulting in one very small 2SB mixer unit. This is especially useful for multipixel receivers.

The new NOEMA Band 2 SIS mixer makes already use of this new IF coupler chip (see following figure).

The NOEMA Band 1 SIS mixer, still to be developed, will also integrate this new IF coupler. Such mixer will employ SIS chips identical to those installed on the EMIR E 0 band.

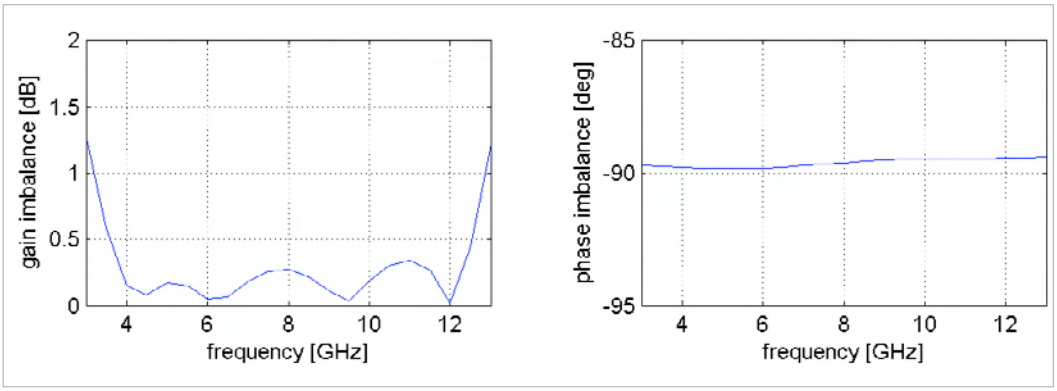


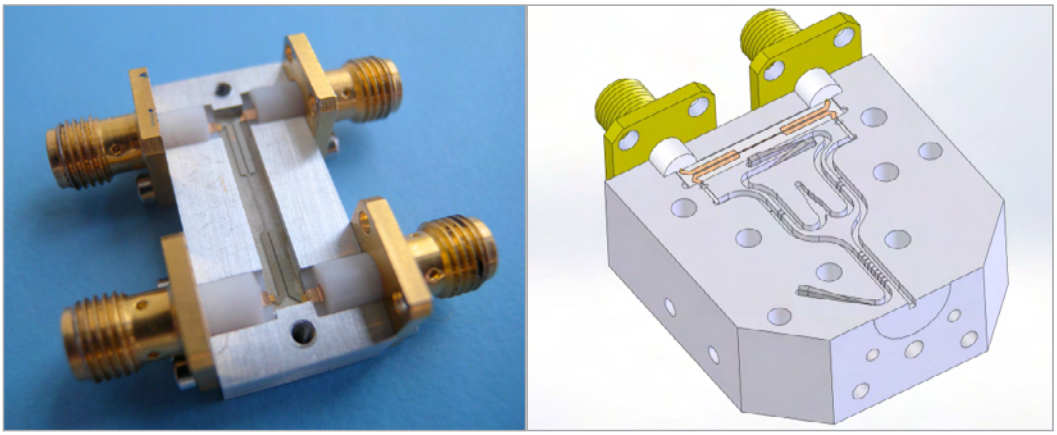

Left: Photo of the IF superconducting hybrid installed in a connectorized block. Right: One half of the new Band 2 2SB mixer with integrated IF superconducting coupler.

## BIAS ELECTRONICS MODULES AND CONTROL BOARDS

New bias electronics modules and control boards based on EtherCAT are under development. These include: 1) a module (see Figure below) capable of biasing the 16 SIS junctions of the mixers of all NOEMA bands; 2) a module for biasing the cryogenic low noise amplifiers; 3) a control board for the warm IF chain and the IF laser link.

A new temperature reading module is also under development.

The design of the fully electronically tuneable 85.744-108.256 GHz NOEMA Band 1 Local Oscillator (LO) prototype was completed. The LO rack shown in the Figure below includes a 14.29-18.04 GHz YIG oscillator cascaded by an Active Multiplier Chain (AMC) predicted to deliver a minimum output power of 6 dBm across the 85.744-108.256 GHz band at the Power Amplifier (PA) input. The PA is followed by a 3 dB recombination coupler which delivers between 12 and 17 dBm output power. A fraction of the AMC output signal is sent to an harmonic mixer, which is pumped by a 13.2-16.4 GHz reference signal,

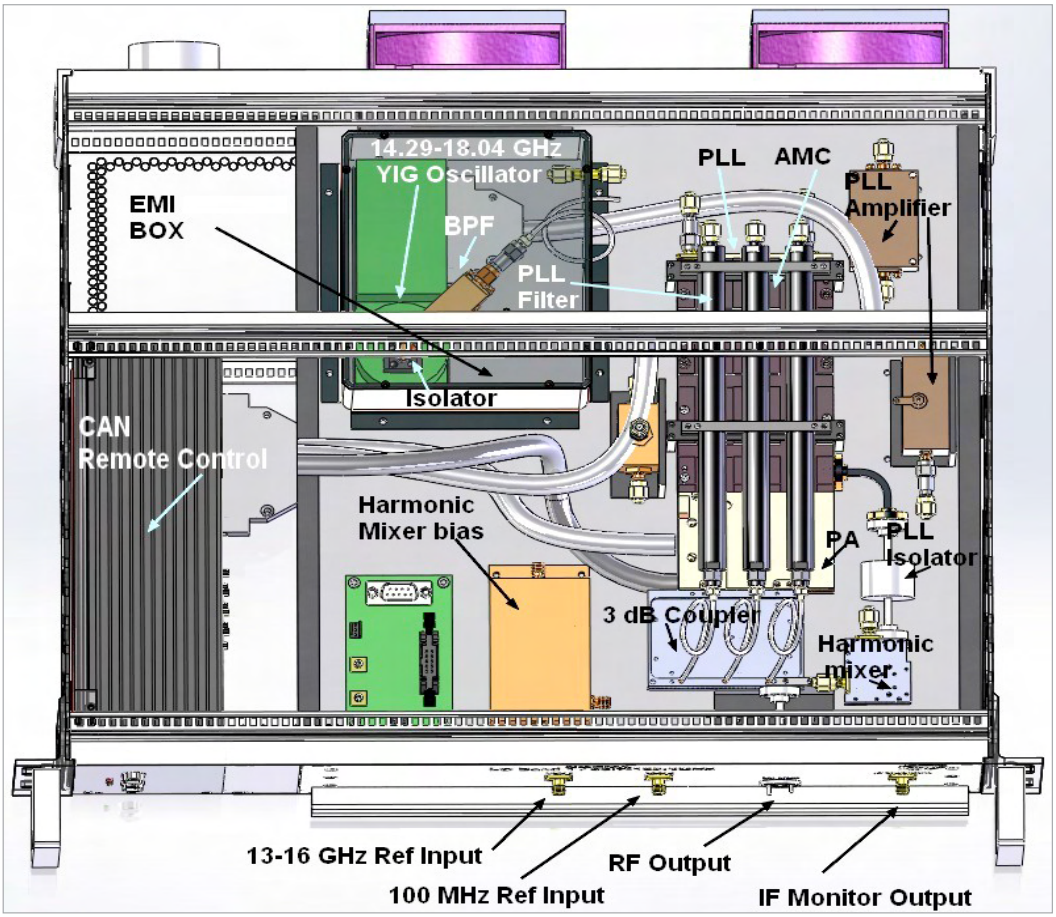


Inner view of the NOEMA Band 1 (85.744-108.256 GHz) LO rack.

and outputs a 100 MHz IF. The 100 MHz IF beat is compared with a 100 MHz second reference in the PLL to lock the YIG. The bias cards and the PLL are remotely controlled using CAN module interfaces.

The details of the AMC, the PA and the 3 dB coupler are shown in the Figure below. The PA and the 3 dB coupler are presented in reverse position (and slightly shifted one to another) compared to the AMC to show the details of the MMICs implantation. In the AMC, the 14.29-18.04 GHz input signal coming from the YIG oscillator goes through a 28.58-36.08 GHz frequency doubler, an amplifier, a band pass filter, and a frequency tripler. At the tripler output, the 85.744-108.256 GHz signal is amplified and filtered by a pass-band filter and pass through a WR10 waveguide using a waveguide to microstrip line transition. A fraction of the AMC output signal pass through a -10 dB coupler and is sent to the PLL output which is connected outside with the PLL harmonic mixer. The AMC output signal is split by a 3dB hybrid coupler and amplified in the PA module. The two PA outputs are then recombined by a second 3 dB hybrid coupler. This hybrid arrangement optimizes the saturated power level and the output return loss.

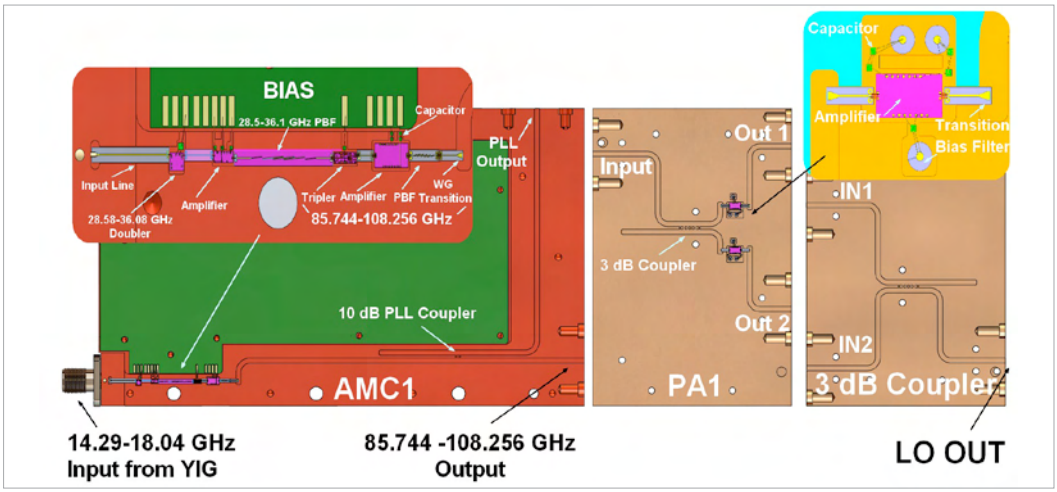


Details of the Active Multiplier Chain (AMC1), of the Power Amplifier (PA 1) and of the 3 dB coupler which are parts of the NOEMA 85.744-108.256 GHz Local Oscillator system.

## UPGRADES AND NEW DEVELOPMENTS FOR PICO VELETA

No maintenance was needed in 2012, neither for the EMIR quadri-band receiver nor for the HERA 1 mm multibeam receiver.

The performance of the 1.3 mm band E 2 2SB SIS mixer installed last year on EMIR was monitored throughout 2012. The miniature permanent magnets used in that mixer proved to reliably suppress the Josephson currents through the superconducting SIS junctions also in the antenna electromagnetic environment. Following this successful result, it was decided to adopt the same type of mixer also for NOEMA Band 3.

### UPGRADE OF HOLOGRAPHY RECEIVER

The 39.592 GHz dual channel holography receiver built in 1996 for the measurement of the 30 meter Pico-Veleta telescope surface was upgraded. That receiver employed the Right Hand Circular (RHC) polarized source signal from the now obsolete ITALSAT satellite. The receiver was upgraded to work with the 45 degrees linear polarized signal at 39.402 GHz emitted by the ALPHASAT TDP 5 satellite module. The satellite is scheduled to be launched in July 2013 and to start broadcasting in Autumn 2013. The local oscillators which match the new beacon frequency and the 45 degrees R&L waveguide twists were provided to IRAM-Granada for the installation in the receiver and in the mountain transmitter.

### 3 MM BAND MULTIBEAM RECEIVER FOR THE 30M TELESCOPE

Good progress was made on the design of a 5x5 pixels dual-polarization 2SB SIS receiver for the 3 mm band. The receiver baseline design utilizes only one of the two output sidebands per polarization channel and delivers a total of 2 pols x 25 pixels = 50 IF channels, each covering 4-8 GHz instantaneous band. The receiver design allows observation at different sky frequencies on the two polarization channels thanks to the use of two independent local oscillators that can drive the SIS mixers to different frequencies.

### 5-PIXEL DUAL POLARIZATION LINEAR-ARRAY MODULE

One important milestone for this project is the development of a 5-pixel dual polarization linear array prototype module, which will be replicated for the construction of the full 5 x 5 pixels receiver RF module. The design of the 5-pixel linear array module is shown in the Figure.

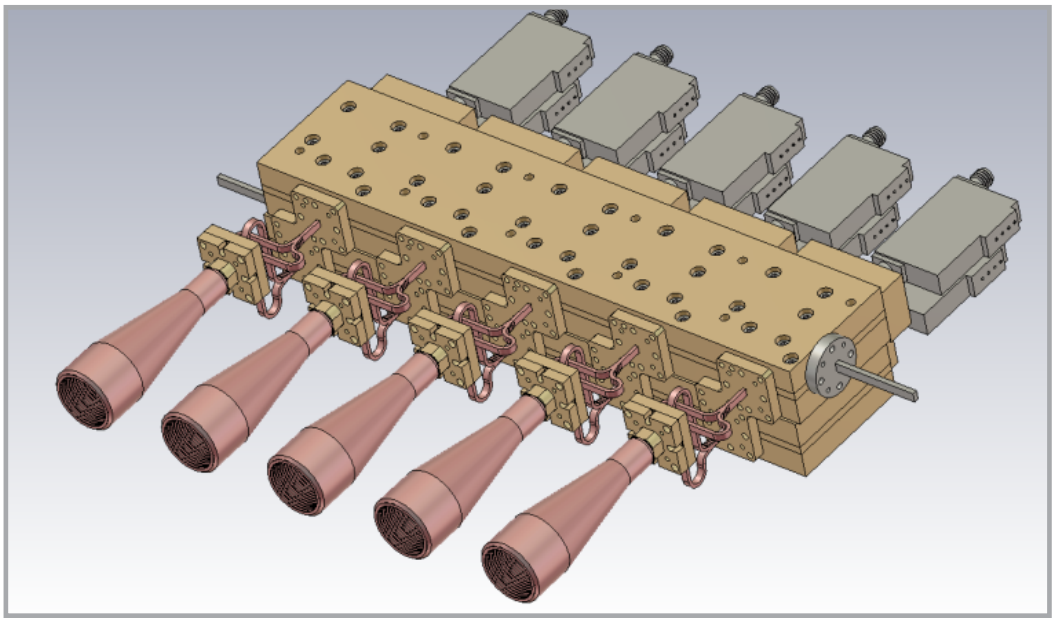

Mechanical drawing of the 5-pixel dual polarization linear array prototype module including the feed-horns, the OMTs, the LO coupler and RF hybrids and the low noise amplifiers.

## WIDEBAND ORTHOMODE TRANSDUCER

A waveguide Ortho Mode Transducer (OMT) was designed to separate two incoming linear polarization signals across a very broadband. The OMT development is common to the 3 mm multi-beam receiver and to the ESO supported ALMA Band 2&3 study in which the IRAM Front-End Group is involved. This OMT, based on a waveguide turnstile junction, was optimized to cover 67-116 GHz, i.e. the ALMA Band 2 (67-90 GHz) and Band 3 (84-116 GHz) combined. This is a challenging project because of the large relative operation bandwidth of the component, which is close to ~54%. Six of these OMTs are being manufactured via electroforming process of Aluminum mandrels (see Figure below, left panel). This design stands on the development of a previous version of such OMT prototype, designed to cover the slightly narrower 70-116 GHz band, which was fabricated and tested. The electroformed OMT unit and its performance measured with the IRAM millimeter vector network analyzer are shown respectively, on the Figures of the central and right panels. That first OMT version performs well and has input reflection of below –17 dB, cross-polarization level of below –35 dB, and insertion losses of order –0.25 dB at room temperature. We expect the newer design to have even lower input reflection and to work down to 67 GHz.

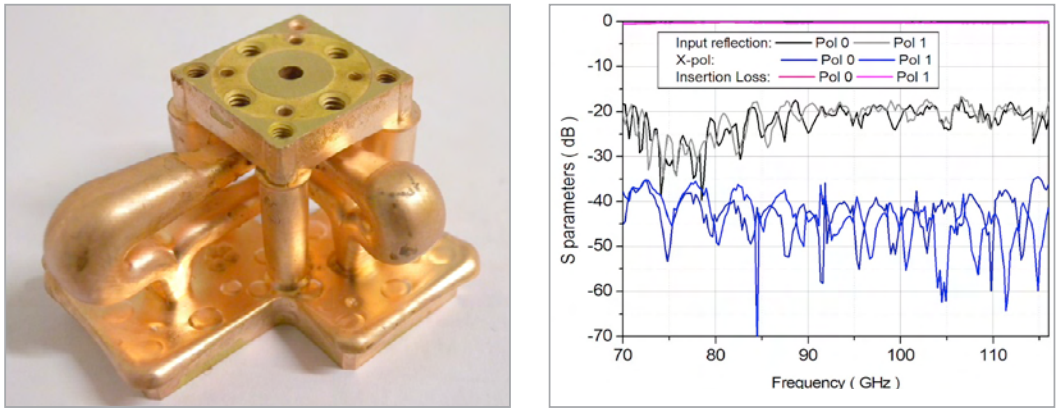


Left: Electroformed OMT designed to cover 70-116 GHz. Right: Measurement results of 70-116 GHz OMT.

## RF HYBRID AND LO DISTRIBUTION COUPLERS

A 1-pixel prototype of a broadband RF hybrid coupler combined to a LO distribution coupler was designed, manufactured and tested. This component consists of three blocks comprising two waveguide circuitries split on opposite sides of a thin block which is sandwiched between two external blocks

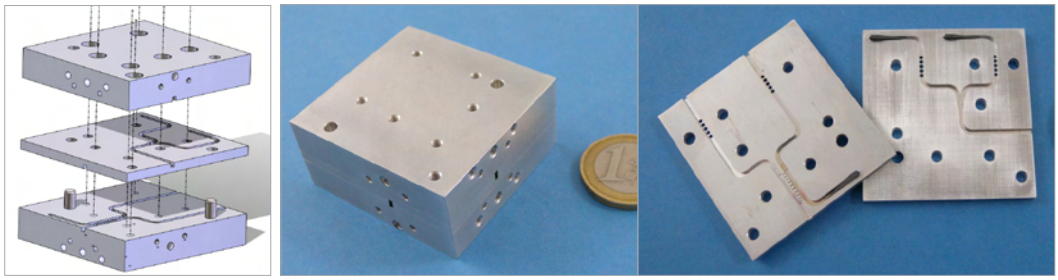

1-pixel RF hybrid and LO coupler. Left: Exploded view of the designed unit. Center: Assembled prototype fabricated at IRAM. Right: Disassembled parts showing the two sides of the central part of the unit (RF waveguide input on the left side, LO waveguide input on the right side).

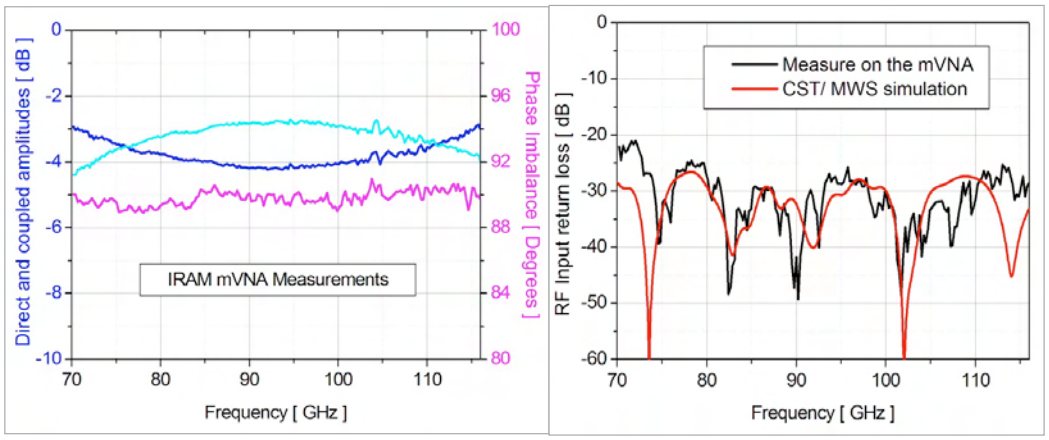


Measured performances of the broadband RF hybrid coupler on IRAM millimeter Vector Network Analyzer.

(see Figure). The unit combines different waveguide technologies: the coupling between the LO and the RF signals is achieved by circular holes on the narrow waveguide side, whereas the 3 dB RF hybrid coupling is obtained through branch lines. This component operates across a very wide band, 70-116 GHz.

Two prototypes of this component were manufactured and tested using the IRAM millimeter vector network analyzer. The measured amplitude imbalance is +/-0.7dB and the measured phase imbalance is of +/-1 degree across the full 70-116 GHz range, with an input reflection of below –20 dB.

## LO AND RF COUPLING DISTRIBUTION FOR 5 PIXELS

The design of the combined LO and RF coupling distribution for 5 pixels, which enables the possibility of using a single local oscillator to pump the 25 pixels array per polarization channel is shown in following figure. Slight differences in the five branch lines coupling regions of the LO signal allow to compensate for the losses along the LO path. As for the 1-pixel prototype, the coupling between the LO and the RF waveguides is obtained through waveguide holes. The simulated electromagnetic performance of the LO distribution to the five pixels predict a maximum difference in the LO coupling values to the RF waveguides of only 1.5 dB.

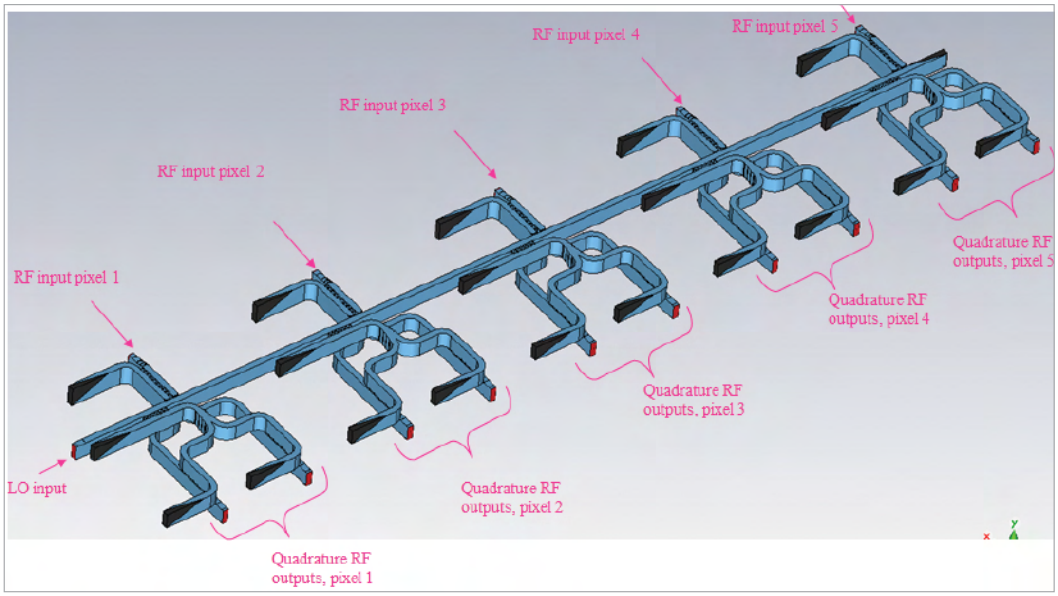


Waveguide path for the LO distribution into a 5 pixel linear array combined to the RF hybrid coupling for 5 pixels. The RF signal is distributed through the waveguides visible on the bottom, while the LO signal is distributed through the waveguide visible on the top.

## MILLIMETER-WAVE VECTOR NETWORK ANALYZER EXTENSION MODULES

We developed three millimeter-wave extension modules for a commercial Vector Network Analyzer (VNA) to cover the 70-279 GHz in 3 MVNA bands (see table below). Such development complements the 260-375 GHz extender built in the past and allows the IRAM S-parameter measurement capabilities to span across all the frequency range covered by the NOEMA Front Ends. The Band 2 and Band 3 MVNA extension modules combine a 65-90 GHz high power source (an Active-Multiplier-Chain) and two through-reflect test-sets allowing through-reflect scattering parameters measurement. The Band 1 extension module is a full two-port scattering parameter measurement system with two through-reflect modules. Each Band 1 extension module includes a passive harmonic multiplier used as millimeter source. The extenders are connected to an Agilent $N_5$244A PNAX which drives the RF and the LO frequency in the range of 8 to 29.6 GHz according to


The three MVNA Test-Sets extenders with the AMC power source, the Agilent N5244A PNAX and the power supply.

the used band. Most of the devices, used in the test sets (like the mechanical box, the Schottky harmonic mixers, the waveguide couplers and the kit of calibration standards) were built in house.

| Band # | Frequency Band [GHz] | Transmission dynamic [dB] | Reflection dynamic [dB] |
|---|---|---|---|
| 1 | 70-116 | 80 | 50-60 |
| 2 | 127-179 | 80-100 | 60 |
| 3 | 200-278 | 90-100 | 60 |

## COMPLETION OF ALMA BAND 7 CARTRIDGE PRODUCTION

In December 2012, the ALMA Band 7 (275-373 GHz) cartridge production was successfully completed within cost and allocated timescale.

In 2012, four retrofitted pre-production cartridges and the last 13 production cartridges were assembled, tested and delivered to the ALMA project. Ten spare 2SB mixer assemblies were also fabricated and tested. One of the cartridge test set was reworked prior to its shipment to the ALMA Operation Support Facility (OSF) in Chile.

A first cartridge maintenance training was provided to our Chilean colleagues in June 2012.

The following Figures show the integrated noise temperature and the image band suppression of the 65 production cartridges.

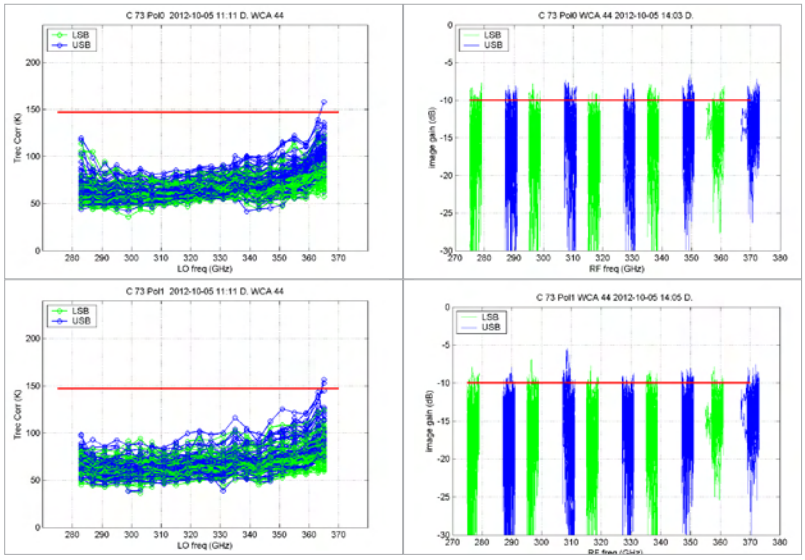


Integrated SSB receiver noise temperature (left) and image band suppression (right) for all 65 ALMA Band 7 production cartridges (#9 to #73).

## AMSTAR+ / AETHER ACTIVITIES

Within the framework of the AMSTAR+ FP7 programme, a collaborative effort of a number of European research institutes which ended in June 2012, IRAM was involved in the two following tasks:

Task 1: the development of a prototype pixel for a W-band dual polarization module using metamorphic HEMT technology to be integrated into a Focal Plane Array;

TasK 2: the development of advanced receiver pixels and LOs for large Focal Plane Arrays in the near mm-wave domain.

The European programme is continuing through the new AETHER project, which started in July 2012.

### AMSTAR+ TASK 1

Waveguide W-band Low Noise Amplifier (LNA) modules integrating metamorphic MMIC amplifiers that were designed and fabricated at IAF (Fraunhofer Institute, Freiburg, Germany) were developed at IRAM in 2012. The mechanical packaging of the W-band LNA integrates the following components: a) one IAF MMIC amplifier; b) two probe chips (waveguide-to-coplanar waveguide CPW transitions); c) one bias board circuit; and d) one DC bias connector from Microtech. Views of a packaged MMIC amplifier and of its internal details are shown in the Figures below.

A number of W-band LNA modules were built and characterized (see Figure below, left panel). The external dimensions of the W-band LNA module were chosen to allow assembly of two LNA units

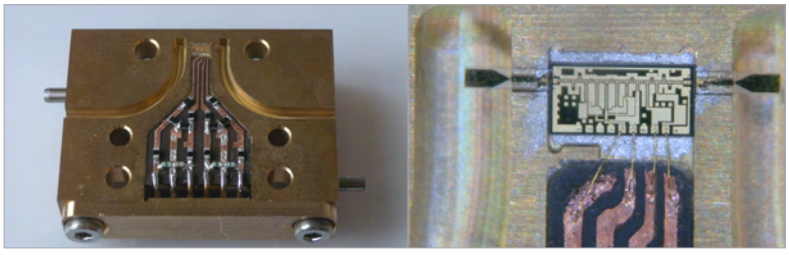

Left: LNA base block (cover block removed) showing the input and output waveguides and DC bias board. Right: IAF MMIC glued to LNA base block in between two waveguide-to-CPW quartz probe chips.

with the waveguide orthomode transducer (OMT), which was also built and tested at IRAM. A complete dual linear polarization module including two LNA units per polarization channel interconnected through a commercial isolator was built and characterized (see Figure below, right panel).

A cryostat equipped with the AMSTAR+ module was installed on the IRAM Pico Veleta 30 m telescope and its performance were measured in July 2012. A full 3 mm band (84-116 GHz) spectrum was taken on IRC+10216 in less than an hour (see Figure below) using the AMSTAR+ prototype receiver and the Fast Fourier-Transform backends (FTS), showing a very good baseline and no contamination from lines on the image sideband. A longer integration time spectrum, taken on the same source, shows the RMS noise closely follows the radiometric noise limit. Allan variance analysis gives results similar to other IRAM SIS receivers.

Left: some of the W-band LNA modules packaged and tested at IRAM. Right: spectral line survey conducted with AMSTAR+ receiver module installed on the IRAM 30 m telescope.

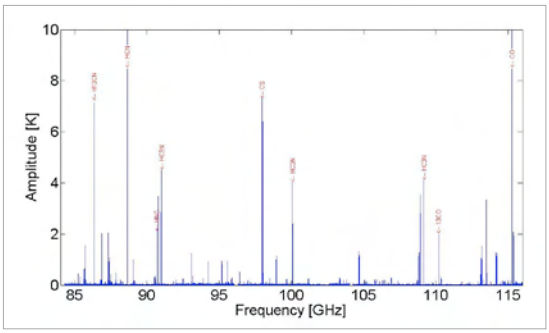


Left: Room temperature S-parameters measurement of one of the W-band LNAs performed with the IRAM mm-wave Vector Network Analyzer across 70-116 GHz. Right: Noise temperature and gain of W-band LNA at 4.2 K.

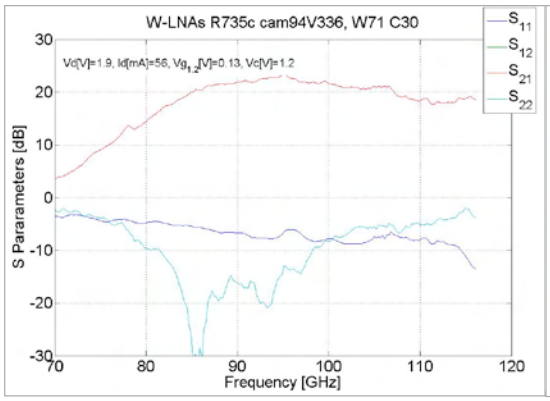


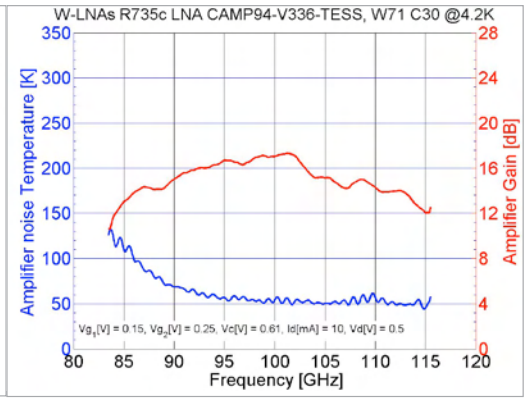


The amplifiers were first characterized at room temperature, then at cryogenic temperature. The results of the characterization of one of the amplifiers are presented on the Figure below.

## AMSTAR+ TASK 2

A small footprint 2SB mixer module for the 200-280 GHz frequency range, having a flat noise response over the 4-12 GHz IF band, had successfully developed at IRAM in 2011 and is currently mounted on the $E_2$ channel of the EMIR receiver. Because of the good results and the already sufficiently small footprint of the 2SB mixer module, the initial project of designing a 2SB mixer-on-a-chip was abandoned. Instead, it was decided to further pursue the integration of the 2SB mixer by designing an IF superconducting hybrid coupler, which can be integrated with the mixer chip into one block. Such IF hybrid, to be employed in the NOEMA Front End, is under development.

Additional tests of the 2SB mixer were performed in conjunction with 4-12 GHz low noise amplifiers (LNAs) with low input reflection coefficient developed at Yebes. Different types of LNAs were tested, which were based on MMIC or hybrid transistor technologies. The results were compared to the measurements obtained with the standard set-up of 2SB mixer cascaded with cryogenic isolators and classic amplifiers (which were retained for NOEMA). The noise temperature of the receiver without isolators was found to be slightly higher than thenoise temperature of the receiver with isolators. A ripple was observed in the measured noise versus IF frequency, at the origin of the reflections between mixer and amplifier. They ripple was more pronounced for the case of the MMIC LNA.

# CONTINUUM ARRAY DEVELOPMENTS FROM THE 30M TELESCOPE

## GISMO

### GISMO(-1) (prototype)

Since April 2012 GISMO has begun the 2nd part of its life: it is now in its nominal configuration and opened to the community with a basis of 2 science runs per year organized in observing pools of 2 weeks each. For the April 2012 and November 2012 pools the median NEFD = 13 and 18 mJy•s$^{1/2}$, and is dominated by sky noise. In both cases a large fraction (~70%) of the scheduled time was lost due to bad weather. However a majority of the projects rms requirements were achieved.

For the 3rd pool run in April 2013, 19 projects have been accepted. A 4th pool run is scheduled for the autumn 2013.

An article from Staguhn et al. has been submitted for publication to ApJ in February 2013. The map studied, called the Gismo Deep Field (GDF), is a portion of the GOODS-N field, containing the detection of 12 sources, 7 of them being discoveries without any known counterpart. This is a good demonstration of the deep integration capacities of GISMO for the study of the far universe.

### GISMO-2 (instrument)

IRAM has been active in designing the optics for GISMO-2, a dual band follow up of GISMO 1. It will be a 2 band system using filled arrays at 150 and 250 GHz and covering a 4'x5' FOV. The GISMO-2 cryostat is now in development, as well as the TES detectors arrays, and the optical elements including large silicon lenses. The delivery for first tests should occur in about one year.

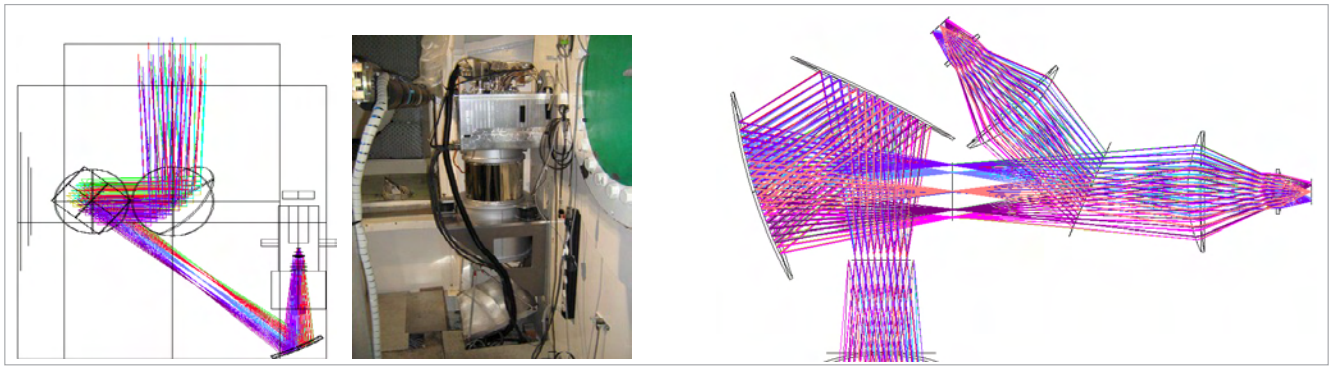

Left: screenshot from Zemax of the GISMO(-1) new optics; centre: GISMO installed at this final permanent position; right: details of the ray tracing inside the GISMO-2 cryostat, the optical elements displayed are the entrance window, the cold pupil stop, 2 folded off-axis mirrors, the field stop, the dichroic separating the 1.2 and 2 mm bands, and 2 lenses for each bands producing an excellent image quality.

## NIKA

### NIKA(-1) (prototype)

The 4th test run of NIKA occurred in June 2012, the goals being the installation and test at the new permanent position. The curved M6 mirror and the HDPE lenses were machined by the IRAM mechanical workshop, with a new kind of large band-pass anti-reflection pyramidal corrugations. The unstable weather allowed toproduce only calibration maps, however sufficient to witness the modifications of several problems seen in the previous runs.

The 5th test run occurred in November 2012. It included the new NIKEL electronics developed at the LPSC, and a KID auto-tuning procedure. Unfortunately an unforeseen saturation of a cold amplifier limited the number of pixels to 69 for the 240 GHz band. Besides, the arrays showed such disparities that in order to appreciate the system performances, it was worth giving 2 numbers per band for the sensitivities: NEFD 140GHz = 31 (18) mJy•s$^{1/2}$ for the 101 (20 best) valid pixels

NEFD 240GHz = 81 (24) mJy•s$^{1/2}$ for the 69 (8 best) valid pixels

Some science observations could be conducted, in particular on the topics of diffuse emission, and the Sunyaev Zeldovich effect.

A change of the cold amplifier and KIDs array is foreseen for the next run in June 2013. The camera could then be opened to external observers on a shared risk basis for the Winter 2013-2014.

## NIKA-2 (instrument)

The development is funded with an ANR proposal of 900 k€, it will also benefit from a Labex Focus (driven by IPAG), and a EU ERC granted 500 k€ to the CEA to support polarimetry, which follows recommendations from the SAC and led to modified specifications accordingly. Hence the cryostat will contain 3 channels for simultaneous observations: a 1000 pixels array for the 150 GHz band, a 2500 pixels array for the 250 GHz band, and possibly another 2500 pixels array at 250 GHz to allow simultaneous polarized observations. Each of these 3 arrays will fully sample a 6.5' FOV diameter, implying 0.75 Fλ pixel angular size.

In the 2nd half of 2012 intense work at IRAM was engaged for the optical design of NIKA-2. With 2.3 m long and about 900 kg, NIKA-2 will be a big instrument. The spacing constraints in the 30m telescope receiver cabin were analyzed, a review meeting was scheduled in April 2013. The electronics will be made with 20 NIKEL boards currently in development at the LPSC. The pixel design is derived from the LEKID arrays tested at Pico Veleta in the NIKA(-1) prototype. Each array will be achieved on a single 4 inches Si wafer. Several developments are ongoing to optimise the sensitivity (e.g. AR coating, bridges, TiN, etc.); G. Coiffard has started a PhD on this subject in the IRAM SIS group.

The NIKA-2 arrays will be tested in laboratory electrically and optically, using a modified NIKA-1 cryostat, which includes an optics designed in the summer 2012 that allows illuminating 4 inches wafers. Thus it is possible to test the arrays while the NIKA-2 cryostat is in fabrication. Some early tests conducted on 1000 pixels arrays have validated the testing facility and demonstrated performances in line with the current 2 inches wafers.

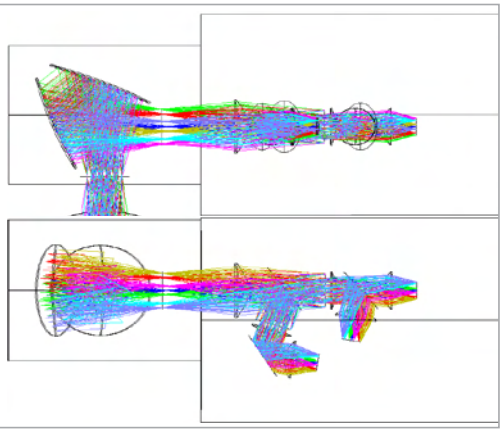

Left: NIKA(-1) installed at its new permanent position; Right: Zemax ray tracing inside the NIKA-2 cryostat viewed from the top (top) and from the side (bottom), the optical elements displayed are the entrance window, the cold pupil stop, 2 folded off-axis mirrors, the field stop, a lens, the dichroic separating the 1.2 and 2 mm bands, the polarizer separating orthogonal polarizations at 1.2 mm, and 2 lenses for each bands allowing producing an excellent image quality on the detector.

## 30M CABIN MIRRORS REFURBISHMENT

The specifications updates and beginning of development of both the bolometric project and the heterodynes FPAs have reactivated the project of the 30m cabin mirrors refurbishment. The most noticeable evolution is the realization that the structures from the 2010 propositions were incompatible with the future instruments sizes and locations. Another evolution was the rationalization of the project steps, in particular the motorization of $M_3$ will not be necessary until a need for more than 7' FOV emerges. Therefore, at the end of 2012 a solution was proposed that is (1) compatible with the receiver cabin and future instruments constraints, (2) preserves the solution of a mechanical Nasmyth system, (3) preserves the possibility of a future 2 axis motorization, and (4) free even more spacing than the current smaller FOV system. This solution is currently studied by the Granada team to define its feasibility (structure stiffness, vibration and thermal characteristics, etc.).

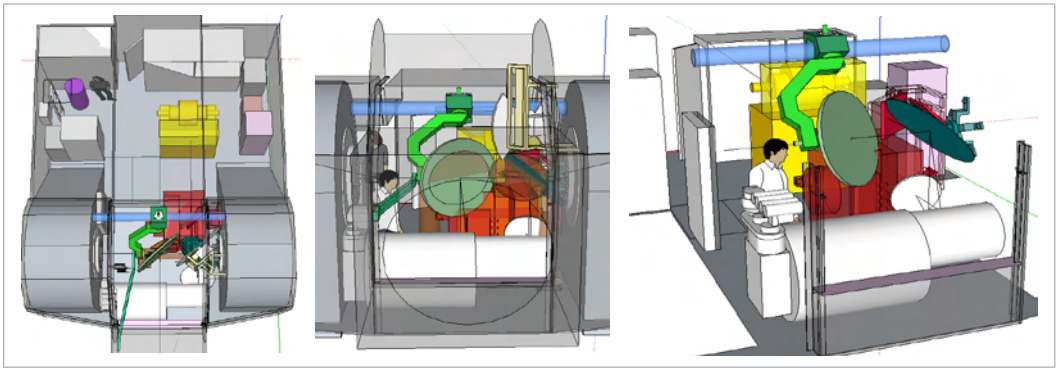

Screenshots from a SketchUp model of the future large FOV optics of the 30m telescope cabin receiver, view from the top (left), front (center), and oblique (right). The future optics systems is in green, the current one in semi-transparent brown, NIKA-2 in white, EMIR in red, and HERA in yellow.

## SIS GROUP

During the year 2012 junction fabrication in the IRAM SIS group has progressed with high pace to be ready for the EMIR upgrades and the NOEMA receivers. Work has focused on new 100 GHz and 150 GHz wideband mixer designs. Other production runs were also performed for modified wideband designs for the 350 GHz band of the SMA.

In the area of kinetic inductance detectors (KIDs), the development of TiN films has gained in quality when the specific sputter equipment was upgraded with a modern mass spectrometer which can work as well as in pre-process UHV conditions as well as during reactive sputtering. At the current stage the pre-sputter conditions could be significantly improved and stabilized, a very difficult but essential task if Ti is deposited due to its high reactivity with background pollutions such as oxygen and water. Progress has also been made in the characterization of deposited TiN films by means of X-Ray diffraction and spectroscopic ellipsometry. For the fabrication of 4" KID detector arrays such as foreseen for the NIKA 2 project on the 30m telescope, the SIS group has upgraded its photolithography line. The work for KID detectors has received support from the French LABEX excellence program FOCUS (PI IPAG Grenoble). The structure of KID arrays as developed in the NEEL/IRAM collaboration is employing long CPW readout lines across the array. Such transmission lines are sensitive to develop undesired asymmetric modes of propagation. Air-bridges to suppress such modes have been started to be developed in 2012 an activity which bases on the process previously developed for cryogenic MEMS applications.

The deposition of membranes, their release and structuring have made important progress in 2012 and the technology blocks for creating complex fully planar membrane supported mm-wave structures have now been assembled. A first application is underway within the collaboration with INAF to fabricate a planar wide band OMT for the 100 GHz range.

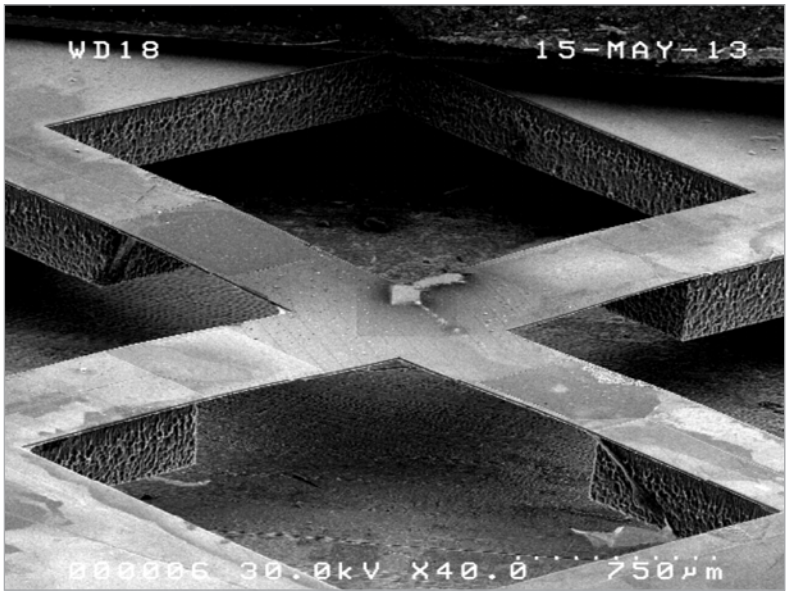


Prototype of a membrane based planar orthomode transducer using a sputtered SiN membrane on high resistivity Silicon substrate and Nb films for the definition of the waveguide probes.

## BACKEND GROUP

### THE HIGH-SPEED ADCS FOR THE NOEMA CORRELATOR ARE IN HOUSE

After a technical evaluation period in close collaboration with the E2V-Grenoble chip designers, it was found that using the EVX5AS210 in two-core mode was a perfectly adequate solution for the PolyFiX correlator design. A probable weakness in the clock tree feeding the two other cores make them less stable, thus not recommended for radio astronomy. However, as a demonstrator, a 4-core, full speed (16Gsps) machine was implemented in the lab and did provide nice single-chunk 8GHz spectra. The PolyFiX application will be less stringent (2-core mode) thus will yield superior performance.

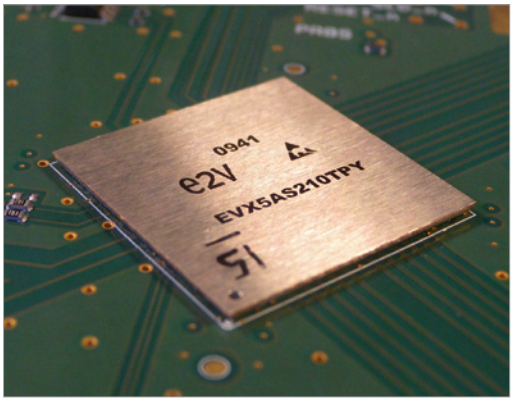


This prototype chip is not commercialized by E2V but 120 pcs have been encapsulated from an existing batch. All of them were individually tested, showing an ENOB better than 4.3 bits on the 2 healthy cores.

## DEVELOPMENT OF CORRELATOR

The digital "LO 3" phase rotators have been designed, simulated and aggregated to the Polyphase Filter Bank on the DiFER platform. Actually the phase shift is not applied on a physical LO 3 but on the baseband signal produced by the PFB. Each digital stream is multiplied by a unity gain complex number that changes with time at a programmable rate. Multiplications are performed in I-Q multipliers made out of DSP blocks from the FPGA. The 16-bit design allows for a 2.46 km maximum baseline and has negligible AM and PM residual modulation.

Filters for the IF processor diplexer have been selected, and two full signal chains prototyped, including their home made synthesized LO's. Phase stability and noise were found very good.

## LO REFERENCE SYSTEM FOR 12 ANTENNAS

The design is completed and most components have been delivered. Several signal chains have been prototyped in order to measure phase stability and cross-talk between antennas. The results are an order of magnitude better than the existing system, due to modern electronics. The computer-closed loop is now implemented in a single PC, yielding a faster transient response.

# MECHANICAL GROUP

## MICROWAVE DRAWING OFFICE AND MECHANICAL WORKSHOP

The IRAM microwave drawing office worked on numerous mechanical designs in close collaboration with the other groups. 80 % of its activities have been dedicated to NOEMA projects. Other work is related to the NIKA project and the prototyping of components for future multibeam systems.

Cold NOEMA optics machined in the IRAM workshop.

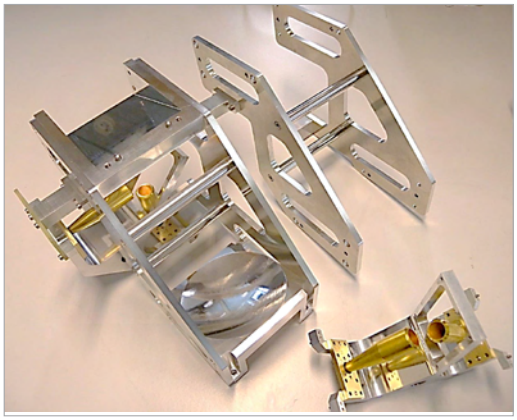

For the NOEMA project, the drawing office and the IRAM mechanical workshop mainly worked on specific improvements of the antenna design, on the prototyping of new receiver components and on the definition of technical specifications in order to optimize component assembly.

The workshop did produce a large number of microwave components, like mixers, couplers, horns and mirrors. 90 % of the parts dedicated to the NOEMA project have been produced in the IRAM workshop.

## WORK FOR THE NOEMA PROJECT

The drawing office worked on many mechanical sub-projects related to improvements of the current PdB antenna for NOEMA. Some of them are described hereafter:

**Reflector mass** The mass of the reflector is an important parameter of the telescope as it determines not only gravitational deformations but also the lowest eigen-frequency and therefore the quality of telescope tracking. Right from the beginning of the NOEMA project, it has been decided to make a dedicated effort on reflector weight reduction and work has focused on the following points:

**Backstructure Nodes** The weight of the nodes close to the panels is 6,2 kg. As there are more than 150 such nodes in the reflector and considering the required counterweights, a mass reduction of the individual nodes has an important impact on the total weight of the reflector. After extensive engineering studies, IRAM succeeded to design a modified node with 20% weight reduction. This generates about 500kg of reflector mass reduction.

At the time being, prototyping for extensive testing of the new nodes is engaged, and if successful, production of the nodes for the first antenna of NOEMA will be started right after.

**Panel actuators** The current mass of actuator is about 500 gr. With our supplier we succeeded to reduce mass by a factor of 1.5. This concept generates a total mass reduction for the reflector of 250 kg.

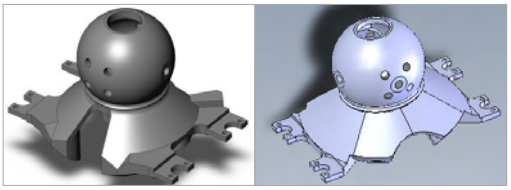

Left: Current node.
Right: New node with 20 % mass reduction

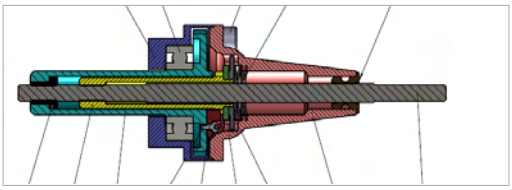

Drawing of the new type of actuator

## DESIGN OF NEW SUBREFLECTOR BACKUP STRUCTURE

One of the main objectives within the antenna development program for NOEMA is to optimize the back up structure of the subreflector. The new SR-BUS must reach the following main goals:

- Improve reliability
- Stay with the same mechanical specifications or better
- No extra weight,
- Easy maintenance
- Limited development and budget risk
- Can be directly integrated in the existing PdB antennas for future upgrades.

Along these lines and in collaboration with SYMETRIE (Nîmes) IRAM has designed a specific hexapod device. The mains characteristics of this hexapod are its possibility for full steering, its carbon fiber based platform and the improved thermal design of the support-mirror ensemble.

Previous connections between support and mirror were made through 4 asymmetrical points; The new hexapod is designed to have 3 symmetrical points with a connection with a specific thermo-mechanical decoupling devices made from INVAR. The improvement on deformations under thermal stress is significant and can be seen in the figure below.

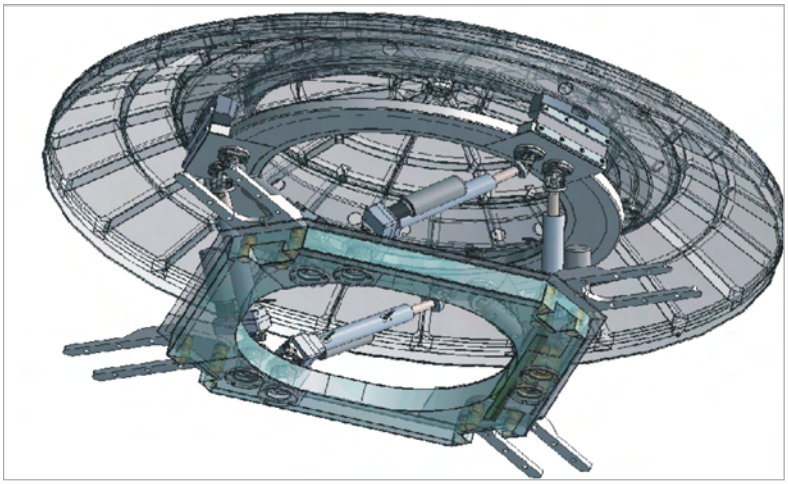

3-D view of NOEMA subreflector mirror with its hexapod support

All components of the NOEMA subreflector hexapod have been designed following the very demanding specifications on environmental conditions at Plateau de Bure and for the composite parts within the system special rapid ageing tests are made for validation.

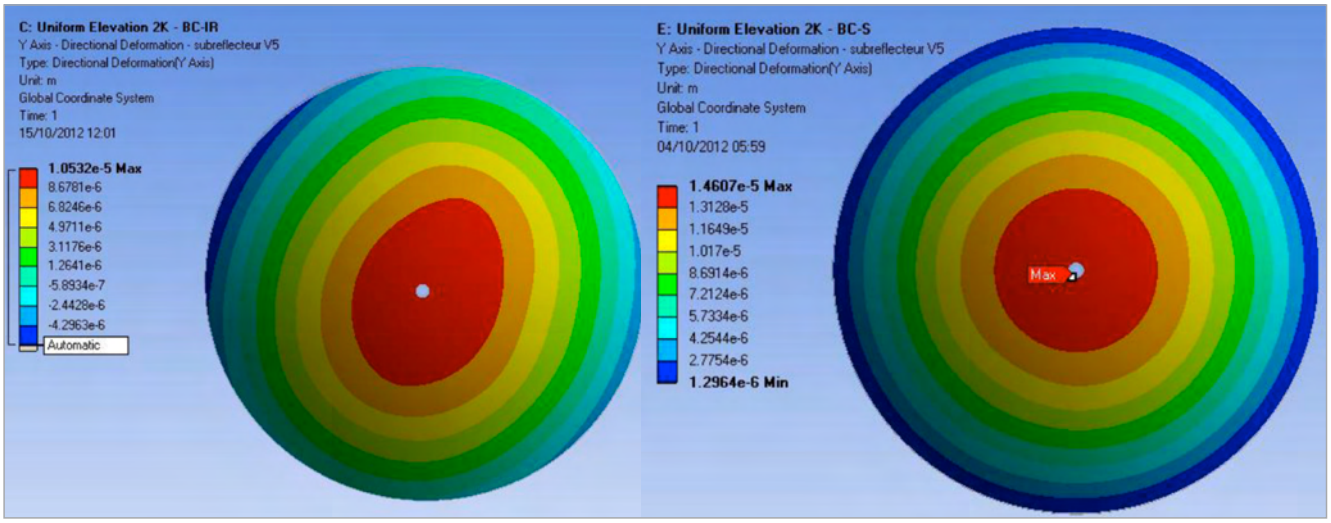


FEM modeling of deformation under thermal stress: actual PdB subreflector (left), and the NOEMA subreflector (right).

## PREPARATION AND CONSTRUCTION START OF ANTENNA 7

Year 2012 has been crucial to prepare our technical team for on site assembling of the NOEMA antennas. A full work break down, from subcomponent acceptance over transport and assembling until final integration and tests, has been established. A full day-to-day planning has been defined together with the personal at Plateau de Bure. A matrix organization involving staff from several groups and well defined responsibilities will be applied and operational planning tools have been created.


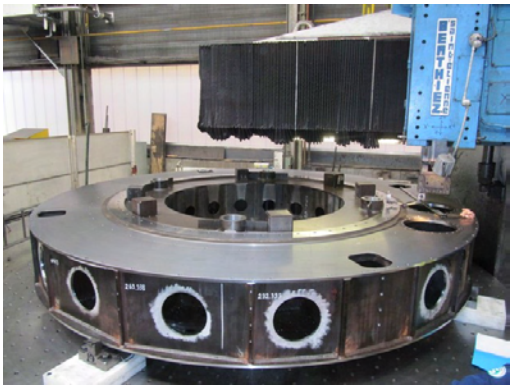


Machining and factory pre-assembling of the first NOEMA antenna mount.

# COMPUTER GROUP

2012 was a pivotal year for the computer group because a quick sequence of leaving for retirement has juxtaposed on the NOEMA project. Fortunately, after some unavoidable delays, a new group leader has finally been appointed and the staff has been reconstituted.

## NETWORK INFRASTRUCTURE

In 2011, the headquarter routers have been replaced by Linux computers. In 2012 the Plateau de Bure routers have received the same treatment. In parallel a new SDSL network link has been subscribed to connect both sites through two different paths. With such Linux routers at both ends, links can be aggregated to a single IP tunnel. The new system offers redundancy and a bigger bandwidth, and it is totally transparent for the users and applications.

Massive fiber optic deployment is now a national goal for the French government, therefore new contacts have been started again with France Telecom and the local authorities to benefit from a high-speed network connection at Bure.

## HARDWARE AND SOFTWARE UPGRADE

Following the NOEMA project, more powerful computers are required to run the last-generation CAD tools in all the technical groups. Therefore a large program has been launched to upgrade the computers. Windows 8 has not been considered as mature enough for IRAM needs, therefore this upgrade program is based on new DELL workstations running Windows 7 64 bits. Unlike Windows 8, Windows 7 requires a very limited training effort for users because almost all of them already use it at home for their personal computers.

## NOEMA SUPPORT

The computer group was heavily involved in many work packages for the NOEMA project. For example it has modified control software to allow the future double array mode and it has also delivered new control boxes for the new YIG local oscillator.

## ANTENNA CONTROL

A mechanical analog for the new antenna drive system has been built to test all the new control for the NOEMA antenna. After that, a scale test with the new selected motors has been run in September 2012 on antenna #5. The test has shown that these new motors suit IRAM needs.

Thanks to the drove anolog, the computer group has also gained a strong experience with EtherCAT on realtime Linux. This precious knowledge will be used to develop the final antenna control software.

## SCIENCE SOFTWARE ACTIVITIES

The main goal of the science software activities at IRAM is to support the preparation, the acquisition and the reduction of data at both the 30m and the Plateau de Bure Interferometer. This includes the delivery of 1) software to the community for proposing and setting-up observations, 2) software to the IRAM staff for use in the online acquisition system and 3) offline software to end users for final reduction of their data. However, the GILDAS suite of software is freely available to and used by other radio telescopes, like Herschel/HIFI, APEX and SOFIA/GREAT.

At the 30m, the advent of broadband spectra (16 GHz per polarization) at high spectral resolution (195 kHz) triggered in 2010 a series of changes in the data processing and analysis of spectra. Many adaptations of the data processing software (CLASS) were finalized in 2012. This includes generalizations in the handling of the spectroscopic axes to remove assumptions valid only for narrow-band spectra. In addition, adaptations were made to take into account the evolution with frequency of telescope parameters, like the beam efficiencies. Moreover, the associated increase of the data rate underlined efficiency problems in MIRA, the online calibration software. In view of the difficulty to solve them, it was decided to develop a new efficient and robust calibration software. A first version of this software, named MRTCAL, should be available end of 2013 or beginning of 2014. The interface to line databases (CDMS, JPL, etc.), developed in 2010 in collaboration with the Observatoire de Grenoble, and released as a CLASS extension named WEEDS, proved its usefulness. A new round of developments thus started in 2012 to generalize this service and to make it available to other GILDAS software. The monitoring of the technical properties (time synchronization, tracking, pointing, focus, calibration, etc.) of the 30m continued. For instance, statistical analyses were developed in MOPSIC to reveal and to understand systematic behaviors. Work started to use the same tools for the Plateau de Bure interferometer.

After a round of software requirements for NOEMA, the Plateau de Bure interferometer extension project, the first developments happened in 2012. At this early time in the project, work focused on preparation. Three main actions happened on the data acquisition side. First, the possibility to separate the array of antenna into two sub-arrays was introduced. This will be essential to enable simultaneously science observations along with commissioning phases of new hardware (antenna, receivers, correlators, etc.) from 2014 to 2017. This implied significant changes in the real-time software to be able to separately control some pieces of hardware from both arrays and to synchronize the access to shared resources (e.g. the noise diodes used for calibration). Second, prototype hardware, like a new tiltmeter, was integrated into one of the existing PdBI antenna, implying new software to command them, store the measurements, and analyze the results. Third, a general review of the codes developed in the last five years happened to base further developments on firm grounds. This includes removal of obsolete commands, debugging, and improvements in the handling of the backward compatibility over the last few generations of receivers. As a consequence, the software that interfaces the online acquisition of the array (OBS) can now be started without hardware resources, a first step towards the implementation of a simulator mode.

Support for science operations continued in 2012. Many improvements were implemented in the calibration pipeline: 1) Efforts were done to identify parasites into the radio-frequency passband; 2) The size of the secondary flux calibrator (MWC349) was taken into account in the flux calibration, as this source starts to be resolved in the A-configuration; 3) A new tool was included to assess whether a faint line is detected inside the receiver bandpass. This is particularly useful to detect galaxies at high redshift. The calibration pipeline is now fully mature, i.e. it provides optimized solutions for all calibration steps, except the flux calibration – work is progressing to bring it to the same level of maturity. Moreover, a tool intended to aid astronomers on duty and operators in optimizing the interferometer's observing schedule on a 24 hours timescale is being developed in collaboration with the Observatoire de Grenoble.

The size of the datasets produced by the current and future radio-instruments experience a tremendous increase (because of the multi-beam receivers, wide bandwidth receivers, spectrometers with thousands of channels, and/or new observing modes like the interferometric on-the-fly). This implied a transversal work to remove the limitations present in all the data formats used in GILDAS. We first concentrated on the GILDAS Data Format (GDF) to store already calibrated data, either position, frequency cubes or calibrated uv-tables. This project (known as GDF-V 2), which was started in 2011, aims at enabling the support of arrays of more than 2 giga elements (the limit that a 32 bits integer can encode). This has implications on all GILDAS software. This change is done so that GILDAS will still be able to read the version 1 of the format to ensure backward compatibility

with existing data sets. The project will converge in 2013. This work is done in collaboration with the Observatoire de Bordeaux. Additionally, we worked on the data formats to store raw data both from the IRAM-30m and the PdBI, i.e. the CLASS and CLIC data format, respectively. While the semantics (i.e. the meaning) of both data format are very different due to the specificities of the single-dish and interferometry techniques, CLASS and CLIC still share the data binary container (i.e. the way the bits are ordered, independent of their science meaning). After an analysis of the different limitations of this data binary container, we progressively removed them. In order to factorize the code, we created a new library, named CLASSIC, which will be used in both CLASS and CLIC. This will decrease maintenance efforts on the medium term.

All the software developments are based on the common GILDAS services, e.g. a set of common low-level libraries, collectively named GILDAS kernel, which take care of the scripting and plotting capabilities of GILDAS. Among the many small improvements which happened in 2012, a particular effort was done to improve the new users' learning curve: the various help documents and demonstration scripts were made easily available inside the main widgets of the different programs. We also ensured that GILDAS is able to import/export the FITS format of the CASA software developed for ALMA and the eVLA. Finally, the PMS (Proposal Management System) project, which will replace the current proposal submission and processing system for the IRAM 30m telescope and Plateau de Bure interferometer, was successfully used during the process of the proposal technical evaluation and during the two program committee meetings in 2012. Work started on the new proposal submission facility, which will first be used in September 2013.


Credit: ALMA (ESO/NAOJ/NRAO)

# IRAM ARC Node

The IRAM astronomy support group has been involved for many years in several ALMA-related activities and software developments, hence building an important expertise in the ALMA instrument. IRAM is now a node of the European ALMA Regional Center (ARC) and provides direct support to ALMA users. On the long term, having access to NOEMA and to the ARC node services should place the IRAM users community in the best possible position to obtain observing time on ALMA, in an extremely competitive environment.

## TELESCOPE CALIBRATION SOFTWARE

IRAM is responsible for the development and maintenance of one of the key software for the real-time operations of ALMA, the Telescope Calibration (TelCal) software. An amendment to the original agreement between ESO and IRAM was signed in 2012 to extend and increase the IRAM contribution for TelCal in 2013 and 2014. TelCal is performing all real-time calibrations necessary to run the array: antenna pointing, focus, baseline measurements, atmospheric parameters, etc. Two IRAM engineers are working on these developments.

2012 was a critical year for TelCal, as this was the first year during which a production version of the software was used all over the year to perform scientific observations (Cycle 0), putting strong constraints on the performances and reliability of the real-time system. In parallel, the array commissioning continued, implying a continuous and important effort to correct, adapt, and further develop TelCal. A stand-alone version of TelCal, interfaced to the CASA off-line package, is also supported, to allow an off-line reprocessing of the real-time calibration. Finally, a specific version of CLIC, used for the ALMA holography processing, is also maintained in the TelCal package.

## ALMA USERS SUPPORT

2012 was a pivotal year for the ARC, as the start of the scientific operations (end of 2011) triggered an important series of activities. The main tasks the IRAM ARC node was involved in were:

- Preparation of the Cycle 1 deadline; various documents were distributed in order to help the IRAM community to prepare their proposals.
- Cycle 0 contact scientists: the ARC node staff act as "Contact Scientists" for the accepted ALMA projects, providing expertise to check and validate the Scheduling Blocks that were created from the initial proposals. The IRAM ARC node supported 20 projects out of the 54 accepted+filler projects in Europe. Specific tools to display and possibly

optimize the correlator setup in the ASTRO software were developed.

- Face-to-face support for data reduction: from July 2012 on, IRAM started to support astronomers visiting the institute for the reduction of their ALMA projects. Procedures similar to the Plateau de Bure rules were used to organize these visits, including financial support for PIs affiliated to the IRAM funding agencies. The data reduction itself turned out to be a somewhat lengthy process, as many calibration parameters have still to be manually checked and optimized, providing in some cases a significant increase of the final maps quality. Data fillers to transfer calibrated data from/to CASA to/from GILDAS were developed, allowing to image the data in both software packages.

## 8TH MM INTERFEROMETRY SCHOOL

IRAM organized its 8th mm-interferometry school from October 15-19, in Grenoble. The lectures covered, as in the previous schools, the fundamentals of millimeter interferometry techniques, the atmospheric phase correction, data calibration, and imaging. The Plateau de Bure array and ALMA were presented in some details, and data reduction tutorials were also organized. 65 participants - out of more than 120 applications - attended the school and gave a very positive feedback at the end of the week. This event was supported, as in 2010, by the EU RadioNet program.

Participants at the 8th IRAM interferometry school

# Personnel and finances

## HUMAN RESOURCES

In 2012, IRAM employed 93 FTE in France and 29.5 FTE in Spain.

Five employees joined IRAM in 2012:
Grégoire Coiffard (PhD-student), Xavier Avrillier, Sabine König and Tessel Van der Laan to reinforce the scientific and technical departments; Isabelle Delaunay in the administration department.

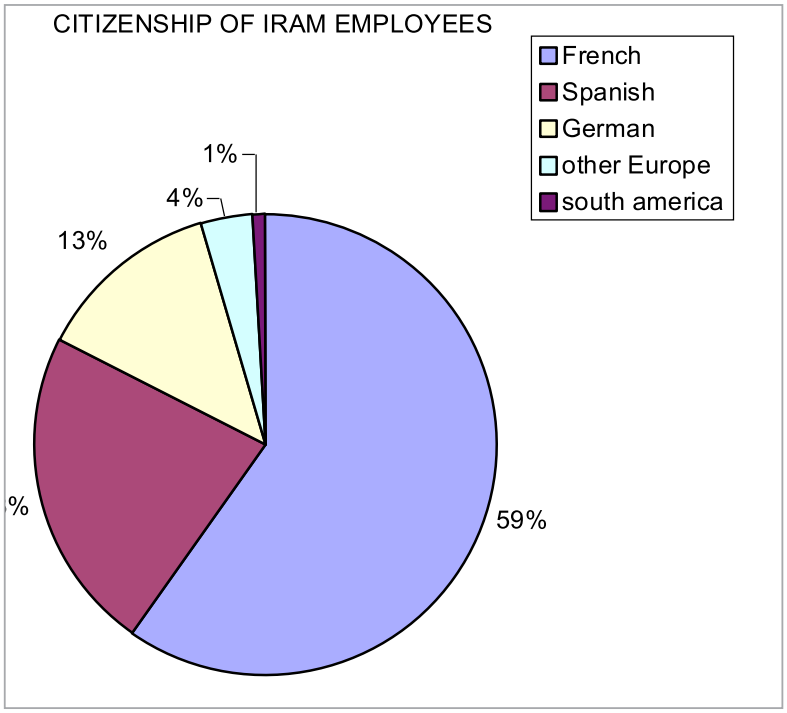


Six employees left IRAM at the same time:
Irvin Stil, Roger Ah Tchou, Markus Rösch (PhD-student), Mathieu Lonjaret and Jean Yves Pierre from the scientific and technical departments ; Raymond Hennequin from the administration department.

IRAM gratefully thanks these persons for their work and involvement through years. IRAM also thanks Martino Calvo (now Inst. Neel) who strengthened the IRAM NIKA team for six months in 2012.

On the whole 34 employees were assigned to science tasks and 82 to technical or administrative positions. IRAM science staff is concerned with the operation of the observatories and the science support of IRAM users. The technical departments of IRAM are in charge of design, production and maintenance of IRAM's equipments. With their work they provide the international scientific community with one of the world finest equipments in the field of millimetre astronomy. The IRAM Administrative staff allows IRAM to find its way through the increasing complexity of national and iternational administrative tasks.

The performance of IRAM's personel is also the result of the high level of qualification and involvement of IRAM staff. To support this, IRAM has carried out an important training policy for years and will continue to do so.

IRAM is also a women-friendly institute, 30% of IRAM employees are women, a percentage which is independent of qualification level.

## OPERATING AND INVESTMENT BUDGETS - 2012

The IRAM associates approved a 2% increase in their base contribution to the operation budget for 2012. The contributions to the investment budget were maintained at their previous level for 2012. In addition, CNRS transferred for 2012 a specific contribution of 1 M€ to the investment budget as part of the participation in the reconstruction of the cable car to access the Plateau de Bure Observatory. Finally, 6,5 M€ were budgeted and transferred by ANR (Agence Nationale de la Recherche)-EQUIPEX to co-finance the NOEMA Phase 1.

| Expenditure | | |
|---|---|---|
| **Budget heading** | **Approved** | **Actual** |
| Operation/Personnel | 8 216 493 | 8 148 292 |
| Operation/Other items | 3 329 937 | 3 683 725 |
| Budgetary excess/loss | 421 143 | -334 315 |
| **TOTAL OPERATION** | **11 967 573** | **11 497 703** |
| Investment base | 1 565 816 | 818 781 |
| Investment NOEMA | 9 595 267 | 1 933 043 |
| Investment Cable Car | 9 384 474 | 210 891 |
| Budgetay excess/loss | | 17 896 315 |
| **TOTAL EXPENDITURE excl. VAT** | **32 513 131** | **32 356 733** |

| Income | | |
|---|---|---|
| **Budget heading** | **Approved** | **Actual** |
| CNRS contributions | 7 276 589 | 7 276 589 |
| MPG contributions | 5 776 589 | 5 776 589 |
| IGN contributions | 737 437 | 737 437 |
| **TOTAL CONTRIBUTION** | **13 790 614** | **13 790 614** |
| Carry forward from previous years | 6 202 287 | 6 202 287 |
| IRAM'own income | 6 020 230 | 5 863 832 |
| ANR EQUIPEX | 6 500 000 | 6 500 000 |
| **TOTAL INCOME excl. VAT** | **32 513 131** | **32 356 733** |

# Annex I – Telescope schedules

The next two tables show the allocations for the telescope time for the 30-meter telescope and the Plateau de Bure Interferometer for the year 2012. In each table, the first column gives the project's identification, the second column the title of the investigation and the third column the names of the Principal Investigators and the co-investigators.

## 30-METER TELESCOPE

| Ident. | Title | Investigators |
|---|---|---|
| 228-09 | A Legacy Survey to Study Cold Gas Scaling Laws in the Local Universe | Kramer, Kauffmann, Buchbender, Catinella, Cortese, Fabello, Fu, Giovanelli, Gracia-Carpio, Guo, Haynes, Heckman, Krumholz, Li, Moran, Rodriguez-Fernandez, Saintonge, Schiminovich, Schuster, Sievers, Tacconi, Wang |
| 225-10 | The complete CO(2-1) map of M33 | Braine, Schuster, Kramer, Gonzalez, Sievers, Rodriguez, Gratier, Brouillet, Herpin, Bontemps, Israel, van der Werf, van der Tak, Tabatabaei, Henkel, Roellig, Combes, Wiedner |
| 271-10 | Physics of Gas and Star Formation in Galaxies at $z$=1.2 | Combes, Tacconi, Genzel, Bolatto, Bournaud, Burkert, Cooper, Cox, Davis, Schreiber, García-Burillo, Gracia-Carpio, Lutz, Naab, Neri, Newman, Sternberg, Weiner |
| 135-11 | Isotopic ratios in Oort cloud comet C/2009P1 (Garradd) | Biver, Bockelée-Morvan, Crovisier, Colom, Moreno, Hartogh, Lis, Boissier, Paubert, Weaver, Russo, Vervack |
| 136-11 | Search for complex organic molecules in pre-stellar cores | Bacmann, Kahane, Taquet, Ceccarelli, Faure |
| 137-11 | Using chemistry to constrain the evolutionary state of prestellar cores | Maret, Tafalla, Bergin, Hily-Blant |
| 138-11 | A search for formamide in the solar-type protostar IRAS 16293-2422 | Kahane, Alexandre, Alexandre, Cecilia, Vianney, Laurent, Roman, Eric |
| 139-11 | Chemical characterisation of the massive cores in IRDC G28.53-00.25 | Padovani, Girart, Palau, Sepulcre, Busquet, Sánchez-Monge, Frau |
| 140-11 | The chemical structure of Orion : Completion of the 2-D line survey at 1mm | Marcelino, Cernicharo, Esplugues, Palau, Bell, Tercero, Guelin |
| 142-11 | Search for ortho-$H_2Cl$+, a new probe of the diffuse ISM | Gerin, Neufeld, De Luca, Kramer, Le Petit, Lis, Menten, Navarro, Pety, Roueff |
| 143-11 | Spectroscopy of Shocks: the role of SiO(8-7) | Codella, Gueth, Cabrit, Ceccarelli, Lefloch, Bachiller, Tafalla, Guilloteau, Benedettini, Gusdorf, Nisini |
| 145-11 | Benchmarking grain-surface chemistry on the Horsehead mane | Pety, Guzman, Bardeau, Belloche, Gerin, Goicoechea, Gratier, Le Bourlot, Le Petit, Roueff, Teyssier, Sievers |
| 146-11 | Search for $^{13}$C Ethanol toward G34.3 +0.15, a star forming region | Bouchez Giret, Bottinelli, Walters, Müller |
| 149-11 | Deuterated water chemistry towards high/low-mass star-forming regions. | Vastel, Gérin, Coutens, Comito, Jastrzebska, Lis, Goldsmith, Herbst, Faure |
| 150-11 | D3O+ and the oxygen budget of L1544 | Bizzocchi, Caselli, Dore, Ceccarelli, van der Tak, Angeloni, Leonardo |
| 152-11 | Deuterium fractionation in the evolution of high-mass protostars | Fontani, Sánchez-Monge, López-Sepulcre, Cesaroni, Walmsley, Beltrán |
| 153-11 | Search for deuterated methyl formate ($DCOOCH_3$) in NGC1333-IRAS4A | Demyk, Bottinelli, Caux, Vastel, Coutens, Ceccarelli, Kahane, Taquet, Wakelam, Quirico, Ratajczak, Aikawa |
| 154-11 | Isotopic fractionation of nitrogen in the dense and cold ISM. | Le Gal, Hily-Blant, Padovani, Faure, Pineau des Forêts, Walmsley, Tafalla |
| 155-11 | A 1 mm high spectral resolution line survey of the Orion Bar PDR | Goicoechea, Cuadrado, Cernicharo, Fuente, Esplugues, García-Burillo, Usero, Marcelino |
| 156-11 | An Unbiased Spectral Survey of the Protostellar Bowshock L1157-B1 | Lefloch, Ceccarelli, Gueth, Cernicharo, Codella, Benedettini, Cabrit, Schuster, Vasta |
| 157-11 | Spectral survey of the intermediate mass protostar OMC2-FIR4 | López-Sepulcre, Kama, Ceccarelli, Lefloch, Fuente, Caselli, Caux, Dominik, Kahane, van der Tak, Wiesenfeld |
| 158-11 | A complete 3mm line survey of dark cloud cores: B1-b and TMC-1 | Marcelino, Cernicharo, Roueff, Thum, Gerin |
| 159-11 | Molecular study of the PDR around the UCHII region Mon R2 | Treviño-Morales, Fuente, Kramer, Gonzalez-Garcia, Pilleri, Cernicharo, Ginard, Berne, Joblin, Ossenkopf, Goicoechea, Garcia-Burillo, Roueff, Viti, Rizzo, Alonso-Albi |
| 161-11 | Unbiased Line Spectral Survey of a Circumstellar Disk | Hily-Blant, Kastner, Forveille, Sacco, Rodriguez, Zuckerman |
| 162-11 | Probing the magnetic field in Supernova Remnant IC 443 | Hezareh, Wiesemeyer, Gusdorf, Thum |
| 163-11 | Preliminary Observations for a Large Zeeman Proposal | Falgarone, Crutcher, Troland, Hily-Blant, Piétu, Paubert, Guilloteau, Beuther, Heiles, Lai, Koch, Tang, Zhang, Henning, Plambeck |
| 164-11 | 3D magnetic fields and deep chemical survey of young magnetized prestellar cores | Frau, Padovani, Girart, Beltrán, Morata, Alves, Franco |
| 165-11 | Magnetic Fields versus Turbulence on Regulating Star Formation | Li, Kainulainen, Houde, Henning |

| Ident. | Title | Investigators |
|---|---|---|
| 167-11 | IRAM-30m follow-up of cold cores detected by the Planck satellite | Pagani, Ristorcelli, Juvela, Bernard, Giard, Mény, Marshall, Montier, Harju, Malinen, Laureijs, Mcgehee, Paladini, Pelkonen, Toth |
| 169-11 | Understanding core formation in clustered environments | Hacar, Tafalla |
| 170-11 | New it Herschel-identified Orion protostars: characterizing an extreme population of cold sources with IRAM | Stutz, Tobin, Thomas Megeath, di Francesco, Henning, Linz, Stanke, Ali, Fischer, Maret, Wilson |
| 171-11 | Outflow Impacts on the Protocluster Serpens South | Plunkett, Arce, Mardones, Chen, Dunham |
| 172-11 | Carbon budget and molecular cloud formation signatures in IRDCs | Ragan, Beuther, Linz, Henning |
| 173-11 | Interaction of cosmic-rays and molecular clouds | Ceccarelli, Dubus, Hily-Blant, Lelfoch, Montmerle, Padovani |
| 174-11 | Tracing infall towards the low-luminosity protostar in CB130 | Lippok, Launhardt, Stutz, Henning, Linz, Pavlyuchenkov, Semenov |
| 175-11 | Rotation Signatures in the Inner Protostellar Envelope: Constraining Angular Momentum | Tobin, Bourke, Stutz, Smith, Wootten, Maret, Bergin, Hartmann |
| 176-11 | The outflow phenomenon at the substellar boundary | Monin, Lefloch, Dougados, Whelan, Cabrit, Oliveira |
| 177-11 | Origin of warm water in deeply embedded low-mass protostars | Persson, Jorgensen, Dishoeck, Harsono, Visser, Kristensen, Bergin |
| 178-11 | MAYS: Mass (and ages) of Young Stars - a CN survey | Guilloteau, Di Folco, Simon, Piétu, Dutrey, Hersant, Wakelam, Ducourant, Grosso, Guillout, Schaefer, White, Teixera, Palla |
| 179-11 | Structure and Kinematics of Hub-Filament Systems in High-Mass Star Formation | Liu, Quintana-Lacaci, Immer, Menten, Wang, Ho, Zhang, Galván-Madrid, Lin, Li, Zhang |
| 180-11 | The systematic trends in the kinematics of massive star forming regions. Observations of HC3N* in hot cores | Rivilla, Martín-Pintado, Jiménez-Serra, Rodríguez-franco, Báez |
| 181-11 | The evolution of outflows in high-mass young stellar objects | Sánchez-Monge, López-Sepulcre, Cesaroni, Walmsley, Codella, Beltrán |
| 182-11 | Probing the large scale chemical evolution in high-mass protostars | Øberg, Fayolle, Dishoeck, Garrod, Bisschop |
| 183-11 | Mass loss on the RGB: reaching the limits | Groenewegen |
| 184-11 | Studying the outer molecular envelope of Betelgeuse | Kamiński, Proedrou, Menten |
| 185-11 | Search for rotating disks around Hot post-AGB stars. | Quintana-Lacaci, Akras |
| 186-11 | Mass-loss properties of AGB stars: the key to understanding wind-ISM interactions | Cox, Groenewegen, Decin, Royer, De Beck |
| 187-11 | Discs around post-AGB stars and the formation of planetary nebulae | Bujarrabal, Winckel, Alcolea, Santander-García, Castro-Carrizo |
| 188-11 | A Line Survey of the Supergiant O-rich star VY CMa | Cernicharo, Quintana-Lacaci, Sánchez Contreras, Velilla, Bujarrabal, Marcelino, Alcolea, Santander, Pearson, Teyssier |
| 190-11 | 2 mm Continuum Observations of the Galactic Center Region | Staguhn, Kovács, Benford, Morris |
| 191-11 | The accretion flow onto Sgr Astar | Thum, Downes, Morris, Sievers, Wiesemeyer |
| 193-11 | EMIR $^{12}$CO and $^{13}$CO maps of the M83 central bar (resubmission) | Abreu Vicente, Kramer, García-Burillo, Israel, Lord, Billot |
| 195-11 | Molecular gas mass distribution in NGC 604 (M 33) | Israel, Braine, Heiner |
| 196-11 | CO in Abell 1367: a probe for interaction mechanisms | Scott, Brinks, Usero, Bravo-Alfaro |
| 197-11 | CO Gas Clouds toward the Virgo Cluster: Progenitors of Dwarf Galaxies | Kent, Mangum |
| 199-11 | A Unique Dynamical Measurement of Star-Formation Thresholds in Five Galaxy Disks | Westfall, Verheijen, Spaans, van der Tak, Bershady, Martinsson, Kramer |
| 200-11 | The Physical State of Dense Molecular Gas in Early-Type Galaxies | Crocker, Bournaud, Juneau, Saintonge, Martig, Bureau |
| 201-11 | Monitoring the HNC/HCN ratio in Arp220 | Aalto, Costagliola, Muller, Martín, Sakamoto, Garcia-Burillo, Cernicharo |
| 203-11 | Constraining the origin of the heating rate in the Perseus Cluster | Bayet, Viti, Hartquist, Williams, Aladro |
| 204-11 | Characterisation of the very dense gas in the outskirts of NGC6946 | Bayet, Viti, Martín-Pintado, Martín, Aladro |
| 208-11 | Exploring Averaged Chemical Composition of GMCs in the Spiral Arm of M51 | Yoshimasa, Sorai, Sakai, Yamamoto |
| 209-11 | Cold dust along the major axis of the spiral galaxy M33 - the HerM33es project. | Quintana-Lacaci, Kramer, Sievers, Bertoldi, Albrecht, Buchbender, Tabatabaei, Akras, Xilouris, Alto, Anderl, Braine, Israel |
| 210-11 | Molecular shocks in the Stephan's Quintet | Usero, García-Burillo, Verdes-Montenegro, Fuente, Sulentic, Brinks |
| 211-11 | Dense gas tracing the collisional past of Andromeda: an atypical inner region? | Melchior, Combes |
| 214-11 | Molecular content of polar ring galaxies | Combes, Reshetnikov, Moiseev |

| Ident. | Title | Investigators |
|---|---|---|
| 216-11 | Molecular gas masses for a sample of local mergers: bridging the gap between normal galaxies and ULIRGs in the Kennicutt-Schmidt law | Coppin, Scudder, Ellison |
| 218-11 | Using IRAM to Construct the First Detailed Timeline of Early Type Galaxy Evolution | Zabludoff, Shirley, Yang, Walter, Narayanan, Smith |
| 219-11 | Star Formation in Void Galaxies | Beygu, Van Der Hulst, Van De Weijgaert, Gorkom, Kreckel |
| 220-11 | Dust and molecular gas in Virgo star-forming dwarf galaxies | Grossi, Corbelli, Hunt, Bianchi, Giovanardi, Magrini, Pappalardo, Madden, Davies, Smith, Bizzocchi, Papaderos, De Looze, Verstappen, Garcia, Vlahakis |
| 221-11 | Mapping the molecular inner ring of M31 | Melchior, Combes |
| 222-11 | CO properties of the most gas-rich massive galaxies up to z~0.2 | Cortese, Catinella, Fabello |
| 223-11 | Are mid-IR spectral signatures of pressure-confined star formation an aspect of major merger mode star formation in galaxies? | Spoon, Aalto, Costagliola, Farrah, Garcia-Burillo, Illana, Graciá-Carpio, Lahuis, Pérez-Beaupuits, Perez-Torres, Rodriguez, Spaans |
| 224-11 | Molecular Tracers of Galaxy Evolution II: Chemistry or Excitation? | Costagliola, Aalto, Spoon, van der Werf, Muller, Jütte, Lahuis, Martín Ruiz, Rodriguez |
| 225-11 | CS 2-1/3-2 mapping along the major axes of nearby gas-rich galaxies | Zhang, Henkel, Gao, Wang, Garcia-Burillo, Graciá-Carpio |
| 226-11 | The nuclear ISM of Luminous IR Galaxies | Baan, Henkel, Papadopoulos, Loenen, Meijerink |
| 227-11 | Molecular Gas Observations of $L_{IR} \geq 10^{11.4} L_{\odot}$ Infrared Galaxies in the Great Observatories All-sky LIRG Survey (GOALS) | Iwasawa, Evans, Aalto, Frayer, Perez-Torres, Herrero-Illana, Surace, Privon, Kim, Mazzarella, Armus, Spoon |
| 229-11 | Probing the kinetic temperature in active galaxies | Rodríguez, Mühle, Aalto, Odriozola, Pérez Torres |
| 230-11 | Characterising the influence of galaxy activity on the properties of the densest molecular gas component | Bayet, Viti, Martín-Pintado, Martín, Aladro |
| 231-11 | Multi-line HCO+ survey in external galaxies - Part I. Starburst | Bayet, Viti, Martín-Pintado, Martín, Aladro |
| 232-11 | The physical conditions of molecular gas in extreme star-forming environments | Davis, Heiderman, Iono, Blanc, Evans, Gebhardt, Papovich, Yun |
| 233-11 | Measuring the intrinsic radio power of AGN in cluster cores with GISMO | Edge, Hogan, Staguhn, Kovács, Benford, Hlavacek-Larrondo, Fabian, Salomé, Grainge |
| 234-11 | Searching for SiO mega-maser in type II AGN | Wang, Zhang |
| 235-11 | The dense gas properties in the AGN with the most turbulent $H^2$ gas motions | Dasyra, Combes |
| 236-11 | MAPI: Monitoring AGN with Polarimetry at the IRAM-30 m | Agudo, Thum, Wiesemeyer, Gómez, Casadio, Molina, Marscher, Jorstad |
| 237-11 | Testing the link between star formation and AGN | Dicken, Nesvadba, Boulanger, Lehnert, Combes, Tadhunter |
| 238-11 | Coordinated cm to mm-monitoring of variability and spectral shape evolution of a selected Fermi blazar sample | Fuhrmann, Zensus, Nestoras, Krichbaum, Angelakis, Schmidt, Ungerechts, Sievers, Readhead |
| 239-11 | A systematic search for absorption lines in z~2 radio galaxies | Nesvadba, Combes, Garcia-Burillo, De Breuck, Collet, Boulanger, Lehnert, Papadopoulos |
| 240-11 | Molecular gas content in radio galaxies at medium redshift (0.3 - 0.6) | Ocaña Flaquer, Leon, Verdes-Montenegro, Scott |
| 241-11 | The molecular gas content of 0.2 < z <0.3 SDSS type 2 quasars. | Villar Martín, De Breuck, Colina, Emonts, Humphrey, Martínez-Sansigre, Pérez-Torres, Rodríguez |
| 242-11 | Interstellar Medium Physical Conditions in a Normal Spiral Galaxy at *z*=1 | Richard, Boone, Dessauges, Egami, Rex, Schaerer, Zamojski, Pello, Combes, Blain, Omont, Kneib |
| 243-11 | CO Study for Dust-Rich Quasars at z <= 2 | Dai, Omont, Bergeron, Willmer, Huang, Rigopoulou, Hatziminaoglou, Perez-Fournon, Elvis, Fazio |
| 244-11 | CO and CI in Intermediate Redshift ULIRGs | Boone, Lim, Gerin, Bayet, Papadopoulos, Dasyra, Combes, Trung, Muller |
| 245-11 | Disentangling SZ Clusters and Dusty Galaxies | Kovács, Staguhn, Benford |
| 246-11 | New strongly lensed galaxies representative of the high-*z* star forming population | De Zotti, Maiolino, González-Nuevo, Andreani, Lapi, Danese, Negrello, Dannerbauer, Omont, Rodighiero, Fan, Serjeant, Birkinshaw, Clements, Smail, Michalowski, Wardlow, Dye |
| 247-11 | COSMO: Characterizing the High Redshift Tail of the SMG Population | Staguhn, Karim, Schinnerer, Smolvcic, Bertoldi, Aravena, Smail, Benford, Kovács |
| 248-11 | Millimeter Photometry of FIR-Bright High Redshift WISE Sources | Benford, Bridge, Eisenhardt, Petty, Tsai, Wright, Wu, Blain |
| 249-11 | GISMO snapshots: Obtaining the flux at 2 mm of the Brightest Herschel-Selected Submm-Galaxies at z>5 | Perez Fournon, Dannerbauer, Bertoldi, Omont, Riechers, Clements, Conley, Cox, Ivison, Michalowski |
| 250-11 | The GDF: The Deepest (Sub-)Millimeter Field Ever | Staguhn, Walter, Kovács, Benford, Decarli, Da Cunha |
| 251-11 | Chasing dust in strongly lensed z>6 star-forming galaxies | Schaerer, Staguhn, Dessauges, Boone, Combes, Kneib, Richard, Zamojski |
| 252-11 | High-J CO lines of lensed high-*z* galaxies discovered by Herschel | van der Werf, Omont, Ivison, Cox, Swinbank, Smail, Dannerbauer, Bertoldi, Rosenberg, Eales, Cooray, Leeuw, Ibar, Vaccari, Coppin, Dunlop, De Zotti, Harris, Baker, Verma, Frayer, Meijerink, Loenen, Berciano, Krips, Lupu, Massardi, Scott, Marrone |

| Ident. | Title | Investigators |
|---|---|---|
| 253-11 | CO Redshift Search for Exceptionally Bright Lensed Herschel Sources | Kneib, Dessauges-Zavadsky, Boone, Combes, Omont, Egami, Rex, Rawle, Schaerer, Smail, Xu |
| 254-11 | Searching for gas in WISE-selected Hyperluminous Galaxies | Blain, Benford, Bridge, Eisenhardt, Jones, Petty, Yan, Tsai, Wu |
| 255-11 | A search for $HeH^+$ at high redshifts | Zinchenko, Dubrovich, Henkel |
| 257-11 | The fragmentation of massive dense cores detected by Herschel | Hennemann, Motte, Csengeri, Schneider, Hill, Luong, Bontemps |
| 260-11 | A complete homogeneous CO survey of northern FU Ori-type objects | Kóspál, Ábrahám, Hogerheijde, Brinch |
| 262-11 | Molecular filament in the Crab Nebula | Salomé, Hily-Blant, Castro-Carrizo, Ferland, Combes, Baldwin, Loh, C Fabian |
| 264-11 | Dense Gas in M 33 - Complementary 12CO(1-0) observations | Buchbender, Kramer, Quintana-Lacaci, Gonzalez-Garcia, Garcia-Burillo, Bertoldi, Anderl, Mookerjea, Braine, Gratier, Billot, Israel |
| D05-11 | CFp as a tracer of Cp, the outermost layers in PDRs | Guzmán, Pety, Gratier, Gerin, Goicoechea, Teyssier, Roueff |
| D06-11 | Isotopic ratios in M82 | LeBourlot |
| D07-11 | Extended submillimeter emission in A2744, galaxies at z>5? | Boone, Schaerer, Lutz, Weiss, Combes, Richard, Dessauges-Zavadsky, Egami, Rex, Rawle, Pello, Staguhn, Edge, Smail, Ivison, Zamojski, Altieri, Kneib, Omont, van der Werf |
| D08-11 | DDT extension for the complete CO(2-1) map of M33 | Braine, Schuster, Kramer, Gonzalez, Sievers, Rodriguez, Gratier, Brouillet, Herpin, Bontemps, Israel, van der Werf, van der Tak, Tabatabaei, Henkel, Roellig, Combes, Wiedner |
| 002-12 | A synoptic view of chemistry in diffuse interstellar gas | Liszt, Pety, Lucas, Gerin |
| 003-12 | The puzzling presence of COMs in prestellar cores: role of photolytic processes | Bacmann, Taquet, Faure, Thiabaud, Quirico, Bonal |
| 004-12 | The role of PAH photo-destruction in the carbon chemistry of PDRs. | Pilleri, Joblin, Berné, Gerin, Montillaud, Fuente, Falgarone, Le Bourlot, Cernicharo, Pety, Kokkin, Goicoechea, González-García, Treviño-Morales, Kramer, Cuadrado, Godard, Le Petit, Teyssier, Habart |
| 005-12 | Deuteration in the PDR around the UCHII region Mon R2 | Treviño-Morales, Fuente, Kramer, Gonzalez-Garcia, Pilleri, Roueff, Gerin, Pety, Cernicharo, Ginard, Berne, Ossenkopf, Goicoechea, Garcia-Burillo, Viti, Rizzo |
| 008-12 | A search for c-$C_3D_2$, a new probe for interstellar deuterium chemistry | Spezzano, Brünken, Schilke, Mccarthy, Caselli |
| 009-12 | A Search for Deuterated Ammonium Ion in Molecular Clouds | Cernicharo, Roueff, Marcelino, Tercero, Fuente, Gerin, Carrasco, Tanarro, Domenech, Herrero |
| 010-12 | $^{15}N$ fractionation at the starting point of star formation | Bizzocchi, Caselli, Leonardo, Dore |
| 011-12 | Nitriles in dark clouds: chemistry and isotopic ratios | Bonal, Faure, Hily-Blant, Le Gal, Quirico, Maret, Rist, Padovani, Pineau des Forêts |
| 012-12 | IRAM Chemical Survey of Sun-Like Star-Forming Regions | Bachiller, Lefloch, Cernicharo, Fuente, Tafalla, De Vicente, Alonso-Albi, Rodriguez, Ceccarelli, Kahane, Bacmann, Hily-Blant, Podio, Le Gall, López-Sepulcre, Faure, Wiesenfeld, Caux, Vastel, Bottinelli, Demyk, Marcelino, Codella, Vasta, Roueff, Gerin, Pineau Des Forets, Cabrit, Gomez-Ruiz, Viti, Caselli, Sakai, Yamamoto, Pety, Gonzalez |
| 013-12 | Unbiased spectral survey of CygX-N63 a unique pre-hot core source | Bontemps, Csengeri, Fechtenbaum, Herpin, Duarte-Cabral, Hennemann, Schneider, Motte, Gursdorf, Lefloch, Wakelam |
| 014-12 | Building a chemical sequence of starless core evolution: a 3mm line survey | Frau, Girart, Beltrán, Tafalla, Morata, Alves, Franco |
| 015-12 | Benchmarking grain-surface chemistry on the Horsehead mane | Guzmán, Pety, Gratier, Gerin, Goicoechea, Bardeau, Belloche, Le Bourlot, Le Petit, Roueff, Teyssier, Sievers |
| 016-12 | An unbiased 3 mm line survey of a protoplanetary disk | Øberg, Graninger, Qi, Wilner |
| 017-12 | A Line Survey of the Supergiant O-rich star VY CMa. II | Cernicharo, Quintana-Lacaci, Sánchez Contreras, Velilla, Bujarrabal, Marcelino, Alcolea, Santander, Pearson, Teyssier |
| 019-12 | From Gas Motions to Star-Forming Cores in Perseus B1-E | Sadavoy, di Francesco, Shirley, André, Hatchell, Pezzuto |
| 020-12 | The Stability of Super-Jeans Starless Cores | Schnee, di Francesco, Johnstone, Sadavoy |
| 021-12 | Using chemistry to constrain the evolutionary state of prestellar cores | Maret, Tafalla, Bergin, Hily-Blant |
| 022-12 | Probing core growth through filamentary accretion in Taurus | Palmeirim, André, Didelon, Peretto, Hennebelle, Arzoumanian, Könyves, Menshchikov |
| 024-12 | Infall and outflow in young IRDC cores | Ragan, Beuther, Linz, Henning |
| 025-12 | Large scale kinematics of the dense gas in IRDCs | Henshaw, Caselli, Tan, Jimenez-Serra, Fontani, Hernandez |
| 027-12 | Observations of $C^{18}O$ J = 1-0 & 2-1: A Direct Method to Obtain Total Column Densities in Hot Cores | Plume, Caux, Bergin, Lis, Cernicharo, Menten, Schilke., Stutzki, Wang |
| 028-12 | Dust properties in star-forming cores | Launhardt, Stutz, Lippok, Henning, Krause, Nielbock, di Francesco, Staguhn, Kovács |
| 029-12 | Understanding the nature of coreshine | Pagani, Andersen, Bacmann, Steinacker |
| 031-12 | Short spacing data for SMA observations of S255 | Zinchenko, Liu, Su |
| 032-12 | Angular Momentum Transportation from Envelopes to Disks | Yen, Takakuwa, Ohashi, Ho |
| 033-12 | The chemical sub-structure of Orion-KL: SMA & 30 m in concert | Feng, Beuther, Semenov, Henning |

| Ident. | Title | Investigators |
|---|---|---|
| 034-12 | MAYS: Mass (and ages) of Young Stars - a CN survey in ρ Oph | Guilloteau, Di Folco, Simon, Piétu, Dutrey, Hersant, Wakelam, Ducourant, Grosso, Guillout, Schaefer, White, Teixera, Palla |
| 035-12 | A quest for high-mass star formation in two families of molecular clumps | Cesaroni, Beltrán, Elia, Molinari, Moscadelli, Olmi, Pestalozzi, Sánchez-Monge, Schisano |
| 037-12 | Molecular fingerprints of an unbiased sample of Galactic MSF clumps | Wyrowski, Csengeri, König, Urquhart, Schuller, Menten, Bontemps, Herpin, Schilke, Beuther, Walmsley, Motte, Garay, Zavagno |
| 040-12 | Polarization study of CN emission towards the massive protostellar objects Cyg-N3 and Cyg-N63: How strong is the role of the magnetic field in the cloud fragmentation? | Herpin, Bontemps, Csengeri, Hezareh, Schneider, Wiesemeyer |
| 041-12 | A Study of the Pumping Mechanisms of SiO masers in Evolved Stars | Cernicharo, Rizzo, Quintana, Dayou, Balanca, Godard, Velilla, Sánchez Contreras |
| 042-12 | Nucleosynthesis in AGB stars traced by isotopic ratios | Decin, Ramstedt, Olofsson, Daza, Milam |
| 044-12 | X-ray induced chemistry: systematic observations of planetary nebulae | Bujarrabal, Kastner, Montez, Alcolea, Castro-Carrizo, Agundez, Santander-García, Balick |
| 045-12 | On the circumstellar envelopes of semi-regular long-period variables | Alcolea, Bujarrabal, Castro-Carrizo |
| 046-12 | Spatially resolved chemistry around SNR IC 443 | Martín Ruiz, Jimenez-Serra, Wesson, Aladro, Viti |
| 047-12 | TIME VARIABILITY OF MOLECULAR LINES IN IRC+10216 | Cernicharo, Quintana-Lacaci, Guélin, Agúndez, Kahane, Teyssier, Pearson, Decin, De Beck, Barlow, Garcia-Lario, Neufeld |
| 048-12 | G0.25+0.02: The Cradle of an Arches-like cluster? | Johnston, Beuther, Longmore, Rathborne, Ragan, Keto |
| 049-12 | 2 mm Continuum Observations of the Galactic Center Region | Staguhn, Kovács, Benford, Morris |
| 050-12 | Molecular gas in luminous M33 HII region complexes | Israel, Braine, Buchbender, Heiner |
| 054-12 | The gas-to-dust ratio in edge-on spiral galaxies | Allaert, Gentile, Baes, Verstappen |
| 055-12 | Low-metallicity star formation: where is the molecular gas? | Lebouteiller, Cormier, Madden, Galliano, Hony, Bayet, Hughes, Barlow, Karczewski, Viti |
| 056-12 | Star formation laws and efficiency from the centre to the outer edge of the XUV disk of the isolated galaxy CIG 96 | Scott, Leon, Montenegro-Verdes, Gil De Paz, Dobbs, Usero, Burillo |
| 057-12 | How Do Stars Form in Extragalactic Spiral Arms? | Topal, Bureau, Bayet, Yildiz, Davis, Ozeren, Yildiz, Etli |
| 058-12 | Mapping galactic disk breaks in CO | Munoz-Mateos, Leroy, Sheth |
| 059-12 | The Behaviour of Cold Gas in Damp-Mergers | Brassington, Duc, Belles, Lisenfeld, Brinks, Mundell |
| 061-12 | Chemical differentiation in the giant molecular halo of M 82 | González-García, García-Burillo, Fuente, Usero, Aladro, Abreu, Pilleri, Berné, Bayet |
| 062-12 | Unleashing the ISM chemistry in isolated galaxies | Martín, Verdes-Montenegro, Aladro, Espada, Kramer, Scott |
| 063-12 | Spectral Line Surveys toward Nearby Spiral Galaxy M51 in 3 mm Band | Yoshimasa, Sorai, Sakai, Yamamoto |
| 064-12 | A Complete Characterization of the Star-forming ISM in M51 with EMIR | Bigiel, Schinnerer, Usero, Leroy, Gonzalez, Pety, Dumas, Hughes, Colombo, Garcia-Burillo |
| 065-12 | Origin of the deviation from the LFIR-LHCN correlation in the most isolated galaxies | Ocaña Flaquer, Scott, Leon, Martín, Verdes-Montenegro |
| 067-12 | Determining the Resolved Star Formation Law and Dust Masses in NGC 6946 | Dwek, Staguhn, Arendt, Eufrasio |
| 069-12 | The gas content of high sSFR galaxies in the local volume: implications for distant galaxies | Lehnert, Driel |
| 070-12 | CO and Star Formation in Gas-dominated Massive Galaxies | Haynes, Huang, Giovanelli, Adams, Brinchmann, Chengalur, Hallenbeck, Hunt, Masters, Saintonge, Spekkens |
| 071-12 | CO and Star Formation Efficiency in Mass-Selected Major Mergers | Gao, Xu, Lisenfeld, Yun, Jarrett |
| 072-12 | Star formation efficiencies and XCO in intermediate mass galaxies | Saintonge, Tacconi, Kauffmann, Kramer, Schiminovich, Buchbender, Catinella, Cortese, Fabello, Genzel, Gracia-Carpio, Giovanelli, Haynes, Heckman, Moran, Schuster, Sternberg, Wang |
| 073-12 | The Role of Molecular Gas in Galaxy Disk Growth and Evolution | Bigiel, Kauffmann, Usero, Saintonge, Gonzalez, Catinella, Wang, Jozsa, Serra |
| 074-12 | Using IRAM to Construct the First Detailed Timeline of Early-Type Galaxy Evolution | Zabludoff, Shirley, Yang, Walter, Narayanan, Smith |
| 075-12 | Dust and molecular gas in Virgo star-forming dwarf galaxies | Grossi, Corbelli, Hunt, Bianchi, Giovanardi, Magrini, Pappalardo, Madden, Bomans, Davies, Smith, Bizzocchi, De Medeiros, Papaderos, De Looze, Verstappen, Garcia, Vlahakis |
| 076-12 | Molecular Gas and Nuclear Activity in Isolated, Non-Interacting Luminous Infrared Galaxies | Iwasawa, Evans, Aalto, Frayer, Perez-Torres, Privon, Herrero-Illana, Surace, Kim, Mazzarella, Armus, Stierwalt, Conway |
| 077-12 | Dense Gas in the HerCULES Sample | Weiss, van der Werf, Rosenberg, Greve, Downes, Papadopoulos, Walter, Aalto |
| 078-12 | The KS Law, Nitrogen Chemistry, and Nucleosynthesis in Nearby Vigorously Star Forming Galaxies | Henkel, García-Burillo, Aalto, Papadopoulos, Zhang, Gao, Graciá-Carpio, Mühle, Asiri, Pérez-Beaupuits, Mauersberger, Baan, Costagliola, Spaans, Ao |
| 079-12 | Understanding AGN feedback with gas chemistry in NGC 1266 | Davis, Bayet, Martín, Meier, Young, Alatalo, Crocker, Bureau, Blitz |

| Ident. | Title | Investigators |
|---|---|---|
| 082-12 | Testing the link between star formation and AGN | Dicken, Nesvadba, Boulanger, Lehnert, Combes, Tadhunter |
| 083-12 | Radio cores shedding light on molecular outflows | Dasyra, Combes |
| 085-12 | The variability of the intrinsic radio power of AGN in cluster cores with GISMO | Edge, Hogan, Staguhn, Kovács, Benford, Hlavacek-Larrondo, Fabian, Salomé, Grainge |
| 086-12 | MAPI: Monitoring AGN with Polarimetry at the IRAM-30 m | Agudo, Thum, Gómez, Casadio, Molina, Marscher, Jorstad, Wiesemeyer |
| 087-12 | Coordinated cm to mm monitoring of variability and spectral evolution of a selected it Fermi blazar sample | Fuhrmann, Zensus, Nestoras, Krichbaum, Angelakis, Schmidt, Karamanavis, Ungerechts, Sievers, Readhead |
| 089-12 | Measuring the ISM content of optically luminous Type 2 QSOs | Petric, Ho, Omont, Billot |
| 090-12 | TANGO: Molecular gas content in radio galaxies at medium redshift | Ocaña Flaquer, Leon, Verdes-Montenegro, Scott |
| 091-12 | CO Study for Dust-Rich Quasars at Intermediate Redshifts | Dai, Bergeron, Omont, Elvis, Fazio, Huang, Hatziminaoglou, Perez-Fournon, Rigopoulou, Willmer |
| 092-12 | The molecular gas content of 0.2< z < 0.35 SDSS type 2 quasars. | Villar Martín, Colina, García-Burillo, Pérez-Torres, Rodríguez, De Breuck, Emonts, Humphrey, Martínez-Sansigre |
| 093-12 | Obtaining CO(1-0) and CO(2-1) for ULIRGs with mid and high-J CO measurements from Herschel-SPIRE-FTS | Spoon, Farrah, Afonso, Bernard-Salas, Borys, Clements, Connolly, Connolly, Cooray, Cormier, Efstathiou, Lebouteiller, Oliver, Pearson, Rigopoulou, Roseboom, Rowan-Robinson, Surace, Verma, Wang, Wardlow, Westmoquette |
| 094-12 | Bridging local and high-*z* ULIRGs; A detailed study of the ISM in z~0.5 ULIRGs | Magdis, Rigopoulou, Cox, Herrero, Omont, Heywood, Oliver, Bock, Pearson, Farrah, Virdee, Huang, Valtchanov |
| 095-12 | Search for a cosmological variation of the proton-electron mass ratio via methanol | Ubachs, Henkel, Bagdonaite, Menten |
| 097-12 | GISMO snapshots: Obtaining the flux at 2 mm of Ultra-Red Herschel Galaxies | Perez Fournon, Dannerbauer, Bertoldi, Omont, Riechers, Clements, Conley, Cox, Ivison, Michalowski |
| 098-12 | The GISMO 2 mm GDF: Pushing the Deepest (Sub-) Millimeter Field To the Confusion Limit | Staguhn, Walter, Kovács, Benford, Decarli, Da Cunha |
| 099-12 | Disentagling SZ Clusters and Dusty Galaxies. | Kovács, Staguhn, Benford |
| 102-12 | CO Redshift Search for Exceptionally Bright Lensed Herschel Sources | Kneib, Dessauges-Zavadsky, Boone, Combes, Omont, Egami, Rex, Rawle, Swinbank, Schaerer, Smail |
| 103-12 | Variation of Physical Constants: molecular absorption at high z | Lattanzi, Combes, Petitjean, Salome |
| 104-12 | Extreme Star formation in five QSOs at z~4.8 | Salomé, Combes, Dasyra |
| 105-12 | Ambipolar diffusion and magnetic fields in envelopes of prestellar cores | Lippok, Launhardt, Li, Pavlyuchenkov, Stutz, Henning |
| 106-12 | Probing $C^{18}O$ in the envelope of the intermediate mass (IM) protostar NGC 7129 FIRS 2 | Fuente, Caselli, Mccoey, Cernicharo, Johnstone, Castro-Carrizo, Fich, Dishoeck, Kempen, Tisi, Alonso-Albi |
| 111-12 | Looking for embedded compact sources in cold, massive clumps revealed by ATLASGAL | Csengeri, Wyrowski, Urquhart, Menten, Schuller, Bontemps |
| D01-12 | Completing the chemical survey with the template source Orion-KL (053-11) | Beuther, Gerner, Linz, Henning, Vasyunina, Semenov, Banerjee, Dullemond |

## PLATEAU DE BURE INTERFEROMETER

| Ident. | Title of investigation | Authors |
|---|---|---|
| Q052 | Deep study of the circumstellar envelopes of AGB & early post-AGB stars | Castro-Carrizo, Alcolea, Bujarrabal, Grewing, Lindqvist, Lucas, Neri, Olofsson, Quintana-Lacaci, Schöier, Winters |
| S0D7 | Star Forming Histories and Gas Fractions of Galaxies from *z*=1-3 | Genzel, Tacconi, Davis, Bolatto, Bournaud, Burkert, Combes, Cooper, Cox, Schreiber, Garcia-Burillo, Gracia-Carpio, Lutz, Naab, Neri, Omont, Shapiro, Shapley, Sternberg, Weiner |
| T0C5 | The [CII]-forest: a new powerful tool for cosmology | Maiolino, Gallerani, Ferrara, Lutz, Genzel, Tacconi |
| T0CC | IRAM Lensing Survey: Probing Galaxy Formation in the Early Universe | Kneib, Clément, Cuby, Peroux, Ilbert, Jablonka, Boone, Combes, Neri, Krips, Lagache, Beelen, Pello, Courbin, Meylan, Schaerer, Dessauges, Knudsen, van der Werf, Richard, Smail, Swinbank, Chapman, Ivison, Egami, Altieri, Valtchanov |
| U052 | Class 0 protostars with PdBI: Solving the angular momentum problem? | André, Maury, Testi, Launhardt, Codella, Cabrit, Gueth, Lefloch, Maret, Bottinelli, Bacmann, Belloche, Bontemps, Hennebelle, Klessen, Dullemond |
| U09E | An Exploratory Redshift Survey in the Hubble Deep Field North | Walter, Carilli, Daddi, Cox, Riechers, Decarli, Bertoldi, Weiss, Neri, Menten, Dannerbauer, Bell, Dickinson, Ellis, Chiu, Krumholz, Robertson |
| U0DE | Physics of Gas and Star Formation in Galaxies at *z*=1.2 | Tacconi, Combes, Genzel, Bolatto, Bournaud, Burkert, Cooper, Cox, Davis, Förster Schreiber, García-Burillo, Graciá-Carpio, Lutz, Naab, Neri, Newman, Sternberg, Weiner |
| V--8 | A high-resolution map in C[II] of HDF850.1. - A possible example of a merger at z = 5.2 | Cox, Neri, Walter, Downes, Krips |
| V--A | Influence of environment on cold gas in galaxies at moderate redshift | Jablonka, Combes, Rines, Finn |

| Ident. | Title of investigation | Authors |
|---|---|---|
| V--B | Confirming pure rotational emission from TiO and TiO2 toward VY CMa | Menten, Kaminśki, Young, Patel, Gottlieb |
| V007 | Revealing substructure in a very young starless core in the Pipe Nebula | Girart, Frau, Palau, Padovani, Morata, Beltrán, Estalella |
| V021 | Physical conditions in the interstellar medium of early-type galaxies | Bureau, Topal, Bayet, Krips, Crocker, Young, Blitz, Combes, Davis, Alatalo, Cappellari, Emsellem, Krajnovic, McDermid |
| V043 | Continuum imaging of the brightest mm sources from H-ATLAS | Bertoldi, Dannerbauer, Cox, Omont, Neri, Beelen, Negrello, Dunne, Verma, Ivison, Eales, Cooray, Glenn, Michalowski, van der Werf, Bussmann, Riechers, de Zotti, Ibar |
| V04A | An efficient Program for Finding Lensed Galaxies at z>4 - II | Krips, Cox, Dannerbauer, Eales, Omont, Beelen, Bertoldi, Dunne, Aretxaga, Hughes, Ivison, Cooray, Dye, Frayer, Negrello, Smail |
| V053 | The nucleus and inner coma of comet C/2009 P1 (Garradd) | Boissier, Bockelée-Morvan, Groussin, Biver, Crovisier, Moreno, Colom, Jorda, Lamy |
| V054 | Mapping the D/H ratio in the Martian atmosphere | Fouchet, Moreno, Lellouch, Montmessin |
| V059 | The origin of molecules in protostellar jets: a pilot study of HH 111 | Lefloch, Cabrit, Yvart, Gueth, Codella, Pineau des Forêts, Podio, Dougados |
| V05A | Nature of a candidate first protostellar core discovered with Herschel & MAMBO | Maury, André, Könyves, Men'shchikov, Bontemps, Pezzuto, Testi, Ward-Thompson, Commerçon, Hennebelle |
| V05B | Precise measurements of the deuteration of water in low-mass protostars | Persson, Jørgensen, Dishoeck, Harsono |
| V060 | Fragmentation and monolithic collapse to form high-mass stars | Bontemps, Csengeri, Duarte-Cabral, Schneider, Motte, Gueth, Herpin, Bonnell, Commerçon, Hennebelle |
| V061 | The fragmentation of massive dense cores detected by Herschel | Hennemann, Motte, Csengeri, Schneider, Hill, Luong, Bontemps |
| V064 | The Physical Structure of Embedded Disks | van Dishoeck, Harsono, Jørgensen, Hogerheijde, San Jose Garcia |
| V065 | The innermost regions of high-mass accretion disks | Beuther, Linz, Henning |
| V06C | A complete homogeneous CO survey of northern FU Ori-type objects | Kóspál, Ábrahám, Hogerheijde, Brinch |
| V06E | UY Aurigae: a prototypical circumbinary disk? | Piétu, Tang, Dutrey, Guilloteau, Di Folco, Boehler, Gueth, Beck, Barry, Simon |
| V06F | Dust in low-weight disks: constraining models of grain evolution | Testi, Benisty, Natta, Ricci, Birnstiel, Neri |
| V074 | Masers and shocks in the gas around HVC stars | Quintana-Lacaci, Castro-Carrizo, Bujarrabal, Alcolea |
| V075 | Testing the anion chemistry II: the case of CN- | Guélin, Cernicharo, Agundez, Winters, Thaddeus, Gottlieb, McCarthy |
| V077 | The mass loss properties of the Red Supergiant stars | Quintana-Lacaci, Castro-Carrizo, Bujarrabal |
| V078 | Molecular filament in the Crab Nebula | Salomé, Hily-Blant, Castro-Carrizo, Ferland, Combes, Baldwin, Loh, Fabian |
| V07E | Chemistry and environment of M 82 and IC 342: a mapping survey | Henkel, Mauersberger, Martin, Aladro, Bayet, Viti, Wiklind, Peck, Vila-Vilaro, Sawada, Matsushita, Papadopoulos |
| V085 | Dense Molecular Gas around AGN | Davies, Sternberg, Graciá-Carpio, Mark, Orban de Xivry, Dodds-Eden |
| V086 | Imaging the remarkable dense AGN wind from the ULIRG Mrk231 | Aalto, Garcia-Burillo, Costagliola, Muller, van der Werf, Henkel, Winters, Neri |
| V087 | Towards a physical understanding of the massive outflow in Mrk 231 | Feruglio, Fiore, Maiolino, Piconcelli, Cicone, Krips, Chang, Aussel |
| V088 | A new molecular outflow and/or streamer in NGC6240 | Feruglio, Fiore, Maiolino, Piconcelli, Cicone, Sturm, Davies |
| V08A | Cygnus A: AGN feedback and cooling flow | Casasola, Combes, Nakai, Salomé, Prandoni, Mignano, García-Burillo, Paladino, Hunt, Magrini, Rossetti |
| V08B | Mapping the HCN and HCO+ emission in NGC 1275 | Salomé, Edge, Combes, Downes, Lim, Egami, Fabian, Johnstone, Oonk, Mittal, McNamara, Ferland, Boulanger, Nesvadba |
| V08C | Resolving Molecular Outflows in LIRGs/ULIRGs: the case of IRAS17208-0014 | García-Burillo, Colina, Alonso-Herrero, Aalto, Combes, Canadas, Arribas, van der Werf, Villar-Martin, Costagliola, Usero, Henkel, Hunt, Neri, Muller, Planesas |
| V094 | The nature of the unique source SWIFT J1644+57 | Guziy, Agudo, Castro-Tirado, Bremer, Winters, Gorosabel, Gómez, Sánchez-Ramirez, Tello |
| V095 | First detections of molecular emission in damped Lyman-α systems | Dessauges-Zavadsky, Kanekar, Fumagalli, Prochaska |
| V09A | The Molecular Component of a Massive Outflow at $z$=1.2 | Hailey-Dunsheath, Stacey, Brisbin, Nikola, Ferkinhoff |
| V09D | Searching for Molecular Gas in a Highly Amplified Star-Forming Spiral Galaxy at $z$=1.49 | Swinbank, Bower, Livermore, Richard, Smail |
| V09E | 2 in 1: Gas fractions in a z = 1.4 elliptical & its enigmatic neighbour | Sargent, Daddi, Onodera, Strazzullo, Dannerbauer, Bournaud, Martig |
| V0A2 | Connecting QSOs and SMGs: Completing the sample. | Smail, Swinbank, Simpson, Danielson, Cox, Bonfield, van der Werf, Jarvis, Coppin, Ivison, Hughes, Vaccari, Dunlop, Verma, Clements, Leeuw, Smith |
| V0A3 | Understanding the link between SMGs and "main sequence" star forming galaxies | Bothwell, Chapman, Genzel, Tacconi, Lutz, Greve, Bertoldi, Neri, Omont, Cox, Smail, Ivison, Biggs, Blain, Casey, Muxlow, Beswick |
| V0A6 | Understanding the Nature of Herschel-Selected Submillimeter Galaxies | Riechers, Omont, Perez-Fournon, Cox, Cooray, Wardlow, Neri, Clements, Ivison, Bock, Oliver |

| Ident. | Title of investigation | Authors |
|---|---|---|
| V0A7 | Hi-res imaging of a uniquely bright sample of SMGs - II | Cox, Ivison, Bertoldi, Omont, Fournon, Cooray, Eales, Frayer, Jarvis, Krips, Negrello, Neri, Smail, Swinbank, van der Werf, Leeuw, Dannerbauer, Verma |
| V0A9 | A Systematic Study of CO Excitation in High-Redshift Quasar Host Galaxies | Riechers, Walter, Carilli, Neri, Cox, Weiss, Bertoldi |
| V0AA | The nature of star formation in merging-driven starburts at z>2 | Magdis, Daddi, Sargent, Dickinson, Strazzullo, Elbaz, Pannella, Galliano, Walter, Feruglio |
| V0B0 | Identification of the highest redshift H-ATLAS and HerMES galaxies | Bertoldi, Perez-Fournon, Omont, Dannerbauer, Lagache, Bethermin, Michalowski, Ivison, Clements, Negrello, White, Benford, Temi, Vaccari, Riechers, Bock, Vieira, Cooray, Wardlow, Coppin, Frayer, DeZotti, Massardi, Cava |
| V0B1 | Exploring emission in high-*z* strongly lensed Herschel galaxies | Omont, van der Werf, Neri, Cox, Krips, Riechers, Harris, Weiss, Gavazzi, Baker, Bertoldi, Beelen, Clements, Cooray, Dannerbauer, Eales, Frayer, Guélin, Ivison, Lehnert, Lupu, Michalowski, Negrello, Leeuw |
| V0B2 | A survey of ionized Nitrogen ([NII]) at high redshift. | Decarli, Walter, Maiolino, Carilli, Riechers, Bertoldi, Weiss, Cox, Neri |
| V0B3 | Minor mergers and quasar feedback at *z*=4 | Maiolino, Gallerani, Neri, Walter, Martin, de Breuck, Caselli, Krips, Meneghetti, Nagao, Wagg, Walmsley |
| V0B6 | Faint CO Emitters in the Hubble Deep Field North | Walter, Carilli, Daddi, Cox, Riechers, Decarli, da Cunha, Bertoldi, Weiss, Neri, Elbaz, Menten, Dannerbauer, Bell, Dickinson, Ellis, Chiu, Krumholz |
| V0B8 | Comprehensive Study of an Exceptionally Bright Lensed SMG at z~4.6 | Boone, Combes, Egami, Omont, Dessauges-Zavadsky, Schaerer, Richard, Kneib, Smail, Swinbank, Edge, Ivison, van der Werf, Rex, Rawle, Gurwell, Casey, Smith, Pham, Pello |
| V0B9 | A first [CII] imaging survey of z>4 galaxies | Bertoldi, Knudsen, Walter, Riechers, Cox, Carilli, Wang, Maiolino, Omont, Weiss, Neri, Schinnerer |
| V0BA | Constraining the gas content of main sequence galaxies at 4.4 < z < 5.6 | Daddi, Sargent, Dickinson, Walter, Bournaud, Madden, Dekel, Dannerbauer, Elbaz, Magdis, Feruglio |
| V0BD | A Detailed Investigation of the ISM in the Most Distant Starburst Galaxy | Riechers, Perez-Fournon, Omont, Cox, Bradford, Clements, Cooray, Wardlow, Neri, Krips, Dowell, Ivison, Conley, Vieira, Bock, Oliver |
| V0BE | Nature and Excitation of Submillimeter $H^2O$ Emission at *z*=6.42 | Riechers, Weiss, Walter, Neri, van der Werf, Cox, Carilli, Bertoldi, Wang, Omont, Maiolino |
| V0C0 | Atomic and Molecular Gas in a Spectroscopically Confirmed Quasar Host Galaxy at *z*=7.1 | Venemans, Walter, Decarli |
| V0C2 | Unveiling the population of highly obscured and high-*z* gamma-ray bursts (ToO) | Castro-Tirado, Bremer, Winters, Gorosabel, Guziy, de Ugarte Postigo, Pérez-Ramírez, Castro Cerón, Tello, Sánchez-Ramírez |
| W--1 | A likely z ~3 galaxy cluster detected with Planck, Herschel, and Spitzer [DDT] | Dole, Nesvadba, König, Krips, Chary, Beelen, Flores-Cacho, Frye, Giard, Guery, Lagache, Montier, Omont, Pointecouteau, Puget, Welikala, Yan |
| W--2 | Luminous CO in bright Herschel-ATLAS galaxies at z~3 | Neri, Cox, Omont, Downes, Ivison, Krips |
| W--3 | High-velocity molecular gas around SgrA*: feeding the monster | Cernicharo, Lefloch |
| W--5 | DDT proposal: Characterizing the ISM in a z~11 Galaxy | Walter, Riechers, Carilli, Decarli, Cox, Neri, Bertoldi, Weiss |
| W005 | Outflow shocks traced in SiO: early hints for star formation in IRDCs | Linz, Ragan, Beuther, Vasyunina, Schmiedeke |
| W009 | Looking for embedded compact sources in cold, massive clumps revealed by ATLASGAL | Csengeri, Wyrowski, Urquhart, Menten, Schuller, Bontemps |
| W00A | HDO and complex molecules in a deeply embedded low-mass protostar | Persson, Jørgensen, Dishoeck, Harsono, Bisschop |
| W00B | Ambipolar diffusion and magnetic fields in envelopes of prestellar cores | Lippok, Launhardt, Li, Pavlyuchenkov, Stutz, Henning |
| W00D | Probing $C^{18}O$ in the envelope of the intermediate mass (IM) protostar NGC 7129 FIRS 2 | Fuente, Caselli, McCoey, Cernicharo, Johnstone, Castro-Carrizo, Fich, Dishoeck, Kempen, Tisi, Alonso-Albi |
| W00F | Probing the expansion of a hypercompact HII region | Sánchez-Monge, Moscadelli, Cesaroni, Beltrán, Neri |
| W010 | Investigating Molecular outflows in Brown Dwarfs | Dougados, Whelan, Monin, Lefloch, Alves, Cabrit |
| W013 | Grain growth in transitional disks | Pinilla, Ricci, Benisty, Isella, Natta, Testi |
| W014 | Constraining the evolution of solids in protoplanetary disks with the PdBI | Ricci, Testi, Williams, Wilner, Neri |
| W016 | MaYS, Mass (and ages) of Young Stars: Dynamical masses from CN(2-1) | Guilloteau, Di Folco, Simon, Piétu, Dutrey, Hersant, Wakelam, Ducourant, Grosso, Guillout, Schaefer, White, Teixera, Palla, Chapillon |
| W018 | Structure and excitation in the CSEs around C-stars with high expansion velocity | Quintana-Lacaci, Castro-Carrizo, Bujarrabal, Alcolea |
| W019 | Testing the anion chemistry in IRC+10216 (3): Where is $C_4H$? | Guélin, Cernicharo, Agundez, Winters, Thaddeus, McCarthy |
| W01D | Peering into a site of cosmic rays acceleration | Ceccarelli, Hily-Blant, Vaupré |
| W01E | A cold gas reservoir to fuel M31 nuclear black hole and stellar cluster | Melchior, Combes |
| W022 | Mapping the molecular gas conditions in nearby starburst galaxies | Rodríguez, Mühle, Aalto, Alberdi, Pérez-Torres |
| W026 | Massive molecular outflows and negative feedback in active galaxies | Sturm, Graciá-Carpio, Maiolino, González-Alfonso, Hailey-Dunsheath, Davies, Veilleux, Fischer, Feruglio, Piconcelli, Fiore, Garcia-Burillo, Aalto, Cicone |
| W027 | CO-to-$H_2$ conversion factor in Mrk 231 | Feruglio, Aalto, Maiolino, Sturm, Cicone, Fiore, Garcia-Carpio, Veilleux, Piconcelli, Garcia-Burillo, Bremer, Winters, Aussel, Krips, Chang |

| Ident. | Title of investigation | Authors |
|---|---|---|
| W028 | Vibrationally excited HCN in Mrk231 - Probing the hot core and the nuclear outflow | Aalto, Muller, Costalgiola, Garcia-Burillo, van der Werf, Winters, Henkel, Gonzalez-Alfonso, Neri |
| W02B | A molecular outflow in the advanced merger NGC 1614 | García-Burillo, Usero, Casznadas, Colina, Aalto, Alonso-Herrero, Combes, Hunt, Tacconi, Graciá-Carpio, Neri, Planesas, Arribas |
| W02D | Monitoring periodic flux variations of 3C 66B | Iguchi, Okuda, Sudou, Matsuzawa, Yoshiike, Nagai |
| W02E | The nature of the unique source SWIFT J1644+57 | Agudo, Castro-Tirado, Guziy, Bremer, Winters, Gorosabel, Gómez, Sánchez-Ramirez, Tello |
| W032 | The highest density starbursts in the Universe | Hickox, Geach, Diamond-Stanic, Moustakas, Robania, Rudnick, Tremonti |
| W034 | The Interplay Between Feedback and Gas Supply at Intermediate Redshift | Rubin, Decarli, Cucchiara, Walter, Hennawi, Prochaska, Fumagalli |
| W036 | Deciphering the impact of the environment on cold gas in cluster galaxies | Jablonka, Combes, Kneib, Jauzac, Egami, Haines, Pereira |
| W037 | Galaxy Evolution and Star Formation Efficiency at 0.6 < z < 1. | Combes, García-Burillo, Braine, Schinnerer, Walter, Colina |
| W039 | First mm observations of a massive black hole binary candidate. | Decarli, Dotti, Volonteri, Walter |
| W03A | Feedback & Mergers in Luminous AGN at *z*=1.3 | Rosario, Lutz, Genzel, Tacconi, Combes, Saintonge |
| W03E | Molecular Gas in a Galaxy Cluster at z = 1.4 | Casasola, Magrini, Combes, Fontani, Mignano, Paladino, Sani |
| W03F | The Molecular Gas in High-*z* Star-Forming Galaxies from HiZELS | Swinbank, Smail, Simpson, Sobral, Best, Geach, van der Werf |
| W041 | First detection of CO in a high-*z* Compton-Thick QSO | Feruglio, Daddi, Fiore, Comastri, Elbaz, Alexander, Dickinson, Piconcelli, Gilli, Brusa, Vignali, Onodera, Bournaud, Sargent, Pannella, Krips |
| W042 | Measuring molecular gas in strongly lensed star-forming galaxies | Dessauges-Zavadsky, Combes, Boone, Omont, Schaerer, Zamojski, Richard, Kneib, Egami, Rex, Rawle, van der Werf, Péroux |
| W043 | CO in high-*z* lensed galaxies with Herschel spectra | Nesvadba, Malhotra, Combes, Rhoads, Guerin, Lehnert, Frye |
| W044 | Does AGN activity in galaxies correlate with their gas content? | Mullaney, Daddi, Sargent, Juneau, Elbaz, Dickinson |
| W045 | Herschel Extreme Starbursts at Redshift ~2 | Rodighiero, Lutz, Tacconi, Genzel, Förster Schreiber, Wuyts, Popesso, Berta, Renzini, Cimatti, Gruppioni, Zamorani, Andreani, Daddi, Carollo, Lilly, Onodera, Bschorr, Franceschini, Baronchelli, Lo, Faro, Silverman |
| W046 | Confirming the membership of SMGs in the most distant galaxy cluster | Dannerbauer, Daddi, Strazzullo, Gobat, Sargent, Carollo, Cimatti, Figoguenov, Onodera, Pannella, Renzini, Ziegler |
| W04A | Understanding the Nature of Herschel-Selected Submillimeter Galaxies | Riechers, Omont, Perez-Fournon, Neri, Cox, Cooray, Wardlow, Clements, Ivison, Magdis, Bock, Oliver |
| W04C | CO in the most overdense cluster known at z>2. | Chapman, Aravena, Smail, Steidel |
| W04D | Exploring the Cores of Lensed Herschel Galaxies Using $H_2O$ Lines | Omont, van der Werf, Yang, Neri, Beelen, Krips, Ivison, Cox, Riechers, Harris, Weiss, Gavazzi, Baker, Bertoldi, Bussmann, Cooray, Dannerbauer, Eales, Gao, Fu, Guélin, Lehnert, Lupu, Menten, Negrello |
| W04E | Revealing the Nature of Lyman-α Nebulae in the Distant Universe | Yang, Walter, Decarli, Weiss, Bertoldi |
| W052 | Identification of the highest redshift H-ATLAS and HerMES galaxies | Bertoldi, Perez-Fournon, Omont, Dannerbauer, Lagache, Bethermin, Michalowski, Ivison, Clements, Negrello, White, Benford, Temi, Vaccari, Riechers, Bock, Vieira, Cooray, Wardlow, Coppin, Frayer, DeZotti |
| W053 | Small-scale structure of molecular gas at *z*=5.243 | Boone, Combes, Richard, Egami, Rex, Rawle, Smail, Ivison, Omont, Dessauges-Zavadsky, Schaerer, van der Werf, Pham |
| W054 | A systematic search for CO in a flux limited sample of *z*=6 quasars | Venemans, Walter, Decarli |
| W056 | Exploring the Unusual CO and $H_2O$ Excitation of z~6 Quasars | Riechers, Neri, Walter, Carilli, Wang, Cox, Weiss, Bertoldi, Omont, van der Werf, Fan, Maiolino |
| W058 | A Detailed Investigation of the ISM in the Most Distant Starburst Galaxy | Riechers, Perez-Fournon, Omont, Neri, Cox, Bradford, Clements, Cooray, Wardlow, Krips, Dowell, Ivison, Kamenetzky, Conley, Vieira, Bock, Oliver |
| W059 | Mapping a quasar-driven massive outflow in the early Universe | Maiolino, Gallerani, Neri, Cicone, Ferrara, Genzel, Lutz, Sturm, Tacconi, Walter, Feruglio, Fiore, Pinconcelli |
| W05A | Blind redshifts for ultra-red Herschel galaxies | Krips, Ivison, Bertoldi, Omont, Cox, Neri, Koenig, van der Werf, Dannerbauer, Eales, Valiante, Clements, Swinbank |
| W05E | Unveiling the population of highly obscured and high-*z* gamma-ray bursts (ToO) | Castro-Tirado, Bremer, Winters, Gorosabel, Guziy, De Ugarte Postigo, Pérez-Ramírez, Castro Cerón, Tello, Sánchez-Ramírez |
| W061 | First high resolution mapping of $C_3H^+$ in the ISM | Guzmán, Pety, Gratier, Goicoechea, Gerin |
| W069 | Imaging the spectral signature of a protostellar J-shock | Codella, Gueth, Benedettini, Busquet, Cabrit, Ceccarelli, Lefloch, Nisini, Gómez-Ruiz |
| W075 | How much water in the protoplanetary disk of DG-Tau | Podio, Codella, Cabrit, Kamp, Nisini, Dougados, Gueth, Bacciotti |
| W09C | The nature of the unique source SWIFT J1644+57 | Agudo, Castro-Tirado, Guziy, Bremer, Winters, Gorosabel, Gómez, Sánchez-Ramirez, Tello |
| W0AC | Building Up CO Ladders in Lyman-α Blobs | Yang, Walter, Decarli, Weiss, Bertoldi |
| W0AD | Resolving the morphology of the first WISE-identified ULIRG | Blain, Benford, Bridge, Eisenhardt, Jones, Yan, Tsai, Wu |
| W0B4 | Probing the Excitation of $H_2O$ in Lensed Herschel Galaxies | Omont, van der Werf, Yang, Neri, Beelen, Krips, Ivison, Cox, Riechers, Harris, Weiss, Gavazzi, Spaans, Baker, Bertoldi, Bussmann, Dannerbauer, Downes, Eales, Gao, Fu, Guélin, Lehnert, Lupu, Menten, Michalowski, Negrello, Temi, Valiante |

| Ident. | Title of investigation | Authors |
|---|---|---|
| W0B7 | Ionized Nitrogen ([NII]) at high redshift | Decarli, Walter, Maiolino, Carilli, Riechers, Bertoldi, Weiss, Cox, Neri |
| W0BD | Identification of the highest redshift H-ATLAS and HerMES galaxies | Bertoldi, Perez Fournon, Omont, Dannerbauer, Lagache, Bethermin, Michalowski, Ivison, Clements, Negrello, White, Benford, Temi, Vaccari, Riechers, Bock, Vieira, Cooray, Wardlow, Coppin, Frayer, DeZotti, Massardi, Cava, Smail, Swinbank, Bremer, Verma, Rigopoulou, Aretxaga, Hughes, Marrone, van Kampen, Eales, van der Werf, Bussmann, Conley, Oliver, Valiante |
| W0C3 | A Quasar-Starburst Merger System at the Epoch of Reionization? | Wang, Carilli, Neri, Walter, Riechers, Fan, Willott, Cox, Bertoldi, Omont, Menten, Strauss, Wagg |
| W0CA | Unveiling the population of highly obscured and high-*z* gamma-ray bursts (ToO) | Castro-Tirado, Bremer, Winters, Gorosabel, Guziy, Pérez-Ramírez, Castro Cerón, Tello, Sánchez-Ramírez |

# Annex II – Publications in 2012

the list of refereed publications, conferences and workshop papers as well as thesis based upon data obtained using the IRAM instruments are provided in the following two tables : the first table gives the publications with the IRAM staff members as co-author (including technical publications by the IRAM staff), and the second table those with results from the user's community.

The running number is the cumulative number since the first annual report was published for the year 1987.

## 2012 PUBLICATION LIST: IRAM (CO)AUTHORS :

| | | | |
|---|---|---|---|
| 1651 | Faint high-redshift AGN in the Chandra deep field south: the evolution of the AGN luminosity function and black hole demography | Fiore F., Puccetti S., Grazian A., Menci N., Shankar F., Santini P., Piconcelli E., Koekemoer A. M., Fontana A., Boutsia K., Castellano M., Lamastra A., Malacaria C., Feruglio C., Mathur S., Miller N., Pannella M. | A&A 537, A16 |
| 1652 | Detection of HCN, $HCO^+$, and HNC in the Mrk 231 molecular outflow. Dense molecular gas in the AGN wind | Aalto S., Garcia-Burillo S., Muller S., Winters J. M., van der Werf P., Henkel C., Costagliola F., Neri R. | A&A 537, A44 |
| 1653 | Chemistry in disks. VI. CN and HCN in protoplanetary disks | Chapillon E., Guilloteau S., Dutrey A., Piétu V., Guélin M. | A&A 537, A60 |
| 1654 | The Herschel M 33 extended survey (HerM33es): PACS spectroscopy of the star forming region BCLMP 302 (Corrigendum) | Mookerjea B., Kramer C., Buchbender C., Boquien M., Verley S., Relaño M., Quintana-Lacaci G., Aalto S., Braine J., Calzetti D., Combes F., Garcia-Burillo S., Gratier P., Henkel C., Israel F., Lord S., Nikola T., Röllig M., Stacey G., Tabatabaei F. S., van der Tak F., van der Werf P. | A&A 537, 3 |
| 1655 | Pre-ALMA observations of GRBs in the mm/submm range | de Ugarte Postigo A., Lundgren A., Martìn S., Garcia-Appadoo D., de Gregorio Monsalvo I., Peck A., MichaŃowski M. J., Thöne C. C., Campana S., Gorosabel J., Tanvir N. R., Wiersema K., Castro-Tirado A. J., Schulze S., De Breuck C., Petitpas G., Hjorth J., Jakobsson P., Covino S., Fynbo J. P. U., Winters J. M., Bremer M., Levan A. J., Llorente A., Sánchez-Ramìrez R., Tello J. C., Salvaterra R. | A&A 538, A44 |
| 1656 | The EMIR multi-band mm-wave receiver for the IRAM 30-m telescope | Carter M., Lazareff B., Maier D., Chenu J.-Y., Fontana A.-L., Bortolotti Y., Boucher C., Navarrini A., Blanchet S., Greve A., John D., Kramer C., Morel F., Navarro S., Peñalver J., Schuster K. F., Thum C. | A&A 538, A89 |
| 1657 | Dust and gas power spectrum in M 33 (HERM33ES) | Combes F., Boquien M., Kramer C., Xilouris E. M., Bertoldi F., Braine J., Buchbender C., Calzetti D., Gratier P., Israel F., Koribalski B., Lord S., Quintana-Lacaci G., Relaño M., Röllig M., Stacey G., Tabatabaei F. S., Tilanus R. P. J., van der Tak F., van der Werf P., Verley S. | A&A 539, A67 |
| 1658 | Ammonia and other parent molecules in comet 10P/Tempel 2 from Herschel/HIFI and ground-based radio observations | Biver N., Crovisier J., Bockelée-Morvan D., Szutowicz S., Lis D. C., Hartogh P., de Val-Borro M., Moreno R., Boissier J., Kidger M., Küppers M., Paubert G., Dello Russo N., Vervack R., Weaver H. | A&A 539, A68 |
| 1659 | On the physical structure of IRC +10216. Ground-based and Herschel observations of CO and $C_2H$ | De Beck E., Lombaert R., Agúndez M., Daniel F., Decin L., Cernicharo J., Müller H. S. P., Min M., Royer P., Vandenbussche B., de Koter A., Waters L. B. F. M., Groenewegen M. A. T., Barlow M. J., Guélin M., Kahane C., Pearson J. C., Encrenaz P., Szczerba R., Schmidt M. R. | A&A 539, A108 |
| 1660 | The first IRAM/PdBI polarimetric millimeter survey of active galactic nuclei. II. Activity and properties of individual sources | Trippe S., Neri R., Krips M., Castro-Carrizo A., Bremer M., Piétu V., Winters J. M. | A&A 540, A74 |
| 1661 | Imaging diffuse clouds: bright and dark gas mapped in CO | Liszt H. S., Pety J. | A&A 541, A58 |
| 1662 | 3C 286: a bright, compact, stable, and highly polarized calibrator for millimeter-wavelength observations | Agudo I., Thum C., Wiesemeyer H., Molina S. N., Casadio C., Gómez J. L., Emmanoulopoulos D. | A&A 541, A111 |
| 1663 | Simultaneous Planck, Swift, and Fermi observations of X-ray and X-ray selected blazars | Giommi P., Polenta G., Lähteenmäki A., Thompson D. J., Capalbi M., Cutini S., Gasparrini D., González-Nuevo J., León-Tavares J., López-Caniego M., Mazziotta M. N., Monte C., Perri M., Rainò S., Tosti G., Tramacere A., Verrecchia F., Aller H. D., Aller M. F., Angelakis E., Bastieri D., Berdyugin A., Bonaldi A., Bonavera L., Burigana C., Burrows D. N., Buson S., Cavazzuti E., Chincarini G., Colafrancesco S., Costamante L., Cuttaia F., D'Ammando F., de Zotti G., Frailis M., Fuhrmann L., Galeotta S., Gargano F., Gehrels N., Giglietto N., Giordano F., Giroletti M., Keihänen E., King O., Krichbaum T. P., Lasenby A., Lavonen N., Lawrence C. R., Leto C., Lindfors E., Mandolesi N., Massardi M., Max-Moerbeck W., Michelson P. F., Mingaliev M., Natoli P., Nestoras I., Nieppola E., Nilsson K., Partridge B., Pavlidou V., Pearson T. J., Procopio P., Rachen J. P., Readhead A., Reeves R., Reimer A., Reinthal R., Ricciardi S., Richards J., Riquelme D., Saarinen J., Sajina A., Sandri M., Savolainen P., Sievers A., Sillanpää A., Sotnikova Y., Stevenson M., Tagliaferri G., Takalo L., Tammi J., Tavagnacco D., Terenzi L., Toffolatti L., Tornikoski M., Trigilio C., Turunen M., Umana G., Ungerechts H., Villa F., Wu J., Zacchei A., Zensus J. A., Zhou X. | A&A 541, A160 |
| 1664 | Herschel/HIFI observation of highly excited rotational lines of HNC toward IRC +10 216 | Daniel F., Agúndez M., Cernicharo J., De Beck E., Lombaert R., Decin L., Kahane C., Guélin M., Müller H. S. P. | A&A 542, A37 |
| 1665 | On the calibration of full-polarization 86 GHz global VLBI observations | Martì-Vidal I., Krichbaum T. P., Marscher A., Alef W., Bertarini A., Bach U., Schinzel F. K., Rottmann H., Anderson J. M., Zensus J. A., Bremer M., Sanchez S., Lindqvist M., Mujunen A. | A&A 542, A107 |
| 1666 | Giant molecular clouds in the Local Group galaxy M 33* | Gratier P., Braine J., Rodriguez-Fernandez N. J., Schuster K. F., Kramer C., Corbelli E., Combes F., Brouillet N., van der Werf P. P., Röllig M. | A&A 542, A108 |
| 1667 | The structure of hot gas in Cepheus B | Mookerjea B., Ossenkopf V., Ricken O., Güsten R., Graf U. U., Jacobs K., Kramer C., Simon R., Stutzki J. | A&A 542, L17 |

| | | | |
|---|---|---|---|
| 1668 | Spectral line survey of the ultracompact HII region Monoceros R2 | Ginard D., González-Garcìa M., Fuente A., Cernicharo J., Alonso-Albi T., Pilleri P., Gerin M., Garcìa-Burillo S., Ossenkopf V., Rizzo J. R., Kramer C., Goicoechea J. R., Pety J., Berné O., Joblin C. | A&A 543, A27 |
| 1669 | Molecular abundances in the inner layers of IRC +10216 | Agúndez M., Fonfrìa J. P., Cernicharo J., Kahane C., Daniel F., Guélin M. | A&A 543, A48 |
| 1670 | Cool and warm dust emission from M 33 (HerM33es) | Xilouris E. M., Tabatabaei F. S., Boquien M., Kramer C., Buchbender C., Bertoldi F., Anderl S., Braine J., Verley S., Relaño M., Quintana-Lacaci G., Akras S., Beck R., Calzetti D., Combes F., Gonzalez M., Gratier P., Henkel C., Israel F., Koribalski B., Lord S., Mookerjea B., Rosolowsky E., Stacey G., Tilanus R. P. J., van der Tak F., van der Werf P. | A&A 543, A74 |
| 1671 | The physics and the structure of the quasar-driven outflow in Mrk 231 | Cicone C., Feruglio C., Maiolino R., Fiore F., Piconcelli E., Menci N., Aussel H., Sturm E. | A&A 543, A99 |
| 1672 | Resolved [CII] emission in a lensed quasar at z = 4.4 | Gallerani S., Neri R., Maiolino R., Martìn S., De Breuck C., Walter F., Caselli P., Krips M., Meneghetti M., Nagao T., Wagg J., Walmsley M. | A&A 543, A114 |
| 1673 | The IRAM-30m line survey of the Horsehead PDR. I. $CF^+$ as a tracer of $C^+$ and as a measure of the fluorine abundance | Guzmán V., Pety J., Gratier P., Goicoechea J. R., Gerin M., Roueff E., Teyssier D. | A&A 543, L1 |
| 1674 | Spectrally resolved C II emission in M 33 (HerM33es). Physical conditions and kinematics around BCLMP 691 | Braine J., Gratier P., Kramer C., Israel F. P., van der Tak F., Mookerjea B., Boquien M., Tabatabaei F., van der Werf P., Henkel C. | A&A 544, A55 |
| 1675 | CN Zeeman observations of the NGC 2264-C protocluster | Maury A. J., Wiesemeyer H., Thum C. | A&A 544, A69 |
| 1676 | Submillimeter line emission from LMC 30 Doradus: The impact of a starburst on a low-metallicity environment | Pineda J. L., Mizuno N., Röllig M., Stutzki J., Kramer C., Klein U., Rubio M., Kawamura A., Minamidani T., Benz A., Burton M., Fukui Y., Koo B.-C., Onishi T. | A&A 544, A84 |
| 1677 | Herschel/HIFI observations of CO, $H_2O$ and $NH_3$ in Monoceros R2 | Pilleri P., Fuente A., Cernicharo J., Ossenkopf V., Berné O., Gerin M., Pety J., Goicoechea J. R., Rizzo J. R., Montillaud J., González-Garcìa M., Joblin C., Le Bourlot J., Le Petit F., Kramer C. | A&A 544, A110 |
| 1678 | Two short mass-loss events that unveil the binary heart of Minkowski's Butterfly Nebula | Castro-Carrizo A., Neri R., Bujarrabal V., Chesneau O., Cox P., Bachiller R. | A&A 545, A1 |
| 1679 | Variability of the blazar 4C 38.41 (B3 1633+382) from GHz frequencies to GeV energies | Raiteri C. M., Villata M., Smith P. S., Larionov V. M., Acosta-Pulido J. A., Aller M. F., D'Ammando F., Gurwell M. A., Jorstad S. G., Joshi M., Kurtanidze O. M., Lähteenmäki A., Mirzaqulov D. O., Agudo I., Aller H. D., Arévalo M. J., Arkharov A. A., Bach U., Benìtez E., Berdyugin A., Blinov D. A., Blumenthal K., Buemi C. S., Bueno A., Carleton T. M., Carnerero M. I., Carosati D., Casadio C., Chen W. P., Di Paola A., Dolci M., Efimova N. V., Ehgamberdiev S. A., Gómez J. L., González A. I., Hagen-Thorn V. A., Heidt J., Hiriart D., Holikov S., Konstantinova T. S., Kopatskaya E. N., Koptelova E., Kurtanidze S. O., Larionova E. G., Larionova L. V., León-Tavares J., Leto P., Lin H. C., Lindfors E., Marscher A. P., McHardy I. M., Molina S. N., Morozova D. A., Mujica R., Nikolashvili M. G., Nilsson K., Ovcharov E. P., Panwar N., Pasanen M., Puerto-Gimenez I., Reinthal R., Richter G. M., Ros J. A., Sakamoto T., Schwartz R. D., Sillanpää A., Smith N., Takalo L. O., Tammi J., Taylor B., Thum C., Tornikoski M., Trigilio C., Troitsky I. S., Umana G., Valcheva A. T., Wehrle A. E. | A&A 545, A48 |
| 1680 | BR1202-0725: an extreme multiple merger at z = 4.7 | Salomé P., Guélin M., Downes D., Cox P., Guilloteau S., Omont A., Gavazzi R., Neri R. | A&A 545, A57 |
| 1681 | Herschel/HIFI observations of red supergiants and yellow hypergiants. I. Molecular inventory | Teyssier D., Quintana-Lacaci G., Marston A. P., Bujarrabal V., Alcolea J., Cernicharo J., Decin L., Dominik C., Justtanont K., de Koter A., Melnick G., Menten K. M., Neufeld D. A., Olofsson H., Planesas P., Schmidt M., Soria-Ruiz R., Schöier F. L., Szczerba R., Waters L. B. F. M. | A&A 545, A99 |
| 1682 | Winds of change - a molecular outflow in NGC 1377? The anatomy of an extreme FIR-excess galaxy | Aalto S., Muller S., Sakamoto K., Gallagher J. S., Martìn S., Costagliola F. | A&A 546, A68 |
| 1683 | The circumstellar disk of AB Aurigae: evidence for envelope accretion at late stages of star formation? | Tang Y.-W., Guilloteau S., Piétu V., Dutrey A., Ohashi N., Ho P. T. P. | A&A 547, A84 |
| 1684 | Millimeter imaging of submillimeter galaxies in the COSMOS field: redshift distribution | Smolčić V., Aravena M., Navarrete F., Schinnerer E., Riechers D. A., Bertoldi F., Feruglio C., Finoguenov A., Salvato M., Sargent M., McCracken H. J., Albrecht M., Karim A., Capak P., Carilli C. L., Cappelluti N., Elvis M., Ilbert O., Kartaltepe J., Lilly S., Sanders D., Sheth K., Scoville N. Z., Taniguchi Y. | A&A 548, A4 |
| 1685 | A detailed view of a molecular cloud in the far outer disk of M 33. Molecular cloud formation in M 33 | Braine J., Gratier P., Contreras Y., Schuster K. F., Brouillet N. | A&A 548, A52 |
| 1686 | The IRAM-30 m line survey of the Horsehead PDR. II. First detection of the $l\text{-}C_3H^+$ hydrocarbon cation | Pety J., Gratier P., Guzmán V., Roueff E., Gerin M., Goicoechea J. R., Bardeau S., Sievers A., Le Petit F., Le Bourlot J., Belloche A., Talbi D. | A&A 548, A68 |
| 1687 | Chemistry in disks. VIII. The CS molecule as an analytic tracer of turbulence in disks | Guilloteau S., Dutrey A., Wakelam V., Hersant F., Semenov D., Chapillon E., Henning T., Piétu V. | A&A 548, A70 |
| 1688 | The hyperfine structure in the rotational spectrum of $CF^+$ | Guzmán V., Roueff E., Gauss J., Pety J., Gratier P., Goicoechea J. R., Gerin M., Teyssier D. | A&A 548, A94 |
| 1689 | Radio-to-g-ray monitoring of the narrow-line Seyfert 1 galaxy PMN J0948 + 0022 from 2008 to 2011 | Foschini L., Angelakis E., Fuhrmann L., Ghisellini G., Hovatta T., Lahteenmaki A., Lister M. L., Braito V., Gallo L., Hamilton T. S., Kino M., Komossa S., Pushkarev A. B., Thompson D. J., Tibolla O., Tramacere A., Carramiñana A., Carrasco L., Falcone A., Giroletti M., Grupe D., Kovalev Y. Y., Krichbaum T. P., Max-Moerbeck W., Nestoras I., Pearson T. J., Porras A., Readhead A. C. S., Recillas E., Richards J. L., Riquelme D., Sievers A., Tammi J., Tornikoski M., Ungerechts H., Zensus J. A., Celotti A., Bonnoli G., Doi A., Maraschi L., Tagliaferri G., Tavecchio F. | A&A 548, A106 |
| 1690 | High SiO abundance in the $HH^212$ protostellar jet | Cabrit S., Codella C., Gueth F., Gusdorf A. | A&A 548, L2 |
| 1691 | First Detection of Hydrogen Chloride Toward Protostellar Shocks | Codella C., Ceccarelli C., Bottinelli S., Salez M., Viti S., Lefloch B., Cabrit S., Caux E., Faure A., Vasta M., Wiesenfeld L. | ApJ 744, 164 |

| | | | |
|---|---|---|---|
| 1692 | Constraining Dust and Molecular Gas Properties in Lya Blobs at z ~ 3 | Yang Y., Decarli R., Dannerbauer H., Walter F., Weiss A., Leipski C., Dey A., Chapman S. C., Le Floc'h E., Prescott M. K. M., Neri R., Borys C., Matsuda Y., Yamada T., Hayashino T., Tapken C., Menten K. M. | ApJ 744, 178 |
| 1693 | The Metallicity Dependence of the CO ⟶ $H_2$ Conversion Factor in z ≥ 1 Star-forming Galaxies | Genzel R., Tacconi L. J., Combes F., Bolatto A., Neri R., Sternberg A., Cooper M. C., Bouché N., Bournaud F., Burkert A., Comerford J., Cox P., Davis M., Förster Schreiber N. M., Garcia-Burillo S., Gracia-Carpio J., Lutz D., Naab T., Newman S., Saintonge A., Shapiro K., Shapley A., Weiner B. | ApJ 746, 69 |
| 1694 | Molecular Gas in Infrared Ultraluminous QSO Hosts | Xia X. Y., Gao Y., Hao C.-N., Tan Q. H., Mao S., Omont A., Flaquer B. O., Leon S., Cox P. | ApJ 750, 92 |
| 1695 | Multi-wavelength Observations of Blazar AO 0235+164 in the 2008-2009 Flaring State | Ackermann M., Ajello M., Ballet J., Barbiellini G., Bastieri D., Bellazzini R., Blandford R. D., Bloom E. D., Bonamente E., Borgland A. W., Bottacini E., Bregeon J., Brigida M., Bruel P., Buehler R., Buson S., Caliandro G. A., Cameron R. A., Caraveo P. A., Casandjian J. M., Cavazzuti E., Cecchi C., Charles E., Chekhtman A., Chiang J., Ciprini S., Claus R., Cohen-Tanugi J., Cutini S., D'Ammando F., de Palma F., Dermer C. D., Silva E. d. C. e., Drell P. S., Drlica-Wagner A., Dubois R., Favuzzi C., Fegan S. J., Ferrara E. C., Focke W. B., Fortin P., Fuhrmann L., Fukazawa Y., Fusco P., Gargano F., Gasparrini D., Gehrels N., Germani S., Giglietto N., Giommi P., Giordano F., Giroletti M., Glanzman T., Godfrey G., Grenier I. A., Guiriec S., Hadasch D., Hayashida M., Hughes R. E., Itoh R., Jóhannesson G., Johnson A. S., Katagiri H., Kataoka J., Knödlseder J., Kuss M., Lande J., Larsson S., Lee S.-H., Longo F., Loparco F., Lott B., Lovellette M. N., Lubrano P., Madejski G. M., Mazziotta M. N., McEnery J. E., Mehault J., Michelson P. F., Mitthumsiri W., Mizuno T., Monte C., Monzani M. E., Morselli A., Moskalenko I. V., Murgia S., Naumann-Godo M., Nishino S., Norris J. P., Nuss E., Ohsugi T., Okumura A., Omodei N., Orlando E., Ozaki M., Paneque D., Panetta J. H., Pelassa V., Pesce-Rollins M., Pierbattista M., Piron F., Pivato G., Porter T. A., Rainò S., Rando R., Rastawicki D., Razzano M., Readhead A., Reimer A., Reimer O., Reyes L. C., Richards J. L., Sbarra C., Sgrò C., Siskind E. J., Spandre G., Spinelli P., Szostek A., Takahashi H., Tanaka T., Thayer J. G., Thayer J. B., Thompson D. J., Tinivella M., Torres D. F., Tosti G., Troja E., Usher T. L., Vandenbroucke J., Vasileiou V., Vianello G., Vitale V., Waite A. P., Winer B. L., Wood K. S., Yang Z., Zimmer S., Fermi-LAT Collaboration, Moderski R., Nalewajko K., Sikora M., Villata M., Raiteri C. M., Aller H. D., Aller M. F., Arkharov A. A., Benìtez E., Berdyugin A., Blinov D. A., Boettcher M., Bravo Calle O. J. A., Buemi C. S., Carosati D., Chen W. P., Diltz C., Di Paola A., Dolci M., Efimova N. V., Forné E., Gurwell M. A., Heidt J., Hiriart D., Jordan B., Kimeridze G., Konstantinova T. S., Kopatskaya E. N., Koptelova E., Kurtanidze O. M., Lähteenmäki A., Larionova E. G., Larionova L. V., Larionov V. M., Leto P., Lindfors E., Lin H. C., Morozova D. A., Nikolashvili M. G., Nilsson K., Oksman M., Roustazadeh P., Sievers A., Sigua L. A., Sillanpää A., Takahashi T., Takalo L. O., Tornikoski M., Trigilio C., Troitsky I. S., Umana G., GASP-WEBT Consortium, Angelakis E., Krichbaum T. P., Nestoras I., Riquelme D., F-GAMMA, Krips M., Trippe S., Iram-PdBI, Arai A., Kawabata K. S., Sakimoto K., Sasada M., Sato S., Uemura M., Yamanaka M., Yoshida M., Kanata, Belloni T., Tagliaferri G., RXTE, Bonning E. W., Isler J., Urry C. M., SMARTS, Hoversten E., Falcone A., Pagani C., Stroh M., (Swift-XRT | ApJ 751, 159 |
| 1696 | Detection of Atomic Carbon [C II] 158 mm and Dust Emission from a z = 7.1 Quasar Host Galaxy | Venemans B. P., McMahon R. G., Walter F., Decarli R., Cox P., Neri R., Hewett P., Mortlock D. J., Simpson C., Warren S. J. | ApJ 751, L25 |
| 1697 | Ionized Nitrogen at High Redshift | Decarli R., Walter F., Neri R., Bertoldi F., Carilli C., Cox P., Kneib J. P., Lestrade J. F., Maiolino R., Omont A., Richard J., Riechers D., Thanjavur K., Weiss A. | ApJ 752, 2 |
| 1698 | Evidence for Low Extinction in Actively Star-forming Galaxies at z > 6.5 | Walter F., Decarli R., Carilli C., Riechers D., Bertoldi F., Weiß A., Cox P., Neri R., Maiolino R., Ouchi M., Egami E., Nakanishi K. | ApJ 752, 93 |
| 1699 | On the Variations of Fundamental Constants and Active Galactic Nucleus Feedback in the Quasi-stellar Object Host Galaxy RXJ0911.4+0551 at z = 2.79 | Weiß A., Walter F., Downes D., Carrili C. L., Henkel C., Menten K. M., Cox P. | ApJ 753, 102 |
| 1700 | CO Emission in Optically Obscured (Type-2) Quasars at Redshifts z ≈ 0.1-0.4 | Krips M., Neri R., Cox P. | ApJ 753, 135 |
| 1701 | Herschel Far-infrared Photometric Monitoring of Protostars in the Orion Nebula Cluster | Billot N., Morales-Calderón M., Stauffer J. R., Megeath S. T., Whitney B. | ApJ 753, L35 |
| 1702 | The Arp 220 Merger on kpc Scales | König S., Garcìa-Marìn M., Eckart A., Downes D., Scharwächter J. | ApJ 754, 58 |
| 1703 | Circumbinary Gas Accretion onto a Central Binary: Infrared Molecular Hydrogen Emission from GG Tau A | Beck T. L., Bary J. S., Dutrey A., Piétu V., Guilloteau S., Lubow S. H., Simon M. | ApJ 754, 72 |
| 1704 | Chemistry in Disks. VII. First Detection of $HC_3N$ in Protoplanetary Disks | Chapillon E., Dutrey A., Guilloteau S., Piétu V., Wakelam V., Hersant F., Gueth F., Henning T., Launhardt R., Schreyer K., Semenov D. | ApJ 756, 58 |
| 1705 | The Sources of HCN and $CH_3OH$ and the Rotational Temperature in Comet 103P/Hartley 2 from Time-resolved Millimeter Spectroscopy | Drahus M., Jewitt D., Guilbert-Lepoutre A., Waniak W., Sievers A. | ApJ 756, 80 |
| 1706 | The Impact of Interactions, Bars, Bulges, and Active Galactic Nuclei on Star Formation Efficiency in Local Massive Galaxies | Saintonge A., Tacconi L. J., Fabello S., Wang J., Catinella B., Genzel R., Graciá-Carpio J., Kramer C., Moran S., Heckman T. M., Schiminovich D., Schuster K., Wuyts S. | ApJ 758, 73 |
| 1707 | The Molecular Gas Content of z = 3 Lyman Break Galaxies: Evidence of a Non-evolving Gas Fraction in Main-sequence Galaxies at z > 2 | Magdis G. E., Daddi E., Sargent M., Elbaz D., Gobat R., Dannerbauer H., Feruglio C., Tan Q., Rigopoulou D., Charmandaris V., Dickinson M., Reddy N., Aussel H. | ApJ 758, L9 |
| 1708 | The ATLAS$^{3D}$ project - XI. Dense molecular gas properties of CO-luminous early-type galaxies | Crocker A., Krips M., Bureau M., Young L. M., Davis T. A., Bayet E., Alatalo K., Blitz L., Bois M., Bournaud F., Cappellari M., Davies R. L., de Zeeuw P. T., Duc P.-A., Emsellem E., Khochfar S., Krajnović D., Kuntschner H., Lablanche P.-Y., McDermid R. M., Morganti R., Naab T., Oosterloo T., Sarzi M., Scott N., Serra P., Weijmans A.-M. | MNRAS 421, 1298 |
| 1709 | COLD GASS, an IRAM legacy survey of molecular gas in massive galaxies - III. Comparison with semi-analytic models of galaxy formation | Kauffmann G., Li C., Fu J., Saintonge A., Catinella B., Tacconi L. J., Kramer C., Genzel R., Moran S., Schiminovich D. | MNRAS 422, 997 |

| | | | |
|---|---|---|---|
| 1710 | Discovery of a detached H I gas shell surrounding a Orionis | Le Bertre T., Matthews L. D., Gérard E., Libert Y. | MNRAS 422, 3433 |
| 1711 | Physical properties of dense molecular gas in centres of Seyfert galaxies | Sani E., Davies R. I., Sternberg A., Graciá-Carpio J., Hicks E. K. S., Krips M., Tacconi L. J., Genzel R., Vollmer B., Schinnerer E., Garcìa-Burillo S., Usero A., Orban de Xivry G. | MNRAS 424, 1963 |
| 1712 | A search for linear polarization in the active galactic nucleus 3C 84 at 239 and 348 GHz | Trippe S., Bremer M., Krichbaum T. P., Krips M., Neri R., Piétu V., Winters J. M. | MNRAS 425, 1192 |
| 1713 | Evidence of strong quasar feedback in the early Universe | Maiolino R., Gallerani S., Neri R., Cicone C., Ferrara A., Genzel R., Lutz D., Sturm E., Tacconi L. J., Walter F., Feruglio C., Fiore F., Piconcelli E. | MNRAS 425, L66 |
| 1714 | Comprehensive multiwavelength modelling of the afterglow of GRB 050525A | Resmi L., Misra K., Jóhannesson G., Castro Tirado A. J., Gorosabel J., Jelìnek M., Bhattacharya D., Kubánek P., Anupama G. C., Sota A., Sahu D. K., de Ugarte Postigo A., Pandey S. B., Sánchez Ramìrez R., Bremer M., Sagar R. | MNRAS 427, 288 |
| 1715 | An ALMA survey of submillimetre galaxies in the Extended Chandra Deep Field-South: detection of [C II] at $z = 4.4$ | Swinbank A. M., Karim A., Smail I., Hodge J., Walter F., Bertoldi F., Biggs A. D., de Breuck C., Chapman S. C., Coppin K. E. K., Cox P., Danielson A. L. R., Dannerbauer H., Ivison R. J., Greve T. R., Knudsen K. K., Menten K. M., Simpson J. M., Schinnerer E., Wardlow J. L., Weiß A., van der Werf P. | MNRAS 427, 1066 |
| 1716 | The intense starburst HDF850.1 in a galaxy overdensity at $z \approx 5.2$ in the Hubble Deep Field | Walter F., Decarli R., Carilli C., Bertoldi F., Cox P., da Cunha E., Daddi E., Dickinson M., Downes D., Elbaz D., Ellis R., Hodge J., Neri R., Riechers D. A., Weiss A., Bell E., Dannerbauer H., Krips M., Krumholz M., Lentati L., Maiolino R., Menten K., Rix H.-W., Robertson B., Spinrad H., Stark D. P., Stern D. | Nature 486, 233 |
| 1717 | Spectral Energy Distributions of a set of H II regions in M33 (HerM33es) | Relaño M., Verley S., Pérez I., Kramer C., Xilouris M., Boquien M., Braine J., Calzetti D., Henkel C., Henkel | IAU Symp. 284, 122 |
| 1718 | Variation in the dust spectral index across M33 | Tabatabaei F. S., Braine J., Kramer C., Xilouris M., Boquien M., Verley S., Schinnerer E., Calzetti D., Combes F., Israel F., Henkel C., Henkel | IAU Symp. 284, 125 |
| 1719 | Polarization of the Recombination Line Maser in MWC349 | Thum C., Morris D., Wiesemeyer H. | IAU Symp. 287, 49 |
| 1720 | Low CO Luminosities in Dwarf Galaxies | Schruba A., Leroy A. K., Walter F., Bigiel F., Brinks E., de Blok W. J. G., Kramer C., Rosolowsky E., Sandstrom K., Schuster K., Usero A., Weiss A., Wiesemeyer H. | Astron. J 143, 138 |
| 1721 | Imaging On-the-fly ALMA Observations | Rodrìguez-Fernández N., Pety J., Lonjaret M., Roche J. C., Gueth F. | ASP Conf. Series 461, 715 |
| 1721 | Blind decomposition of Herschel-HIFI spectral maps of the NGC 7023 nebula | Berné O., Joblin C., Deville Y., Pilleri P., Pety J., Teyssier D., Gerin M., Fuente A. | SF2A-2012 conf., 507 |
| 1722 | Millimeter radio spectro-imaging | Gratier P., Pety J. | SF2A-2012 conf., 529 |
| 1723 | The first months in the lifetime of the newly born jet associated to Swift J1644+57 | Castro-Tirado A. J., Gómez J. L., Agudo I., Guerrero M. A., Bremer M., Winters J. M., Gorosabel J., Guziy S., Jelinek M., Tello J. C., Sánchez-Ramìrez R., Pérez-Ramìrez D., Reyes-Iturbide J., Park I. H., Jeong S., Pozanenko A. S. | Tidal Disruption Events and AGN Outbursts, EPJ Web of Conf. 39, 4002 |
| 1724 | Herschel far-infrared photometric monitoring of protostars in the Orion Nebula Cluster | Billot N., Morales-Calderon M., Stauffer J., Megeath T. | Symp. Proceedings of "from Atoms to Pebbels: Herschel's view of Star and Planet Formation" |
| 1725 | Division VI / Commission 34 / Working Group Astrochemistry | van Dishoeck E. F., Herbst E., Aikawa Y., Black J. H., Blake G. A., Caselli P., Cernicharo J., Garay G., Guelin M., Jørgensen U. G., Maier J. P., Menten K. M., Millar T. J., Kwok S., Salama F., Sims I., Sternberg A. | IAU Transactions 7, Issue T28A, 236 |
| 1726 | TAPAS, a VO archive at the IRAM 30-m telescope | Leon S., Espigares V., Ruìz J. E., Verdes-Montenegro L., Mauersberger R., Brunswig W., Kramer C., Santander-Vela J. d. D., Wiesemeyer H. | Experimental Astron. 34, 65 |
| 1727 | Imaging the heart of astrophysical objects with optical long-baseline interferometry | Berger J.-P., Malbet F., Baron F., Chiavassa A., Duvert G., Elitzur M., Freytag B., Gueth F., Hönig S., Hron J., Jang-Condell H., Le Bouquin J.-B., Monin J.-L., Monnier J. D., Perrin G., Plez B., Ratzka T., Renard S., Stefl S., Thiébaut E., Tristram K. R. W., Verhoelst T., Wolf S., Young J. | A&A Review 20, 53 |
| 1728 | Structural Variability of 3C111 on Parsec Scales | Grossberger C., Kadler M., Wilms J., Müller C., Beuchert T., Ros E., Ojha R., Aller M., Aller H., Angelakis E., Fuhrmann L., Nestoras I., Schmidt R., Zensus J. A., Krichbaum T. P., Ungerechts H., Sievers A., Riquelme D. | Acta Polytechnica 52, 18 |
| 1729 | A 3mm band dual polarization MMIC receiver for the 30-m Pico Veleta Radio Telescope | Serres P., Garnier O., Bortolotti Y., Navarro S., John D., Pissard B., Navarrini A., Schuster K. F. | SPIE 8452, 84522X - 84522X-10 |
| 1730 | An 8 GHz digital spectrometer for millimeter-wave astronomy | Garcìa R. G., Gentaz O., Baldino M., Torres M. | SPIE 8452, 84522T-84522T-8 |
| 1731 | A 3mm multipixel SIS receiver for IRAM 30-m Pico Veleta Telescope | Fontana A.-L., Boucher C., Serres P., Bortolotti Y., Cope F., Stil I., Lefranc B., Garnier O., Butin G., Mattiocco F., Navarro S., John D., Navarrini A., Schuster K. F. | SPIE 8452, 84522E-84522E-11 |
| 1732 | The GISMO-2 bolometer camera | Staguhn J. G., Benford D. J., Fixsen D. J., Hilton G., Irwin K. D., Jhabvala C. A., Kovacs A., Leclercq S., Maher S. F., Miller T. M., Moseley S. H., Sharp E. H., Wollack E. J. | SPIE 8452, 84520T-84520T-9 |
| 1733 | The NIKA 2011 run: results and perspectives towards a permanent camera for the Pico Veleta observatory | Calvo M., Roesch M., Désert F. X., Monfardini A., Benoit A., Ade P., Boudou N., Bourrion O., Camus P., Cruciani A., Doyle S., Hoffmann C., Leclercq S., Macias-Perez J. F., Mauskopf P., Ponthieu N., Schuster K., Tucker C., Vescovi C. | SPIE 8452, 845203-845203-7 |
| 1734 | Modeling and Measuring the Optical Coupling of Lumped Element Kinetic Induction Detectors at 128 - 180 GHz | Roesch M., Mattiocco F., Scherer T. A., Siegel M., Schuster K.-F. | IEEE Trans. on Ant. and Prop., pp, 99 (DOI 10.1109/TAP.2012.2231933) |
| 1735 | The ALMA Band-7 Cartridge | Mahieu S., Maier D., Lazareff B., Navarrini A., Celestin G., Chalain J., Geoffroy D., Laslaz F., Perrin G. | IEEE Trans. on THz Sci. and Tech., 2, 29 |
| 1736 | Upgrade of EMIR's Band 3 and Band 4 Mixers for the IRAM 30-m Telescope | Maier D., Reverdy J., Billon-Pierron D., Barbier A. | IEEE Trans. on THz Sci. and Tech., 2, 215 |
| 1737 | F-GAMMA: On the phenomenological classification of continuum radio spectra variability patterns of Fermi blazars | Angelakis E., Fuhrmann L., Nestoras I., Fromm C. M., Perucho-Pla M., Schmidt R., Zensus J. A., Marchili N., Krichbaum T. P., Ungerechts H., Sievers A., Riquelme D., Pavlidou V. | J. of Physics Conf. Series 372, 012007 |

| | | | |
|---|---|---|---|
| 1738 | g-ray emission region located in the parsec scale jet of OJ287 | Agudo I., Jorstad S. G., Marscher A. P., Larionov V. M., Gómez J. L., Lähteenmäki A., Gurwell M., Smith P. S., Wiesemeyer H., Thum C., Heidt J. | J. of Physics Conf. Series 355, 012032 |
| 1739 | Disk-Halo interaction: The molecular clouds in the Galactic center region | Riquelme D., Martìn-Pintado J., Mauersberger R., Amo-Baladrón M. A., Martìn S., Bronfman L. | J. of Physics Conf. Series 372, 012027 |
| 1740 | Multiple-Line Study of NGC 1068: Hot Molecular Gas Caused by Jet-Gas Interaction in the Central 100pc? | Krips M. | J. of Physics Conf. Series 372, 012038 |
| 1741 | Location of the g-RAY Flaring Emission in the Parsec-Scale Jet of the BL Lac Object AO 0235+164 | Agudo I., Marscher A. P., Jorstad S. G., Larionov V. M., Gómez J. L., Lähteenmäki A., Smith P. S., Nilsson K., Readhead A. C. S., Aller M. F., Heidt J., Gurwell M., Thum C., Wehrle A. E., Kurtanidze O. M. | Internat. J. of Modern Phys. Conf. Series 8, 271 |
| 1742 | Temporal Variation of the mm/Submm Emission Lines in Comet 103P/Hartley 2: What Does It Tell Us About the Nucleus? | Drahus M., Jewitt D., Guilbert-Lepoutre A., Waniak W., Sievers A., Hoge J., Lis D. C., Yoshida H., Peng R. | Asteroids, Comets, Meteors 2012, Conf. Proc. LPI Contrib. 1667, 6362 |
| 1743 | Molecular Survey of Comet C/2009P1 (Garradd) at mm to Submm Wavelengths | Biver N., Bockelée-Morvan D., Lis D. C., Paubert G., Swinyard B., Crovisier J., Moreno R., Gicquel A., Colom P., Lellouch E., Hartogh P., Boissier J., Cordiner M., Courtin R., de Val-Borro M., Dello Russo N., Kidger M., Küppers M., Milam S., Rengel M., Szutowicz S., Vervack R. J., Weaver H. A., HssO Team, OT1 dbockelee 1 Team | Asteriods, Comets, Meteors 2012, Conf. Proc. LPI Contrib. 1667, 6330 |
| 1744 | X-Ray Imaging Using LEKIDs | Cruciani A., Swenson L. J., Monfardini A., Boudou N., Calvo M., Roesch M. | J. of Low Temp. Physics 167, 311 |
| 1745 | LEKIDs Developments for mm-Wave Astronomy | Calvo M., Hoffman C., Benoit A., Boudou N., Cruciani A., Doyle S., Giordano C., Hoarau C., LeDuc H., Mauskopf P., Monfardini A., Roesch M., Schuster K. | J. of Low Temp. Physics 167, 379 |
| 1746 | The Néel IRAM KID Arrays (NIKA) | Monfardini A., Benoit A., Bideaud A., Boudou N., Calvo M., Camus P., Hoffmann C., Désert F.-X., Leclercq S., Roesch M., Schuster K., Ade P., Doyle S., Mauskopf P., Pascale E., Tucker C., Bourrion A., Macias-Perez J., Vescovi C., Barishev A., Baselmans J., Ferrari L., Yates S. J. C., Cruciani A., De Bernardis P., Masi S., Giordano C., Marghesin B., Leduc H. G., Swenson L. | J. of Low Temp. Physics 167, 834 |
| 1747 | Kinetic inductance detectors for millimeter and submillimeter astronomy | Boudou N., Benoit A., Bourrion O., Calvo M., Désert F.-X., Macias-Perez J., Monfardini A., Roesch M. | Comptes Rendus Physique 13, 62 |
| 1748 | Gamma-ray blazar BL Lacertae: the highest recorded cm/mm radio flux over the past 30 years | Karamanavis V., Myserlis I., Fuhrmann L., Angelakis E., Nestoras I., Krichbaum T. P., Zensus J. A., Ungerechts H., Sievers A., Riquelme D. | Astron. Tel. 4349 |
| 1749 | Follow-up radio observations of Nova Mon 2012 at 10 - 142 GHz | Fuhrmann L., Richards J. L., Bach U., Hovatta T., Bremer M., Nestoras I., Karamanavis V., Mooley K., Myserlis I., Readhead A. C. S., Cheung C. C., Pearson T., Angelakis E. | Astron. Tel. 4376 |
| 1750 | Recent radio activity of the Fermi blazar S5 0716+714 | Myserlis I., Angelakis E., Fuhrmann L., Karamanavis V., Nestoras I., Krichbaum T. P., Zensus J. A., Ungerechts H., Sievers A. | Astron. Tel. 4447 |
| 1751 | Recent radio activity of the Fermi blazar 4C +38.41 | Myserlis I., Angelakis E., Fuhrmann L., Karamanavis V., Nestoras I., Krichbaum T. P., Zensus J. A., Ungerechts H., Sievers A. | Astron. Tel. 4448 |
| 1752 | Recent radio activity of the Fermi blazar CTA 102 | Myserlis I., Angelakis E., Fuhrmann L., Karamanavis V., Nestoras I., Krichbaum T. P., Zensus J. A., Ungerechts H., Sievers A. | Astron. Tel. 4449 |
| 1753 | GRB 121123A: NIKA (New IRAM KID arrays) millimetre observations at the 30-m pico veleta telescope. | Monfardini A., Desert F.-X., Ponthieu N., Adams R., Calvo M., Macias-Perez J., Catalano A., Leclercq S., Mauskopf P., Benoit A., Detectors K. I. | GCN 14088 |
| 1754 | GRB 121212A: PdBI mm observations. | Castro-Tirado A. J., Bremer M., Winters J.-M. | GCN 14083 |
| 1755 | PdB IRAM observation of GRB 121011A. | Gendre B., Feruglio C., Stratta G., Antonelli A., Atteia J. L., Basa S., Boer M., Cutini S., D'Elia V., Klotz A., Piro L. | GCN 13871 |
| 1756 | GRB 120624B: mm detection at PdBI. | Bremer M., Winters J. M., König S., de Ugarte Postigo A., Castro-Tirado A. J. | GCN 13421 |
| 1757 | Spatially Resolved $H_2$ Emission In The GG Tau A Binary System | Bary J. S., Beck T. L., Dutrey A., Guilloteau S., Pietu V. | AAS 219, #437.06 |
| 1758 | The Chemical Structure of Orion KL: A 2D Spectral Line Survey at 1mm | Marcelino N., Cernicharo J., Esplugues G. B., Palau A., Bell T., Tercero B., Guelin M. | AAS 219, #437.01 |
| 1759 | Revisiting the Spiral Density Wave Paradigm in M51 with PAWS | Meidt S., Schinnerer E., Garcia-Burillo S., Hughes A., Colombo D., Pety J., Leroy A., Schuster K., Kramer C., Dumas G., Dobbs C., Thompson T. | AAS 219, #346.16 |
| 1760 | The IRAM Large Program HERACLES: The HERA CO-line Extragalactic Survey | Leroy A. K., Walter F., Schruba A., HERACLES Collaboration | AAS 219, #346.03 |
| 1761 | Formation and Evolution of Circumnuclear Starburst rings | Van Der Laan T., Schinnerer E., Garcia-Burillo S., Combes F., Boeker T., Emsellem E., Boone F., Dumas G., Hunt L. | AAS 219, #323.02 |
| 1762 | The Gismo 2-millimeter Deep Field In GOODS-N | Staguhn J., Kovacs A., Walter F., Dwek E., Decarli R., Benford D., Fixsen D., Irwin K., Jhabvala C., Leclercq S. S., Maher S., Miller T., Moseley S., Sharp E., Wollack E. | AAS 220, #308.01 |

## 2012 PUBLICATION LIST: IRAM COMMUNITY

| | | | |
|---|---|---|---|
| 1678 | Dense molecular gas around AGN: HCN/CO in NGC 3227 | Davies R., Mark D., Sternberg A. | A&A 537, A133 |
| 1679 | Ram pressure stripping of the multiphase ISM and star formation in the Virgo spiral galaxy NGC 4330 | Vollmer B., Soida M., Braine J., Abramson A., Beck R., Chung A., Crowl H. H., Kenney J. D. P., van Gorkom J. H. | A&A 537, A143 |
| 1680 | Chemical differentiation toward the Pipe nebula starless cores | Frau P., Girart J. M., Beltrán M. T. | A&A 537, L9 |

| | | | |
|---|---|---|---|
| 1681 | The onset of high-mass star formation in the direct vicinity of the Galactic mini-starburst W43 | Beuther H., Tackenberg J., Linz H., Henning T., Krause O., Ragan S., Nielbock M., Launhardt R., Schmiedeke A., Schuller F., Carlhoff P., Nguyen-Luong Q., Sakai T. | A&A 538, A11 |
| 1682 | Rotational spectrum of a chiral amino acid precursor, 2-aminopropionitrile, and searches for it in Sagittarius B2(N) | Møllendal H., Margulès L., Belloche A., Motiyenko R. A., Konovalov A., Menten K. M., Guillemin J. C. | A&A 538, A51 |
| 1683 | Microwave and submillimeter spectroscopy and first ISM detection of $^{18}$O-methyl formate | Tercero B., Margulès L., Carvajal M., Motiyenko R. A., Huet T. R., Alekseev E. A., Kleiner I., Guillemin J. C., Møllendal H., Cernicharo J. | A&A 538, A119 |
| 1684 | Looking for outflow and infall signatures in high-mass star-forming regions | Klaassen P. D., Testi L., Beuther H. | A&A 538, A140 |
| 1685 | A bright z = 5.2 lensed submillimeter galaxy in the field of Abell 773. HLSJ091828.6+514223 | Combes F., Rex M., Rawle T. D., Egami E., Boone F., Smail I., Richard J., Ivison R. J., Gurwell M., Casey C. M., Omont A., Berciano Alba A., Dessauges-Zavadsky M., Edge A. C., Fazio G. G., Kneib J.-P., Okabe N., Pelló R., Pérez-González P. G., Schaerer D., Smith G. P., Swinbank A. M., van der Werf P. | A&A 538, L4 |
| 1686 | Star-formation laws in luminous infrared galaxies. New observational constraints on models | Garcìa-Burillo S., Usero A., Alonso-Herrero A., Graciá-Carpio J., Pereira-Santaella M., Colina L., Planesas P., Arribas S. | A&A 539, A8 |
| 1687 | A study of deuterated water in the low-mass protostar IRAS 16293-2422 | Coutens A., Vastel C., Caux E., Ceccarelli C., Bottinelli S., Wiesenfeld L., Faure A., Scribano Y., Kahane C. | A&A 539, A132 |
| 1688 | The abundance of C$^{18}$O and HDO in the envelope and hot core of the intermediate mass protostar NGC 7129 FIRS 2 | Fuente A., Caselli P., McCoey C., Cernicharo J., Johnstone D., Fich M., van Kempen T., van Dishoeck E., Yıldız U., Visser R., Kristensen L., Alonso-Albi T., Herpin F., Tisi S. | A&A 540, A75 |
| 1689 | Molecular gas content and SFR in Hickson compact groups: enhanced or deficient? | Martinez-Badenes V., Lisenfeld U., Espada D., Verdes-Montenegro L., Garcìa-Burillo S., Leon S., Sulentic J., Yun M. S. | A&A 540, A96 |
| 1690 | Survival of molecular gas in Virgo's hot intracluster medium: CO near M 86 | Dasyra K. M., Combes F., Salomé P., Braine J. | A&A 540, A112 |
| 1691 | An upper limit to the variation in the fundamental constants at redshift z = 5.2 | Levshakov S. A., Combes F., Boone F., Agafonova I. I., Reimers D., Kozlov M. G. | A&A 540, L9 |
| 1692 | SiO maser emission from red supergiants across the Galaxy . I. Targets in massive star clusters | Verheyen L., Messineo M., Menten K. M. | A&A 541, A36 |
| 1693 | Subarcsecond resolution observations of warm water toward three deeply embedded low-mass protostars | Persson M. V., Jørgensen J. K., van Dishoeck E. F. | A&A 541, A39 |
| 1694 | The quest for complex molecules in space: laboratory spectroscopy of n-butyl cyanide, n-$C_4H_9CN$, in the millimeter wave region and its astronomical search in Sagittarius B2(N) | Ordu M. H., Müller H. S. P., Walters A., Nuñez M., Lewen F., Belloche A., Menten K. M., Schlemmer S. | A&A 541, A121 |
| 1695 | Detection of the hydroperoxyl radical $HO_2$ toward r Ophiuchi A. Additional constraints on the water chemical network | Parise B., Bergman P., Du F. | A&A 541, L11 |
| 1696 | Detection of complex organic molecules in a prestellar core: a new challenge for astrochemical models | Bacmann A., Taquet V., Faure A., Kahane C., Ceccarelli C. | A&A 541, L12 |
| 1697 | The Herschel Virgo Cluster Survey. X. The relationship between cold dust and molecular gas content in Virgo spirals | Corbelli E., Bianchi S., Cortese L., Giovanardi C., Magrini L., Pappalardo C., Boselli A., Bendo G. J., Davies J., Grossi M., Madden S. C., Smith M. W. L., Vlahakis C., Auld R., Baes M., De Looze I., Fritz J., Pohlen M., Verstappen J. | A&A 542, A32 |
| 1698 | Interferometric mapping of the 3.3-mm continuum emission of comet 17P/Holmes after its 2007 outburst | Boissier J., Bockelée-Morvan D., Biver N., Crovisier J., Lellouch E., Moreno R., Zakharov V. | A&A 542, A73 |
| 1699 | APEX-CHAMP$^+$ high-J CO observations of low-mass young stellar objects. III. NGC 1333 IRAS 4A/4B envelope, outflow, and ultraviolet heating | Yıldız U. A., Kristensen L. E., van Dishoeck E. F., Belloche A., van Kempen T. A., Hogerheijde M. R., Güsten R., van der Marel N. | A&A 542, A86 |
| 1700 | Discovery of interstellar mercapto radicals (SH) with the GREAT instrument on SOFIA | Neufeld D. A., Falgarone E., Gerin M., Godard B., Herbst E., Pineau des Forêts G., Vasyunin A. I., Güsten R., Wiesemeyer H., Ricken O. | A&A 542, L6 |
| 1701 | High-J CO emission in the Cepheus E protostellar outflow observed with SOFIA/GREAT | Gómez-Ruiz A. I., Gusdorf A., Leurini S., Codella C., Güsten R., Wyrowski F., Requena-Torres M. A., Risacher C., Wampfler S. F. | A&A 542, L9 |
| 1702 | GREAT confirms transient nature of the circum-nuclear disk | Requena-Torres M. A., Güsten R., Weiß A., Harris A. I., Martìn-Pintado J., Stutzki J., Klein B., Heyminck S., Risacher C. | A&A 542, L21 |
| 1703 | Close encounters of the protostellar kind in IC 1396N | Beltrán M. T., Massi F., Fontani F., Codella C., López R. | A&A 542, L26 |
| 1704 | On the nature of dust clouds in the region towards M 81 and NGC 3077 | Heithausen A. | A&A 543, A21 |
| 1705 | Kinematics of the inner thousand AU region around the young massive star AFGL 2591-VLA3: a massive disk candidate? | Wang K.-S., van der Tak F. F. S., Hogerheijde M. R. | A&A 543, A22 |
| 1706 | The circumstellar disk of HH 30. Searching for signs of disk evolution with multi-wavelength modeling | Madlener D., Wolf S., Dutrey A., Guilloteau S. | A&A 543, A81 |
| 1707 | The high-mass disk candidates NGC 7538IRS1 and NGC 7538S | Beuther H., Linz H., Henning T. | A&A 543, A88 |
| 1708 | Deuterated methanol in Orion BN/KL | Peng T.-C., Despois D., Brouillet N., Parise B., Baudry A. | A&A 543, A152 |

| | | | |
|---|---|---|---|
| 1709 | The search for the magnetic precursor of C-type shocks in young molecular outflows | Roberts J. F., Jiménez-Serra I., Gusdorf A., Martìn-Pintado J. | A&A 544, A150 |
| 1710 | Fragmentation in the massive star-forming region IRAS 19410+2336 | Rodón J. A., Beuther H., Schilke P. | A&A 545, A51 |
| 1711 | The Herschel Virgo Cluster Survey. XI. Environmental effects on molecular gas and dust in spiral disks | Pappalardo C., Bianchi S., Corbelli E., Giovanardi C., Hunt L., Bendo G. J., Boselli A., Cortese L., Magrini L., Zibetti S., di Serego Alighieri S., Davies J., Baes M., Ciesla L., Clemens M., De Looze I., Fritz J., Grossi M., Pohlen M., Smith M. W. L., Verstappen J., Vlahakis C. | A&A 545, A75 |
| 1712 | Modeling the physical and excitation conditions of the molecular envelope of NGC 7027 | Santander-Garcìa M., Bujarrabal V., Alcolea J. | A&A 545, A114 |
| 1713 | Chemistry of $C_3$ and carbon chain molecules in DR21(OH) | Mookerjea B., Hassel G. E., Gerin M., Giesen T., Stutzki J., Herbst E., Black J. H., Goldsmith P. F., Menten K. M., KreŃowski J., De Luca M., Csengeri T., Joblin C., Kaźmierczak M., Schmidt M., Goicoechea J. R., Cernicharo J. | A&A 546, A75 |
| 1714 | Wind mapping in Venus' upper mesosphere with the IRAM-Plateau de Bure interferometer | Moullet A., Lellouch E., Moreno R., Gurwell M., Sagawa H. | A&A 546, A102 |
| 1715 | Dust temperature and CO $\longrightarrow H_2$ conversion factor variations in the SFR-$M_\star$ plane | Magnelli B., Saintonge A., Lutz D., Tacconi L. J., Berta S., Bournaud F., Charmandaris V., Dannerbauer H., Elbaz D., Förster-Schreiber N. M., Graciá-Carpio J., Ivison R., Maiolino R., Nordon R., Popesso P., Rodighiero G., Santini P., Wuyts S. | A&A 548, A22 |
| 1716 | Rotational spectrum of formamide up to 1 THz and first ISM detection of its $n_{12}$ vibrational state | Motiyenko R. A., Tercero B., Cernicharo J., Margulès L. | A&A 548, A71 |
| 1717 | A method to measure CO and $N_2$ depletion profiles inside prestellar cores | Pagani L., Bourgoin A., Lique F. | A&A 548, L4 |
| 1718 | The Late Stages of Protoplanetary Disk Evolution: A Millimeter Survey of Upper Scorpius | Mathews G. S., Williams J. P., Ménard F., Phillips N., Duchêne G., Pinte C. | ApJ 745, 23 |
| 1719 | The Origin of OB Clusters: From 10 pc to 0.1 pc | Liu H. B., Quintana-Lacaci G., Wang K., Ho P. T. P., Li Z.-Y., Zhang Q., Zhang Z.-Y. | ApJ 745, 61 |
| 1720 | The GALEX Arecibo SDSS Survey. V. The Relation between the H I Content of Galaxies and Metal Enrichment at Their Outskirts | Moran S. M., Heckman T. M., Kauffmann G., Davé R., Catinella B., Brinchmann J., Wang J., Schiminovich D., Saintonge A., Gracia-Carpio J., Tacconi L., Giovanelli R., Haynes M., Fabello S., Hummels C., Lemonias J., Wu R. | ApJ 745, 66 |
| 1721 | Initial Conditions for Star Formation in Clusters: Physical and Kinematical Structure of the Starless Core Oph A-N6 | Bourke T. L., Myers P. C., Caselli P., Di Francesco J., Belloche A., Plume R., Wilner D. J. | ApJ 745, 117 |
| 1722 | Barnard 59: No Evidence for Further Fragmentation | Román-Zúñiga C. G., Frau P., Girart J. M., Alves J. F. | ApJ 747, 149 |
| 1723 | Discovery of a Binary System in IRAM 04191+1522 | Chen X., Arce H. G., Dunham M. M., Zhang Q. | ApJ 747, L43 |
| 1724 | Complex Structure in Class 0 Protostellar Envelopes. III. Velocity Gradients in Non-axisymmetric Envelopes, Infall, or Rotation? | Tobin J. J., Hartmann L., Bergin E., Chiang H.-F., Looney L. W., Chandler C. J., Maret S., Heitsch F. | ApJ 748, 16 |
| 1725 | Turbulent Molecular Gas and Star Formation in the Shocked Intergalactic Medium of Stephan's Quintet | Guillard P., Boulanger F., Pineau des Forêts G., Falgarone E., Gusdorf A., Cluver M. E., Appleton P. N., Lisenfeld U., Duc P.-A., Ogle P. M., Xu C. K. | ApJ 749, 158 |
| 1726 | Two Populations of Molecular Clouds in the Antennae Galaxies | Wei L. H., Keto E., Ho L. C. | ApJ 750, 136 |
| 1727 | Properties of Bulgeless Disk Galaxies. II. Star Formation as a Function of Circular Velocity | Watson L. C., Martini P., Lisenfeld U., Wong M.-H., Böker T., Schinnerer E. | ApJ 751, 123 |
| 1728 | CO J = 2-1 Line Emission in Cluster Galaxies at z ~ 1: Fueling Star Formation in Dense Environments | Wagg J., Pope A., Alberts S., Armus L., Brodwin M., Bussmann R. S., Desai V., Dey A., Jannuzi B., Le Floc'h E., Melbourne J., Stern D. | ApJ 752, 91 |
| 1729 | Dust-to-gas Ratio in the Extremely Metal-poor Galaxy I Zw 18 | Herrera-Camus R., Fisher D. B., Bolatto A. D., Leroy A. K., Walter F., Gordon K. D., Roman-Duval J., Donaldson J., Meléndez M., Cannon J. M. | ApJ 752, 112 |
| 1730 | 880 mm Imaging of a Transitional Disk in Upper Scorpius: Holdover from the Era of Giant Planet Formation? | Mathews G. S., Williams J. P., Ménard F. | ApJ 753, 59 |
| 1731 | A Comprehensive View of a Strongly Lensed Planck-Associated Submillimeter Galaxy | Fu H., Jullo E., Cooray A., Bussmann R. S., Ivison R. J., Pérez-Fournon I., Djorgovski S. G., Scoville N., Yan L., Riechers D. A., Aguirre J., Auld R., Baes M., Baker A. J., Bradford M., Cava A., Clements D. L., Dannerbauer H., Dariush A., De Zotti G., Dole H., Dunne L., Dye S., Eales S., Frayer D., Gavazzi R., Gurwell M., Harris A. I., Herranz D., Hopwood R., Hoyos C., Ibar E., Jarvis M. J., Kim S., Leeuw L., Lupu R., Maddox S., Martìnez-Navajas P., MichaŃowski M. J., Negrello M., Omont A., Rosenman M., Scott D., Serjeant S., Smail I., Swinbank A. M., Valiante E., Verma A., Vieira J., Wardlow J. L., van der Werf P. | ApJ 753, 134 |
| 1732 | Warm HCN in the Planet Formation Zone of GV Tau N | Fuente A., Cernicharo J., Agúndez M. | ApJ 754, L6 |
| 1733 | Different Evolutionary Stages in the Massive Star-forming Region W3 Main Complex | Wang Y., Beuther H., Zhang Q., Bik A., Rodón J. A., Jiang Z., Fallscheer C. | ApJ 754, 87 |
| 1734 | Forming an O Star via Disk Accretion? | Qiu K., Zhang Q., Beuther H., Fallscheer C. | ApJ 756, 170 |
| 1735 | A Universal Neutral Gas Profile for nearby Disk Galaxies | Bigiel F., Blitz L. | ApJ 756, 183 |
| 1736 | A Virialized Filamentary Infrared Dark Cloud | Hernandez A. K., Tan J. C., Kainulainen J., Caselli P., Butler M. J., Jiménez-Serra I., Fontani F. | ApJ 756, L13 |

| | | | |
|---|---|---|---|
| 1737 | Detection of Iron Ka Emission from a Complete Sample of Submillimeter Galaxies | Lindner R. R., Baker A. J., Beelen A., Owen F. N., Polletta M. | ApJ 757, 3 |
| 1738 | The Herschel and IRAM CHESS Spectral Surveys of the Protostellar Shock L1157-B1: Fossil Deuteration | Codella C., Ceccarelli C., Lefloch B., Fontani F., Busquet G., Caselli P., Kahane C., Lis D., Taquet V., Vasta M., Viti S., Wiesenfeld L. | ApJ 757, L9 |
| 1739 | Giant Molecular Clouds and Star Formation in the Non-grand Design Spiral Galaxy NGC 6946 | Rebolledo D., Wong T., Leroy A., Koda J., Donovan Meyer J. | ApJ 757, 155 |
| 1740 | The CHESS Survey of the L1157-B1 Shock Region: CO Spectral Signatures of Jet-driven Bow Shocks | Lefloch B., Cabrit S., Busquet G., Codella C., Ceccarelli C., Cernicharo J., Pardo J. R., Benedettini M., Lis D. C., Nisini B. | ApJ 757, L25 |
| 1741 | A 40 Myr Old Gaseous Circumstellar Disk at 49 Ceti: Massive CO-rich Comet Clouds at Young A-type Stars | Zuckerman B., Song I. | ApJ 758, 77 |
| 1742 | Tentative Detection of Deuterated Methane toward the Low-mass Protostar IRAS 04368+2557 in L1527 | Sakai N., Shirley Y. L., Sakai T., Hirota T., Watanabe Y., Yamamoto S. | ApJ 758, L4 |
| 1743 | Observational Limits on the Gas Mass of a z = 4.9 Galaxy | Livermore R. C., Swinbank A. M., Smail I., Bower R. G., Coppin K. E. K., Crain R. A., Edge A. C., Geach J. E., Richard J. | ApJ 758, L35 |
| 1744 | Young Starless Cores Embedded in the Magnetically Dominated Pipe Nebula. II. Extended Data Set | Frau P., Girart J. M., Beltrán M. T., Padovani M., Busquet G., Morata O., Masqué J. M., Alves F. O., Sánchez-Monge Á., Franco G. A. P., Estalella R. | ApJ 759, 3 |
| 1745 | Discovery of the Methoxy Radical, $CH_3O$, toward B1: Dust Grain and Gas-phase Chemistry in Cold Dark Clouds | Cernicharo J., Marcelino N., Roueff E., Gerin M., Jiménez-Escobar A., Muñoz Caro G. M. | ApJ 759, L43 |
| 1746 | Observations of HCN hyperfine line anomalies towards low- and high-mass star-forming cores | Loughnane R. M., Redman M. P., Thompson M. A., Lo N., O'Dwyer B., Cunningham M. R. | MNRAS 420, 1367 |
| 1747 | The relation between line emission and brightest cluster galaxies in three exceptional clusters: evidence for gas cooling from the intracluster medium | Hamer S. L., Edge A. C., Swinbank A. M., Wilman R. J., Russell H. R., Fabian A. C., Sanders J. S., Salomé P. | MNRAS 421, 3409 |
| 1748 | Gas and dust in a *z*= 2.8 obscured quasar | Schumacher H., Martìnez-Sansigre A., Lacy M., Rawlings S., Schinnerer E. | MNRAS 423, 2132 |
| 1749 | Herschel and JCMT observations of the early-type dwarf galaxy NGC 205 | De Looze I., Baes M., Parkin T. J., Wilson C. D., Bendo G. J., Boquien M., Boselli A., Cooray A., Cormier D., Fritz J., Galliano F., Gear W., Gentile G., Lebouteiller V., Madden S. C., Roussel H., Sauvage M., Smith M. W. L., Spinoglio L., Verstappen J., Young L. | MNRAS 423, 2359 |
| 1750 | Residual cooling and persistent star formation amid active galactic nucleus feedback in Abell 2597 | Tremblay G. R., O'Dea C. P., Baum S. A., Clarke T. E., Sarazin C. L., Bregman J. N., Combes F., Donahue M., Edge A. C., Fabian A. C., Ferland G. J., McNamara B. R., Mittal R., Oonk J. B. R., Quillen A. C., Russell H. R., Sanders J. S., Salomé P., Voit G. M., Wilman R. J., Wise M. W. | MNRAS 424, 1042 |
| 1751 | A search of CO emission lines in blazars: the low molecular gas content of BL Lac objects compared to quasars | Fumagalli M., Dessauges-Zavadsky M., Furniss A., Prochaska J. X., Williams D. A., Kaplan K., Hogan M. | MNRAS 424, 2276 |
| 1752 | A search for pre-substellar cores and proto-brown dwarf candidates in Taurus: multiwavelength analysis in the B213-L1495 clouds | Palau A., de Gregorio-Monsalvo I., Morata Ò., Stamatellos D., Huélamo N., Eiroa C., Bayo A., Morales-Calderón M., Bouy H., Ribas Á., Asmus D., Barrado D. | MNRAS 424, 2778 |
| 1753 | Limits on dust emission from z ~ 5 LBGs and their local environments | Davies L. J. M., Bremer M. N., Stanway E. R., Mannering E., Lehnert M. D., Omont A. | MNRAS 425, 153 |
| 1754 | Gas-rich mergers and feedback are ubiquitous amongst starbursting radio galaxies, as revealed by the VLA, IRAM PdBI and Herschel | Ivison R. J., Smail I., Amblard A., Arumugam V., De Breuck C., Emonts B. H. C., Feain I., Greve T. R., Haas M., Ibar E., Jarvis M. J., Kovács A., Lehnert M. D., Nesvadba N. P. H., Röttgering H. J. A., Seymour N., Wylezalek D. | MNRAS 425, 1320 |
| 1755 | Multiwavelength intraday variability of the BL Lacertae S5 0716+714 | Gupta A. C., Krichbaum T. P., Wiita P. J., Rani B., Sokolovsky K. V., Mohan P., Mangalam A., Marchili N., Fuhrmann L., Agudo I., Bach U., Bachev R., Böttcher M., Gabanyi K. E., Gaur H., Hawkins K., Kimeridze G. N., Kurtanidze O. M., Kurtanidze S. O., Lee C.-U., Liu X., McBreen B., Nesci R., Nestoras G., Nikolashvili M. G., Ohlert J. M., Palma N., Peneva S., Pursimo T., Semkov E., Strigachev A., Webb J. R., Wiesemeyer H., Zensus J. A. | MNRAS 425, 1357 |
| 1756 | Probing the physical and chemical structure of the CS core in LDN 673: multitransitional and continuum observations | Morata O., Girart J. M., Estalella R., Garrod R. T. | MNRAS 425, 1980 |
| 1757 | The molecular gas in luminous infrared galaxies - I. CO lines, extreme physical conditions and their drivers | Papadopoulos P. P., van der Werf P. P., Xilouris E. M., Isaak K. G., Gao Y., Mühle S. | MNRAS 426, 2601 |
| 1758 | The evolutionary connection between QSOs and SMGs: molecular gas in far-infrared luminous QSOs at z ~ 2.5 | Simpson J. M., Smail I., Swinbank A. M., Alexander D. M., Auld R., Baes M., Bonfield D. G., Clements D. L., Cooray A., Coppin K. E. K., Danielson A. L. R., Dariush A., Dunne L., de Zotti G., Harrison C. M., Hopwood R., Hoyos C., Ibar E., Ivison R. J., Jarvis M. J., Lapi A., Maddox S. J., Page M. J., Riechers D. A., Valiante E., van der Werf P. P. | MNRAS 426, 3201 |
| 1759 | Interferometric Identification of a Pre-Brown Dwarf | André P., Ward-Thompson D., Greaves J. | Science 337, 69 |
| 1760 | A complete survey of mm line emission from CO and $^{13}CO$ in water fountain stars | Rizzo J. R., Gómez J. F., Miranda L. F., Osorio M., Suárez O. | IAU Symp. 283, 484 |
| 1761 | Estimating the Star Formation Rate at 1 kpc Scales in nearby Galaxies | Leroy A. K., Bigiel F., de Blok W. J. G., Boissier S., Bolatto A., Brinks E., Madore B., Munoz-Mateos J.-C., Murphy E., Sandstrom K., Schruba A., Walter F. | Astron. Journal 144, 3 |
| 1762 | Massive Neutral and Molecular Winds in Nearby Galaxies | Veilleux S. | ASPC 460, 139 |

| | | | |
|---|---|---|---|
| 1763 | CO in Water Fountain Stars: More Than High-Velocity Water | Rizzo J. R., Suárez O., Gómez J. F., Miranda L. F., Osorio M. | ASPC 464, 71 |
| 1764 | Structure of CB 26 protoplanetary disk derived from millimeter dust continuum maps | Akimkin V. V., Pavlyuchenkov Y. N., Launhardt R., Bourke T. | Astronomy Reports 56, 915 |
| 1765 | A Comparison of c-$C_3H^3$ and l-$C_3H^2$ in the Spiral Arm Clouds | Kulczak-Jastrzębska M., Lis D., Gerin M. | Acta Astronomica 62, 313 |
| 1766 | The central structure of Broad Absorption Line QSOs: observational characteristics in the cm-mm wavelength domain | Bruni G., Mack K.-H., Dallacasa D., Montenegro-Montes F. M., Benn C. R., Carballo R., González-Serrano J. I., Holt J., Jiménez-Luján F. | J. of Physics Conf. Series 372, 012031 |
| 1767 | Chemical complexity in NGC 1068 | Aladro R., Viti S., Riquelme D., Martìn S., Mauersberger R., Martìn-Pintado J., Bayet E. | J. of Physics Conf. Series 372, 012039 |
| 1768 | 10 pc Scale Circumnuclear Molecular Gas Imaging of Nearby AGNs | Matsushita S. | J. of Physics Conf. Series 372, 012043 |
| 1769 | The feeding of activity in galaxies: a molecular line perspective | Garcìa-Burillo S., Combes F. | J. of Physics Conf. Series 372, 012050 |
| 1770 | Molecular gas in active environments | Mühle S., Henkel C., de Maio T., Seaquist E. R. | J. of Physics Conf. Series 372, 012052 |
| 1771 | CI, [CII] and CO observations towards TNJ 1338-1942: Probing the ISM in a massive proto-cluster galaxy at z = 4.11 | König S., Greve T. R., Seymour N., Rawlings J. I., Papadopoulos P., Ivison R. J., De Breuck C., Stevens J., Smail I., Kovacs A. | J. of Physics Conf. Series 372, 012064 |
| 1772 | a Confusion Limited Spectral Survey of Orion | Cernicharo J., Tercero B., Marcelino N., Bell T., Palau A. | 67th Internat. Symp on Molec. Spectroscopy, Abstract #$WH^{0}1$ |
| 1773 | The star-forming core ahead of HH 80N: studying the interaction with a parsec scale jet | Masqué Saumell J.-M. | PhDT |
| 1774 | Water deuteration in star-forming regions : Contribution of Herschel/HIFI spectroscopic data | Coutens A. | PhDT |
| 1775 | Characterizing interstellar filaments with Herschel in nearby molecular clouds | Arzoumanian D., André P., Peretto N., Könyves V., Schneider N., Didelon P., Palmeirim P. | Symp. Proceedings of "from Atoms to Pebbels: Herschel's view of Star and Planet Formation", 5 |
| 1776 | A new population of protostars discovered by Herschel | Stutz A. M., Tobin J., Fischer W., S. T. Megeath, Stanke T., Ali B., Henning T. | Symp. Proceedings of "from Atoms to Pebbels: Herschel's view of Star and Planet Formation", 28 |
| 1777 | F-GAMMA program: Unification and physical interpretation of the radio spectra variability patterns in Fermi blazars and detection of radio jet emission from NLSY1 galaxies | Angelakis E. | Proc of the 10th Hellenic Astronom. Conference, 18 |
| 1778 | The Tail-end of Primordial Disk Depletion - a Multiwavelength Gas and Dust Survey in Upper Scorpius | Mathews G. | AAS 219, #327.04 |
| 1779 | The Impact Of Turbulence On The Physical State Of The Molecular Gas And On Star Formation In Galaxy Interactions: The Case Of Stephan's Quintet | Guillard P., Boulanger F., Appleton P., Falgarone E., Gusdorf A., Lisenfeld U., Duc P. | AAS 220, #333.13 |
| 1780 | Low-energy electron irradiation studies of acetonitrile and acetonitrile/acetylene ices relevant to Titan's atmospheric and surface chemistry | Dawley M. M., McLain J., Abbott H. L., Orlando T. M. | American Geophys. Union, Fall Meeting 2011, abstract #P33E-1804 |

# Annex III – Committee members

## EXECUTIVE COUNCIL

R. Bachiller, OAN-IGN, Spain
S. Guilloteau, Obs. Bordeaux, France
A. Barcia Cancio, CAY, Spain
J.M. Hameury, CNRS-INSU, France
R. Genzel, MPE, Germany
K. Menten, MPIfR, Germany
J. Gomez-Gonzalez, IGN, Spain
J.L. Puget, IAS, France
M. Schleier, MPG, Germany

## SCIENTIFIC ADVISORY COMMITTEE

Ph. André, CEA, France
L. Tacconi, MPE, Germany
F. Boulanger, IAS, France
M. Tafalla, OAN-IGN, Spain
D. Jaffe, University of Texas, USA
P. de Vicente, OAN-IGN, Spain
R. Moreno, Obs. de Paris, France
D. Muders, MPIfR, Germany
F. Wyrowski, MPIfR, Germany

## PROGRAM COMMITTEE

H. Beuther, MPIA, Germany
S. Garcia-Burillo, OAN-IGN, Spain
A. Blain, University of Leicester, UK
J. Goicoechea, CSIC/INTA, Spain
S. Bontemps, Obs. Bordeaux, France
C. Henkel, MPIfR, Spain
V. Bujarrabal, OAN-IGN, Spain
B. Lefloch, IPAG, France
C. Codella, INAF, Italy
E. Sturm, MPE, Germany
R. Dave, Steward Observatory, USA
C. Vastel, IRAP, France
H. Dole, IAS, France

## AUDIT COMMISSION

Mr. Adams, CNRS, France
Mrs. Keil, MPG, Germany
Mrs. Maar, MPG, Germany

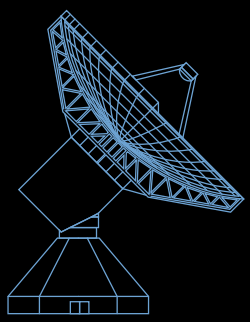

**30-meter diameter telescope, Pico Veleta**

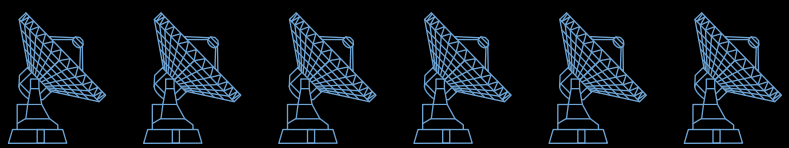

**6 x 15-meter interferometer, Plateau de Bure**

The Institut de Radioastronomie Millimétrique (IRAM) is a multi-national scientific institute covering all aspects of radio astronomy at millimeter wavelengths: the operation of two high-altitude observatories – a 30-meter diameter telescope on Pico Veleta in the Sierra Nevada (southern Spain), and an interferometer of six 15 meter diameter telescopes on the Plateau de Bure in the French Alps – the development of telescopes and instrumentation, radio astronomical observations and their interpretation.

IRAM was founded in 1979 by two national research organizations: the CNRS and the Max-Planck-Gesellschaft – the Spanish Instituto Geográfico Nacional, initially an associate member, became a full member in 1990.

The technical and scientific staff of IRAM develops instrumentation and software for the specific needs of millimeter radioastronomy and for the benefit of the astronomical community. IRAM's laboratories also supply devices to several European partners, including for the ALMA project.

IRAM's scientists conduct forefront research in several domains of astrophysics, from nearby star-forming regions to objects at cosmological distances.

IRAM Partner Organizations:
Centre National de la Recherche Scientifique (CNRS) – Paris, France
Max-Planck-Gesellschaft (MPG) – München, Deutschland
Instituto Geografico Nacional (IGN) – Madrid, España

iram
Institut de
Radioastronomie
Millimétrique